Supporting Information for

Controlled Exchange of Achiral Linkers with Chiral Linkers in Zr-Based UiO-68 Metal-Organic Framework

Chunxia Tan,† Xing Han,† Zijian Li,† Yan Liu,*,† and Yong Cui*,†,‡

†*School of Chemistry and Chemical Engineering and State Key Laboratory of Metal Matrix Composites, Shanghai Jiao Tong University, Shanghai 200240, China*

‡*Collaborative Innovation Center of Chemical Science and Engineering, Tianjin 300072, China*

yongcui@sjtu.edu.cn, liuy@sjtu.edu.cn

Table of Content

1. Materials and general procedures.

All reagents and solvents are commercially available and used without further purification. Powder X-ray diffraction (PXRD) data was collected on a D8 Advance Bruker diffractometer with Cu-*K*α radiation. The CD spectra were carried out on a J-800 spectropolarimeter (Jasco, Japan). Thermogravimetric analyses (TGA) were carried out in an N_2 atmosphere with a heating rate of 10 ^{o}C/min on a STA449C integration thermal analyzer. ICP-OES was performed on Optima 7300DV ICP-OES (Perkin Elmer Coporation, USA). The IR (KBr pellet) spectra were recorded (400-4000 cm^{-1}) on a Nicolet Magna 750 FT-IR spectrometer. Elemental analyses were performed with an EA1110 CHNS-0 CE elemental analyzer. Scanning Electron Microscopy (SEM) images were obtained on a NOVA NanoSEM 230 instrument equipped with an energy dispersive spectroscopy (EDS) detector. Transmission electron microscopy (TEM) images were performed on a Talos F200X/TALOS F200X instrument equipped with an energy dispersive spectroscopy (EDS) detector. The N_2 adsorption isotherms were measured at 77 K by using a Micrometritics ASAP 2020 surface area and porosity analyzer. Before the adsorption measurement, the sample was immersed in fresh DMF at 100 ^{o}C for three days during which the solvent was decanted and freshly replenished at least ten times, and then was Soxhlet extracted with THF for 48 h, and activated at 100 ^{o}C under vacuum (< 10^{-3} torr) for 8 h. The NMR experiments were carried out on a MERCURYplus 400 spectrometer operating at resonance frequencies of 400 MHz. Analytical high performance liquid chromatography (HPLC) was performed on a Shimadzu LC-2010HAT HPLC with UV detection at 200 or 254 nm. Analytical CHIRALCEL OD-H, AD-H, AS-H and OJ-H columns (4.6 mm × 25 cm) from Daicel were used.

X-ray Crystallography. Single-crystal XRD data for compound **UiO-68-Cu** was collected on BL17B beamline (λ = 0.82654 Å) of National Facility for Protein Science in Shanghai Synchrotron Radiation Facility (SSRF) at 100 K. We have collected several sets of data for **UiO-68-Cu**, and the best data set was used for structure solution and refinement. The empirical absorption correction was applied by using the SADABS program (G. M. Sheldrick, SADABS, program for empirical absorption correction of area detector data; University of Göttingen, Göttingen, Germany, 1996). The structure was solved using direct method, and refined by full-matrix least-squares on F^2 (G. M. Sheldrick, SHELXTL97, program for crystal structure refinement, University of Göttingen, Germany, 1997). In the compound, all the non-hydrogen atoms except guest molecules were refined by full-matrix least-squares techniques with anisotropic displacement parameters, and the hydrogen atoms were geometrically fixed at the calculated positions attached to their parent atoms, treated as riding atoms. Due to the high symmetry of the crystal, and the whole Cu(salen) ligand lies on a crystallographic symmetry axis were disorder thus we used the PART -1/PART 0 to restraint it. The final *R1* = 0.0737, *wR2* = 0.2127, GOOF = 1.087 for [$I > 2\mathrm{sigma}(I)$] was achieved for **UiO-68-Cu**. These parameters are reasonable, but the flack value was up to 0.45(4). Note that we used homochiral M(salen) ligands for the PSE process, the chirality of the single-crystal is from the chrial M(salen) ligands. Moreover, CD spectra of the crystal in solid-state show the optical purity of the structures. We think the possible reasons for the high flack parameter may be the disorder of chiral Cu(salen) units, which lies on the crystallographic symmetry axis over two positions of the crystal that weakens the anomalous scattering, leading to the determination of the absolute configuration inaccuracy. Thus the disorder of the chiral units may result in the high flack value.

Crystal data and details of the data collection are given in **Table S2**, and selected bond distances and angles are presented in **Table S3**.

Explanation For The Alert A and B for the UiO-68-Cu

Alert level A

PLAT250_ALERT_2_A Large U3/U1 Ratio for Average U(i,j) Tensor .... 10.1 Note

Discussion: The alert is generated because there is a large amount of disorder in the strucutre due to the whole disorder Cu(salen) ligand lies on the crystallographic symmetry axis over two positions of the crystal.

PLAT602_ALERT_2_A VERY LARGE Solvent Accessible VOID(S) in Structure ! Info

Discussion: The alert is generated because there exist large solvent-accessible void space up to 54% in the structure, and the *SQUEEZE* routine of *PLATON* were ever used but no obvious change.

Alert level B

THETM01_ALERT_3_B The value of sine(theta_max)/wavelength is less than 0.575 Calculated sin(theta_max)/wavelength = 0.5748

Discussion: A full set of data was collected, but the very high angle data was dominated by noise [I/sigma(I)<1.0] and was omitted. This arbitrary theta limit is inappropriate for our highly disordered structures. It would rule out all macromolecular structures. A limit on data/ parameter ratio's that properly consider the number of restraints / constraints and the redundancy of the measurements would be more appropriate. Unfortunately the cif check routine dose no do this. Short contacts between disordered fragments are to be expected.

PLAT049_ALERT_1_B Calculated Density Less Than 1.0 gcm-3 .... 0.8326 Check

Discussion: The alert is generated due to the large solvent-accessible void space in the structure.

PLAT213_ALERT_2_B Atom O3 has ADP max/min Ratio ..... 4.4 prolat

PLAT215_ALERT_3_B Disordered Cu1 has ADP max/min Ratio ..... 4.7 Note

PLAT215_ALERT_3_B Disordered C7 has ADP max/min Ratio ..... 4.2 Note

Discussion: Those alerts are generated because there exists large amount of disorder salen unit in the structure.

2. Synthesis

The $H_2\mathbf{L}^{\mathbf{M}}$ were synthesized according to the literatures[1].

Synthesis of UiO-68-Me: The synthesis of the **UiO-68-Me** was according to the literatures[2]: $ZrCl_4$ (93 mg), H_2Me-TPDC (113 mg), trifluoroacetic acid (1.0 mL) and DMF (20 mL) were charged in Pyrex vial, then the mixture was heated in a 120 ^{o}C oven for 72 h. The colorless crystals of **UiO-68-Me** were obtained (75.3 mg, yield: 63%). Its isostructural feature to **UiO-68** was suggested by PXRD (**Figure S1**). Comparison of unit cell parameters of reported UiO-type MOFs was listed in **Table S1**

Table S1 Unit cell parameters of reported **UiO-68 type** MOFs

MOF	Ligand	Space group	Unit cell	Reference
PCN-56	H_2TPDC-2CH_3	$Fm\bar{3}m$	$a = b = c$ =32.6003(11) V = 34647(2)	*JACS.* **2012**, *134*, 14690
PCN-57	H_2TPDC-4CH_3	$Fm\bar{3}m$	$a = b = c$ =32.657(19) V = 34829(36)	
PCN-58	H_2TPDC-4CH_2N_3	$Fm\bar{3}m$	$a = b = c$ =32.6919(14) V = 34940(3)	
sal-MOF	H2salTPD	$Fm\bar{3}m$	$a = b = c$ =32.6205(16) V = 34711(3)	*JACS.* **2014**, *136*, 13182
UiO-68-alkyne	H_2TPDC-CHC	$Fm\bar{3}m$	$a = b = c$ =32.7304(6) V = 35063.4 (19)	*Inorg. Chem.* **2015**, *54*, 5139.
UiO-68-Me	H_2TPDC-CH_3	$Fm\bar{3}m$	$a = b = c$ =32.5979(5) V = 34639.3 (1)	*this work*

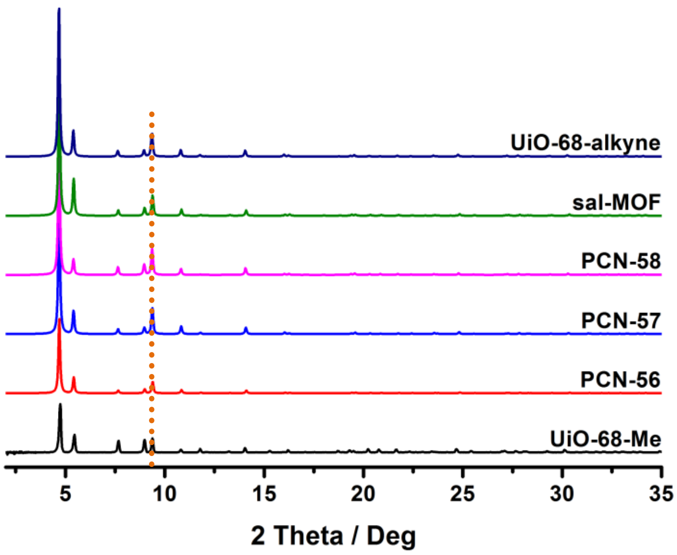

Figure S1. PXRD of UiO-type MOFs

Synthesis of UiO-68-M *via* PSE: The as-prepared **UiO-68-Me** (67.2 mg) was thoroughly washed with fresh DMF, and then was immersed in DMF solution of M(salen) (0.015 mol/L, the H_2**L**$^{\mathbf{M}}$ was about 5.0 equiv of the **L** in the **UiO-68-Me**) at 100 ^{o}C. After 24 h, the exchanged MOFs were thoroughly washed with hot DMF (10 mL × 5) and was then immersed in 10 mL fresh H_2**L**$^{\mathbf{M}}$ solution at 100 ^{o}C for another 24 h. The synthesis of **UiO-68-M** required ten exchange cycles. The obtained sample was immersed in fresh DMF at 100 ^{o}C for three days during which the solvent was decanted and freshly replenished at least ten times until no free M(salen) was detected by ICP-OES, The product can be best formulated based on IR, TGA, EA, NMR and ICP-OES.

UiO-68-Cu: {[$Zr_6O_4(OH)_4$(**TPDC-CH$_3$**)$_{0.33}$(**L**$^{\mathbf{Cu}}$)$_{5.67}$]·5DMF·5H_2O}, Deep purple crystals. Yield: 96%. Elemental analysis: Anal. (%). Calcd for $C_{192}H_{246.3}Cu_{5.7}N_{16.3}O_{53.3}Zr_6$: C, 50.75; H, 5.46; N, 5.03; Found: C, 50.35; H, 5.37; N, 5.02. ICP-OES Anal. (%): Zr, 12.05; Cu, 7.92. Found: Zr, 11.94; Cu, 7.87. IR (KBr pellet, v/cm^{-1}): 3414 (m), 2936 (s), 2858 (m), 1659(m), 1630(m), 1603(s), 1556 (m), 1493(w), 1468(w), 1392(s), 1378(s), 1338(s), 1230(m), 1200(w), 1177(m), 1137(w), 1096(m), 976(w), 933(m), 861(w), 833(w), 795(m), 783(s), 735(w), 707(s), 654(s), 575(m), 519(m).

UiO-68-Mn: {[$Zr_6O_4(OH)_4$(**TPDC-CH$_3$**)$_{0.7}$(**L**$^{\mathbf{Mn}}$)$_{5.3}$]·9DMF·H_2O}, Wine crystals. Yield: 96%. Elemental analysis: Anal. (%). Calcd for $C_{200.7}H_{259}Mn_{5.3}N_{19.6}O_{52.6}Zr_6$: C, 52.11; H, 5.64; N, 5.93; Found: C, 52.35; H, 5.67; N, 5.79. ICP-OES Anal. (%): Zr, 11.83; Mn, 6.29; Found: Zr, 11.99; Mn, 6.337. IR (KBr pellet, v/cm^{-1}): 3492(s), 3056(m), 2943 (s), 2863 (m), 1653(w), 1602(2), 1549 (s), 1412(s), 1385(s), 1336(w), 1308(w), 1202(w), 1180(m), 1145(m), 1103(m), 1022(w), 1004(m), 933(w), 895(w), 863(m), 829(m), 781(s), 713(m), 665(m), 651(m), 549(w), 513(w).471(w).

UiO-68-Cr: {[$Zr_6O_4(OH)_4$(**TPDC-CH$_3$**)$_{0.4}$(**L**$^{\mathbf{Cr}}$)$_{5.6}$]·10DMF ·3H_2O}, Dark yellow crystals. Yield: 95%. Elemental analysis: Anal. (%). Calcd for $C_{206.4}H_{275}Cr_{5.6}N_{21.2}O_{56.2}Zr_6$: C, 51.73; H, 5.81; N, 6.20; O, 18.76; Found: C, 51.36; H, 5.67; N, 6.35. ICP-OES Anal. (%): Zr, 11.42; Cr, 6.08. Found, Zr, 10.98; Cr, 5.854. IR (KBr pellet, v/cm^{-1}): 3406(s), 2942(s), 2860(m), 1709(m), 1653(s), 1602(s), 1562(m), 1488(m), 1468(m), 1421(s), 1392(s), 1382(s), 1331(s), 1256(w), 1228(m), 1200(m), 1180(m), 1143(m), 1101(m), 1025(w), 1004(m), 934(m), 889(w), 865(m), 833(m), 812(m), 784(s), 731(m), 712(s), 653(s), 603(w), 575(m), 558(m), 508(w), 491(w), 464(w).

UiO-68-Fe: {[$Zr_6O_4(OH)_4$(**TPDC-CH$_3$**)$_{1.03}$(**L**$^{\mathbf{Fe}}$)$_{4.97}$]·15DMF·4H_2O}, dark red crystals. Yield: 96%. Elemental analysis: Anal. (%). Calcd for $C_{215.7}H_{300.4}Fe_{4.97}N_{24.9}O_{60.9}Zr_6$: C, 51.38; H, 6.00; N, 6.93. Found: C, 50.96; H, 5.91; N, 6.85. ICP-OES Anal. (%): Zr, 10.85; Fe, 5.50. Found: Zr, 10.76; Fe, 5.471. IR (KBr pellet, v/cm^{-1}): 3417(s), 2944(s), 2863(m), 1697(m), 1603(s), 1556(m), 1448(w). 1468(w), 1392(s), 1380(s), 1335(m), 1313(m), 1291(m), 1232(w), 1201(w), 1180(m), 1136(m), 1120(w), 1105(w), 1048(w), 1028(w), 1005(w), 933(w), 862(m), 831(m), 813(w), 781(s), 735(w), 711(s), 669(s), 651(s), 604(w), 593(w), 572(w), 548(w), 508(m), 487(m).

UiO-68-V: {[$Zr_6O_4(OH)_4$(**TPDC-CH$_3$**)$_{0.92}$(**L**$^{\mathbf{v}}$)$_{5.08}$]·16DMF ·3H_2O}, Green crystals. Yield: 96%. Elemental analysis: Anal. (%). Calcd for $C_{219.7}H_{307.6}N_{26.2}O_{61.2}V_{5..8}Zr_6$: C, 51.74; H, 6.08; N, 7.18. Found: C, 52.07; H, 6.01; N, 7.28. ICP-OES Anal. (%): Zr, 10.73; V, 5.07. Found, Zr, 10.09; V, 4.798. IR (KBr pellet, v/cm^{-1}): 3436(s), 2944(s), 2862(s), 1655(m), 1605(s), 1566(m), 1489(w), 1466(w), 1447(w), 1394(s), 1384(s), 1335(m), 1309(m), 1290(m), 1233(m), 1201(m), 1183(m), 1142(m), 1098(m), 1048(w), 1033(m), 988(s), 935(m), 922(m), 889(w), 862(m), 834(m), 813(m), 791(s), 786(s), 737(m), 710(s), 666(s), 640(s), 594(w), 576(m), 558(m), 527(m), 511(w), 465(w).

Synthesis of UiO-68-Mn-M *via* PSE: Similar to the synthesis of **UiO-68-M**, the newly fabricated **UiO-68-Mn** as a parent material was immersed in 10 mL fresh H_2**L**$^{\mathbf{M}}$ solution at 100 ^{o}C. After 24 h, the exchanged MOFs was thoroughly washed with hot DMF(10 mL × 5) and was then immersed in fresh H_2**L**$^{\mathbf{M}}$ solution at 100 ^{o}C for another 24 h. Repeated for about 5 times (120 h), the obtained sample was immersed in fresh DMF at 100 ^{o}C for three days during which the solvent was decanted and freshly replenished until no free M(salen) was detected by ICP-OES.

The product can be best formulated on the basis of IR, TGA, EA, NMR and ICP-OES.

UiO-68-Mn-Cr. $\{[Zr_6O_4(OH)_4(\mathbf{TPDC\text{-}CH_3})_{0.44}(\mathbf{L^{Mn}})_{2.85}(\mathbf{L^{Cr}})_{2.71}]\cdot 8DMF\cdot 3H_2O\}$ Redlish brown crystals. Yield: 97%. Elemental analysis: Anal. (%). Calcd for $C_{200}H_{261.2}Cr_{2.71}Mn_{2.85}N_{19.1}O_{54.1}Zr_6$: C, 51.73; H, 5.67; N, 5.77; Found: C, 50.95; H, 6.04; N, 5.68. ICP-OES Anal. (%): Cr, 3.03; Mn, 3.37; Zr, 11.78. Found, Cr, 3.07; Mn, 3.22; Zr, 11.86. IR (KBr pellet, v/cm^{-1}): 3418(s), 2944(s), 2865(m), 1654(s), 1604(s), 1549(m), 1485(w), 1410(s), 1384(s), 1335(m), 1308(m), 1292(m), 1252(w), 1204(m), 1180(m), 1145(m), 1104(m), 1047(w), 1020(w), 1006(m), 973(w), 934(w), 865(m), 831(m), 779(s), 738(m), 711(s), 665(s), 652(s), 604(w), 575(m), 557(m), 511(w), 459(w).

UiO-68-Mn-V. $\{[Zr_6O_4(OH)_4(\mathbf{TPDC\text{-}CH_3})_{0.44}(\mathbf{L^{Mn}})_{1.72}(\mathbf{L^{Cr}})_{3.84}]\cdot 3DMF\cdot 12H_2O\}$. Brown crystals. Yield: 96%. Elemental analysis: Anal. (%). Calcd for $C_{185}H_{244.2}Mn_{1.72}N_{141}O_{62}V_{3.84}Zr_{6.}$ C, 49.44; H, 5.48; N, 4.40; Found: C, 48.96; H,5.51; N, 4.60. ICP-OES Anal. (%): Mn, 2.10; V, 4.35; Zr, 12.18. Found, Mn, 2.00; V, 4.46; Zr, 12.21. IR (KBr pellet, v/cm^{-1}): 3426(m), 2966(ms), 2865(m), 1687(s), 1606(s), 1564(m), 1430(w), 1403(s), 1314(s), 1284(m), 1180(m), 1140(m), 1106(m), 1045(w), 1025(w), 938(w), 875(m), 836(m), 748(m), 717(s), 655(s), 606 (w), 5775(m), 567(m), 510(w), 465(w).

3. General procedure for asymmetric catalysis

3.1 Epoxidation of Alkene Catalyzed by UiO-68-Mn: To a suspension of **UiO-68-Mn** (5×10^{-4} mmol) in dry DCM (1 mL), alkene (0.1 mmol) and the oxidant 2-(tert-butylsulfonyl)iodosylbenzene (*s*-PhIO) (2 mg, 6×10^{-3} mmol) were added. The same amount of oxidant was added 18 more times at 15 min intervals. The reaction was carried for 8 h at 0 ^{o}C. After that, the mixture was centrifuged at 9000 rpm for 5 min, and the supernatant was concentrated under vacuum. The concentrate was analyzed by ^{1}H NMR to give the conversion and by HPLC to give the ee value.

3.2 Epoxidation of Alkene Catalyzed by UiO-68-Fe: To a suspension of **UiO-68-Fe** (1×10^{-3} mmol) and alkene (0.1 mmol) in dry chloroform (1 mL), MesIO (0.12 mmol) was added at -20 ^{o}C, and then the reaction was allowed to proceed at -20 ^{o}C for 36 h. After that, the mixture was centrifuged at 9000 rpm for 5 min, and the supernatant was concentrated under vacuum. The concentrate was analyzed by ^{1}H NMR to give the conversion and by HPLC to give the ee value.

3.3 Oxidative Kinetic Resolution of Alcohols by UiO-68-Mn: UiO-68-Mn (5×10^{-3} mmol), racemic secondary alcohols (0.2 mmol), and 1.5 mL mixed solvent (CH_2Cl_2/H_2O, v:v = 1:2) were added to a 10 mL round-bottom flask. After stirring for 5 min, Et_4NBr (1.7 mg, 4.0 mol %) was added. The temperature was cooled down to 0 ^oC and $PhI(OAc)_2$ (45.0 mg,0.14 mmol) was added, and the reaction was allowed to proceed at 0 ^oC for 30 min. After that, the reaction was quenched by a saturated aqueous solution of $Na_2S_2O_3$. The mixture was extracted with Et_2O (3 × 2 mL) and the combined organic extracts were concentrated. The crude product was purified by flash chromatography over silica gel. The ee value and conversion of resulted products were determined by HPLC and ^1H NMR analysis, respectively.

3.4 Cyanation of Aldehyde Catalyzed by UiO-68-V:

Before catalysis, V(IV) of **UiO-68-V** was oxidized to V(V) with m-chloroperoxylbenzoic acid. To a suspension of **UiO-68-V** (100 mg) in CH_2Cl_2 (20 mL) was added a CH_2Cl_2 solution (30 mL) of mCPBA (30 mg, 0.18 mmol). After stirring for 4 h, the mixture was filtered, washed with CH_2Cl_2 (3×8 mL) and dried at 80 ℃ under vacuum to give oxidized **UiO-68-V**.

To a suspension of oxidized **UiO-68-V** (0.025 mmol) and triphenylphosphine oxide (0.5 mmol) in dichloroethane (2 mL), TMSCN (0.6 mmol) was added dropwise. The mixture was stirred at room temperature for 0.5 h and then aldehyde (0.5 mmol) was added dropwise. The reaction was allowed to proceed at 0 ˚C for 36 h. After that, the mixture was centrifuged at 9000 rpm for 5 min, and the supernatant was concentrated under vacuum. The concentrate was analyzed by ^1H NMR to give the conversion. The corresponding trimethylsilyl ether was acidized with 10 w/w% HCl/MeOH (0.2 mL) at room temperature for 10 min. The filtrate was extracted with diethyl ether (10 mL × 3) and washed with brine (20 mL), dried over $MgSO_4$ and evaporated under reduced pressure to give the cyanohydrin.

To a solution of the crude cyanohydrin in CH_2Cl_2 (2 mL) was added pyridine (0.16 mL, 2 mmol) and acetic anhydride (0.14 mL, 1.5 mmol). The mixture was stirred at room temperature for 45 min, diluted with diethyl ether (3 mL) and 1M HCl (0.1 mL). The organic layer was then separated and washed with water (3 mL), and brine (3 mL), dried over Na_2SO_4 and evaporated under reduced pressure to give an o-acetyl cyanohydirn. The ee values were determined by HPLC.

3.5 Aminolysis of Epoxide Catalyzed by UiO-68-Cr: To a suspension of **UiO-68-Cr** (0.01 mmol) in DCM (1 mL) was added epoxide (0.2 mmol) at room temperature under nitrogen. After stirring for 15 min, aniline (0.1 mmol) was added and the reaction mixture was stirred until the disappearance of the amine. After that, the mixture was centrifuged at 9000 rpm for 5 min, and the supernatant was concentrated under vacuum. The concentrate was analyzed by ^{1}H NMR to give the conversion and by HPLC to give the ee value.

3.6 Sequential Epoxidation/Ring-Opening Reactions Catalyzed by UiO-68-Mn-Cr: To a suspension of **UiO-68-Mn-Cr** (5×10^{-4} mmol) in dry DCM (1.0 mL), alkene (0.5 mmol) and S-PhIO (0.01 g, 0.03 mmol) were added. The same amount of oxidant was added 18 more times at 15 min intervals. The reaction was carried out overnight at 0 ^{o}C. After that, nucleophile (0.12 mmol) was added and the reaction mixture was stirred at 0 ^{o}C until the disappearance of the epoxide. Then the mixture was centrifuged at 9000 rpm for 5 min, and the supernatant was concentrated under vacuum. The concentrate was analyzed by ^{1}H NMR to give the conversion and by HPLC to give the ee value.

3.7 Catalyst Recycle Experiments, (using Epoxide Aminolysis as an example): Afterthe reaction, the precipitate was immersed in 3.0 mL fresh CH_2Cl_2 and sonicated for 10 min, then centrifuged at 9000 rpm for 5 min to get the rest catalyst, then wash again for another two times, the recovered catalyst dried in a vacuum oven at 60 ^{o}C, then used for the next run. The recycled experimental of other two catalytic reactions were performed in a similar procedure.

4. Table S2. Crystal data and structure refinement for **UiO-68-Cu** and **UiO-68-Me**

	UiO-68-Cu	**UiO-68-Me**
Empirical formula	$C_{90}H_{78}Cu_3N_6O_{22}Zr_3$	$C_{252}H_{132}O_{64}Zr_{12}$
Formula weight	2059.86	5278.22
Temperature (K)	100(2)	100(2)
Wavelength (Å)	0.82654	0.71073
Crystal system	Cubic	Cubic
Space group	$F432$	$Fm\bar{3}m$
Unit cell dimensions	a = 32.0319(7) Å α= 90 º b = 32.0319(7) Å β= 90 º c = 32.0319(7) Å γ =90 º	a = 32.5979(5) Å α= 90 º b = 32.5979(5) Å β= 90 º c = 32.5979(5) Å γ =90 º
Volume (Å^3), Z	32866(3), 8	34639.3(16), 2
Density (calculated) (mg/m^3)	0.833	0.506
Absorption coefficient (mm^{-1})	0.910	0.200
F(000)	8344.0	5272.0
Limiting indices	-36<=h<=36, -36<=k<=36, -34<=l<=36	-37<=h<=37, -37<=k<=37, -37<=l<=37
Reflections collected / unique	45563 / 2200	86565 / 1416
2Θ range for data collection/ °, Completeness	4.904-56.732, 100%	5.448-48.072, 98.6%
R_{int}	0.0901	0.1121
Refinement method	Full-matrix least-squares on F^2	Full-matrix least-squares on F^2
Data / restraints / parameters	2200 / 297 / 116	1416 / 115 / 53
Goodness-of-fit on F^2	1.093	1.088
Final R indices [I>2sigma(I)]	R_1 = 0.0737, wR_2 = 0.2080	R_1 = 0.0724, wR_2 = 0.1960
R indices (all data)	R_1 = 0.0819, wR_2 = 0.2172	R_1 = 0.0842, wR_2 = 0.2139
Absolute structure parameter	0.43(4)	-
Largest diff. peak and hole (e.Å^{-3})	0.91 and -0.60	0.58/-0.54

[a] $R_1 = \Sigma||F_o| - |F_c||/\Sigma|F_o|$. [b] $wR_2 = [\Sigma[w(F_o^2 - F_c^2)^2]/\Sigma w(F_o^2)^2]^{1/2}$,
$w = 1/[\sigma^2(F_o)^2 + (aP)^2 + bP]$ and $P = (F_o^2 + 2F_c^2)/3$.

5. Table S3a. Selected bond lengths [Å] and angles [°] for **UiO-68-Cu**

Cu(1)-Cu(1)$^{\#1}$	1.798(11)
Cu(1)-O(3)$^{\#1}$	1.569(11)
Cu(1)-O(3)	1.569(11)
Cu(1)-N(1)$^{\#2}$	2.06(2)
Cu(1)-N(1)	2.06(2)
Cu(1)-C(10)	2.06(2)
Cu(1)-C(10)$^{\#2}$	2.06(2)
Zr(1)-Zr(1)$^{\#3}$	3.5066(13)
Zr(1)-Zr(1)$^{\#4}$	3.5066(13)
Zr(1)-Zr(1)$^{\#5}$	3.5066(13)
Zr(1)-Zr(1)$^{\#6}$	3.5066(13)
O(3)-Cu(1)$^{\#1}$	1.569(11)
Zr(1)-O(1)$^{\#7}$	2.142(4)
Zr(1)-O(1)$^{\#8}$	2.142(4)
Zr(1)-O(1)	2.142(4)
Zr(1)-O(1)$^{\#9}$	2.142(4)
Zr(1)-O(2)$^{\#10}$	2.201(5)
Zr(1)-O(2)$^{\#11}$	2.201(5)
Zr(1)-O(2)	2.201(5)
Zr(1)-O(2)$^{\#9}$	2.201(5)
O(1)-Zr(1)$^{\#3}$	2.142(4)
O(1)-Zr(1)$^{\#4}$	2.142(4)
O(3)$^{\#1}$-Cu(1)-O(3)	110.1(6)
O(3)-Cu(1)-N(1)	82.7(6)
O(3)-Cu(1)-N(1)$^{\#2}$	161.9(9)
O(3)$^{\#1}$-Cu(1)-N(1)	161.9(9)
O(3)$^{\#1}$-Cu(1)-N(1)$^{\#2}$	82.7(6)
O(3)-Cu(1)-C(10)$^{\#2}$	161.9(9)
O(3)-Cu(1)-C(10)	82.7(6)
O(3)$^{\#1}$-Cu(1)-C(10)$^{\#2}$	82.7(6)
O(3)$^{\#1}$-Cu(1)-C(10)	161.9(9)
N(1)$^{\#2}$-Cu(1)-N(1)	88.1(12)
C(10)$^{\#2}$-Cu(1)-C(10)	88.1(12)
O(1)$^{\#9}$-Zr(1)-O(1)$^{\#7}$	108.7(6)
O(1)$^{\#7}$-Zr(1)-O(1)$^{\#8}$	70.1(3)
O(1)$^{\#9}$-Zr(1)-O(1)$^{\#8}$	70.1(3)
O(1)$^{\#7}$-Zr(1)-O(1)	70.1(3)
O(1)$^{\#9}$-Zr(1)-O(1)	70.1(3)
O(1)$^{\#8}$-Zr(1)-O(1)	108.7(6)

O(1)$^{\#9}$-Zr(1)-O(2)$^{\#10}$	139.8(3)
O(1)$^{\#9}$-Zr(1)-O(2)$^{\#11}$	78.6(3)
O(1) $^{\#9}$-Zr(1)-O(2)	76.2(3)
O(2)$^{\#10}$-Zr(1)-O(2)$^{\#11}$	121.9(3)
O(2)-Zr(1)-O(2)$^{\#8}$	121.8(3)
O(2)-Zr(1)-O(2)$^{\#10}$	76.34(13)
O(2)-Zr(1)-O(2)$^{\#11}$	76.34(13)
O(2)$^{\#10}$-Zr(1)-O(2)$^{\#8}$	76.34(13)
O(2)$^{\#11}$-Zr(1)-O(2)$^{\#8}$	76.34(13)
O(1)-Zr(1)-O(2)	139.8(3)
O(1)$^{\#7}$-Zr(1)-O(2)	143.7(3)
O(1)$^{\#8}$-Zr(1)-O(2)$^{\#8}$	139.8(3)
O(1)-Zr(1)-O(2)$^{\#10}$	143.7(3)
O(1)$^{\#8}$-Zr(1)-O(2)$^{\#11}$	143.7(3)
O(1)$^{\#8}$-Zr(1)-O(2)	78.6(3)
O(1)-Zr(1)-O(2)$^{\#8}$	78.6(3)
O(1)$^{\#7}$-Zr(1)-O(2)$^{\#11}$	139.8(3)
O(1)$^{\#7}$-Zr(1)-O(2)$^{\#8}$	76.2(3)
O(1)-Zr(1)-O(2)$^{\#11}$	76.2(3)
O(1) $^{\#7}$-Zr(1)-O(2) $^{\#10}$	78.6(3)
O(1) $^{\#8}$-Zr(1)-O(2) $^{\#10}$	76.2(3)
O(1) $^{\#9}$-Zr(1)-O(2) $^{\#8}$	143.7(3)

Symmetry transformations used to generate equivalent atoms:
$^{\#1}$1/2-X, +Y, 3/2-Z; $^{\#2}$1-Z, 1-Y, 1-X;$^{\#3}$1/2-Y, +Z, 1/2-X; $^{\#4}$-1/2+Z, 1/2-X, 1-Y; $^{\#5}$-1/2+Z, 1/2+X, +Y; $^{\#6}$-1/2+Y, +Z, 1/2+X; $^{\#7}$1/2-Y, 1/2-X, 1-Z; $^{\#8}$1/2-Y, 1/2+X, +Z; $^{\#9}$+X, 1-Y, 1-Z; $^{\#10}$+X, +Z, 1-Y; $^{\#11}$+X, 1-Z, +Y; $^{\#12}$-1/2+Z, 1-Y, 1/2+X

Table S3b. Selected bond lengths [Å] and angles [°] for **UiO-68-Me**

Zr(1)-Zr(1)$^{\#1}$	3.4745(10)
Zr(1)-Zr(1)$^{\#2}$	3.4745(10)
Zr(1)-Zr(1)$^{\#3}$	3.4745(10)
Zr(1)-Zr(1)$^{\#4}$	3.4745(10)
Zr(1)-O(1)$^{\#5}$	2.116(3)
Zr(1)-O(1)	2.116(3)
Zr(1)-O(1)$^{\#6}$	2.116(3)
Zr(1)-O(1)$^{\#7}$	2.116(3)
Zr(1)-O(2)$^{\#6}$	2.204(5)
Zr(1)-O(2)$^{\#7}$	2.204(5)
Zr(1)-O(2)	2.204(5)
Zr(1)-O(2)$^{\#5}$	2.204(5)

O(1)-Zr(1)$^{\#1}$	2.116(3)
O(1)-Zr(1)$^{\#2}$	2.116(3)
O(1)$^{\#6}$-Zr(1)-O(1)$^{\#5}$	69.6(2)
O(1)$^{\#7}$-Zr(1)-O(1)$^{\#6}$	69.6(2)
O(1)$^{\#5}$-Zr(1)-O(1)	69.6(2)
O(1)$^{\#6}$-Zr(1)-O(1)	107.6(5)
O(1)$^{\#7}$-Zr(1)-O(1)	69.6(2)
O(1)$^{\#7}$-Zr(1)-O(1)$^{\#5}$	107.6(5)
O(1)$^{\#7}$-Zr(1)-O(2)	78.4(2)
O(1)$^{\#6}$-Zr(1)-O(2)$^{\#5}$	142.06(7)
O(1)$^{\#5}$-Zr(1)-O(2)$^{\#7}$	142.06(7)
O(1)-Zr(1)-O(2)$^{\#7}$	142.06(7)
O(1)$^{\#5}$-Zr(1)-O(2)	142.06(7)
O(1)$^{\#7}$-Zr(1)-O(2)$^{\#7}$	78.4(2)
O(1)-Zr(1)-O(2)	78.4(2)
O(1)$^{\#5}$-Zr(1)-O(2)$^{\#6}$	78.4(2)
O(1)-Zr(1)-O(2)$^{\#6}$	142.06(7)
O(1)$^{\#6}$-Zr(1)-O(2)$^{\#6}$	78.4(2)
O(1)$^{\#7}$-Zr(1)-O(2)$^{\#6}$	142.06(7)
O(1)-Zr(1)-O(2)$^{\#5}$	78.4(2)
O(1)$^{\#7}$-Zr(1)-O(2)$^{\#5}$	142.06(7)
O(2)-Zr(1)-O(2)$^{\#5}$	75.70(17)
O(2)-Zr(1)-O(2)$^{\#6}$	120.4(4)
O(2)$^{\#6}$-Zr(1)-O(2)$^{\#5}$	75.70(17)
O(2)$^{\#6}$-Zr(1)-O(2)$^{\#7}$	75.70(17)
O(2)$^{\#5}$-Zr(1)-O(2)$^{\#7}$	120.4(4)
O(2)-Zr(1)-O(2)$^{\#7}$	75.70(17)
Zr(1)$^{\#2}$-O(1)-Zr(1)	110.4(2)
Zr(1)$^{\#2}$-O(1)-Zr(1)$^{\#3}$	110.4(2)
Zr(1)$^{\#3}$-O(1)-Zr(1)	110.4(2)
O(1)$^{\#7}$-Zr(1)-O(2)$^{\#6}$	142.06(7)
O(1)$^{\#7}$-Zr(1)-O(2)$^{\#5}$	142.06(7)
O(1)$^{\#6}$-Zr(1)-O(2)	142.06(7)
O(1)$^{\#6}$-Zr(1)-O(2)	142.06(7)
O(1)$^{\#6}$-Zr(1)-O(2)$^{\#7}$	78.4(2)

Symmetry transformations used to generate equivalent atoms:

$^{\#1}$1/2-Z,2-Y,-1/2+X; $^{\#2}$+X,1-Z,-1+Y; $^{\#3}$1/2+Z,+Y,1/2-X; $^{\#4}$1-X,1+Z,1-Y; $^{\#5}$3/2-Y,1/2+X,+Z; $^{\#6}$1-X,2-Y,+Z; $^{\#7}$-1/2+Y,3/2-X,+Z; $^{\#8}$+X,1-Z,1-Y; $^{\#9}$1-X,+Y,+Z; $^{\#10}$+X,3/2-Y,1/2-Z

6. Figures S2~S4. Additional X-ray crystallographic structures

6.1 Figure S2. The structure of $[Zr_6O_4(OH)_4(COO)_{12}]$ cluster

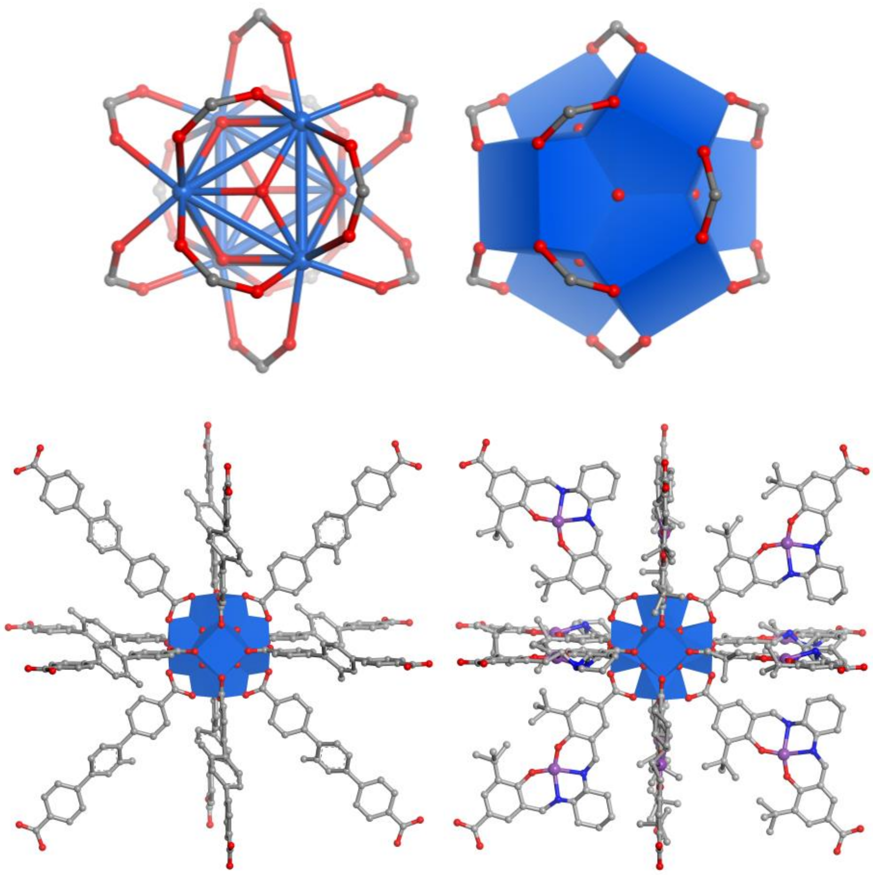

6.2 Figure S3. The structures of the tetrahedron and octahedron cages in **UiO-68-Me** (left) and **UiO-68-Cu** (right) (the cavity was highlighted by a yellow/orange ball)

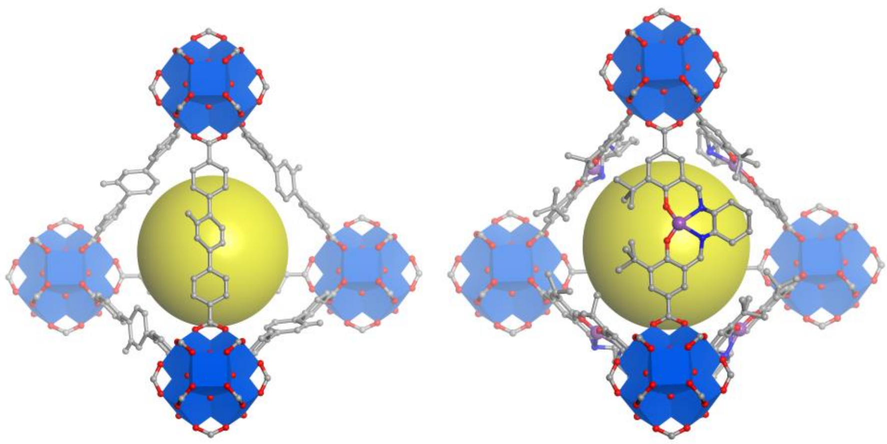

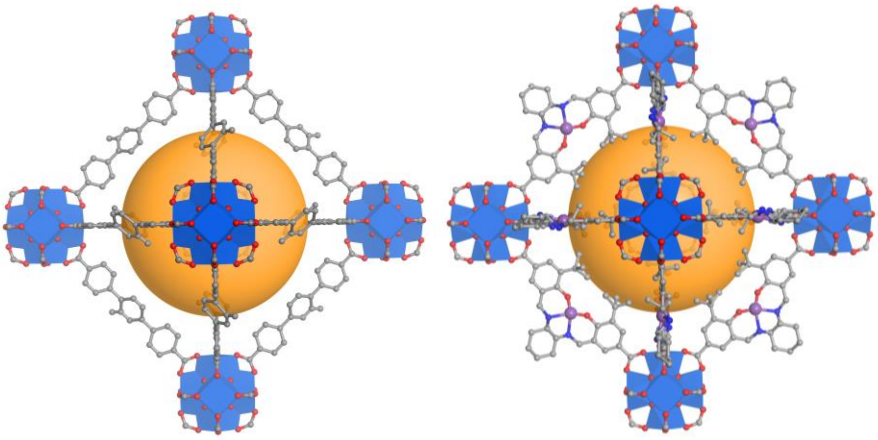

6.3 Figure S4. The packing modes of **UiO-68-Me** (top) and **UiO-68-Cu** (down)

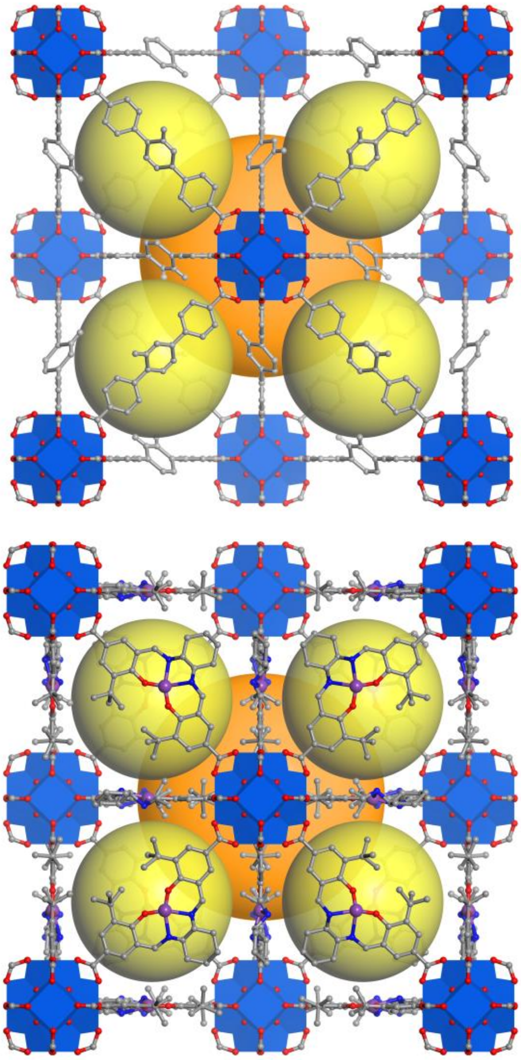

7. Figure S5. PXRD patterns and stability

a)

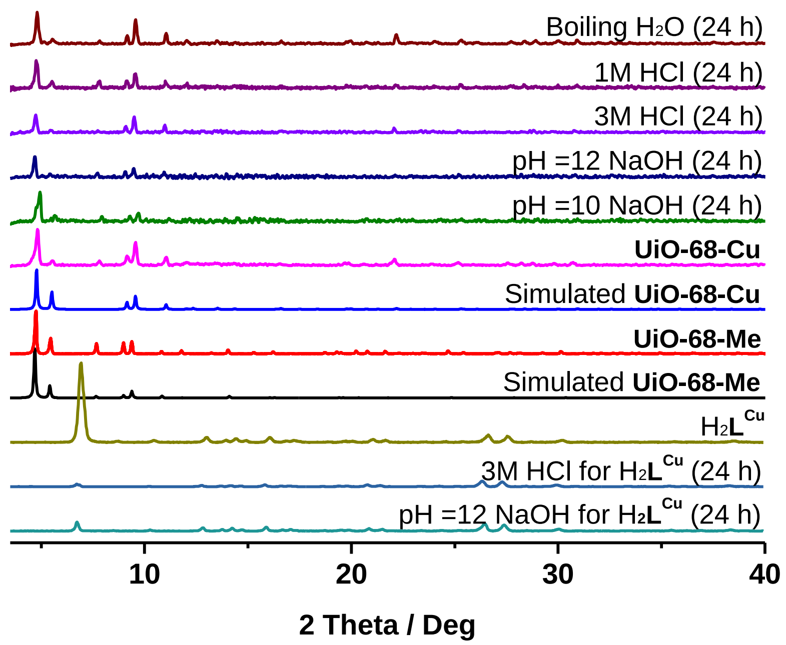

b)

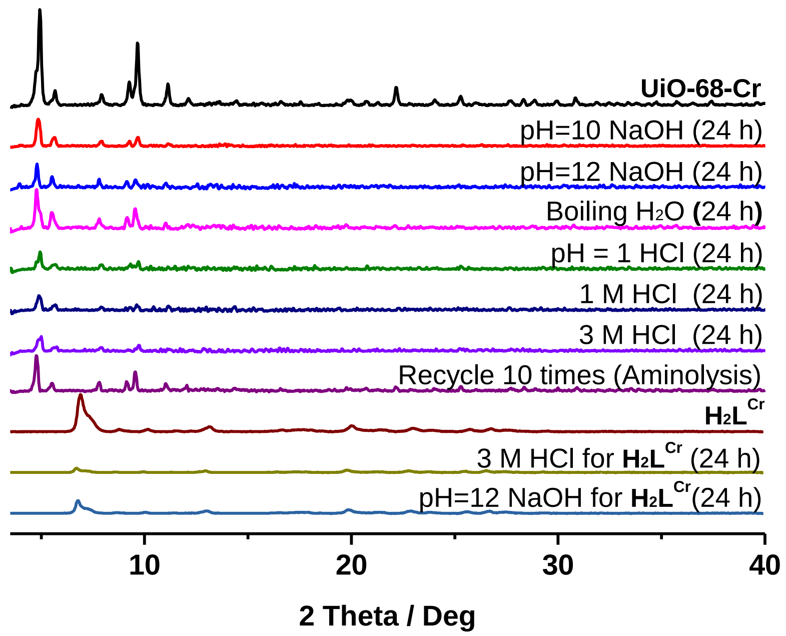

c)

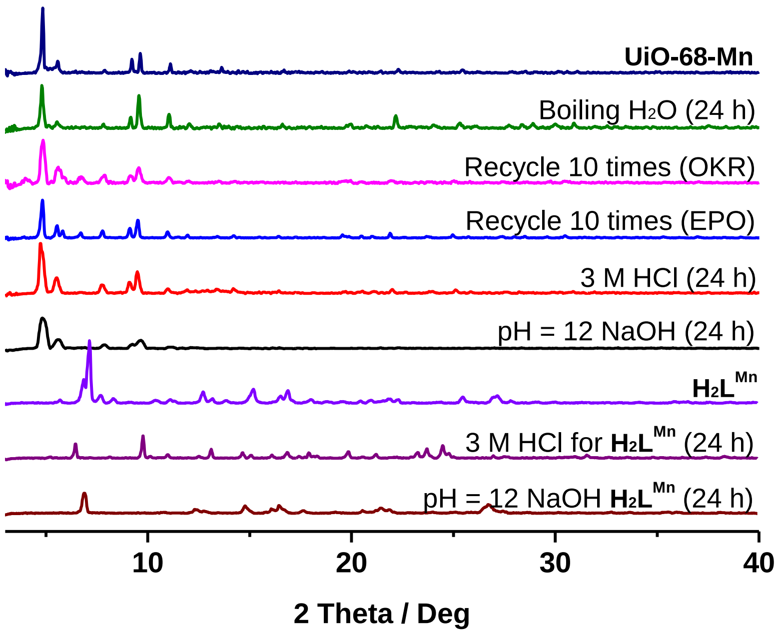
UiO-68-Mn
Boiling H_2O (24 h)
Recycle 10 times (OKR)
Recycle 10 times (EPO)
3 M HCl (24 h)
pH = 12 NaOH (24 h)
H_2L^{Mn}
3 M HCl for H_2L^{Mn} (24 h)
pH = 12 NaOH H_2L^{Mn} (24 h)
10
20
30
40
2 Theta / Deg

d)

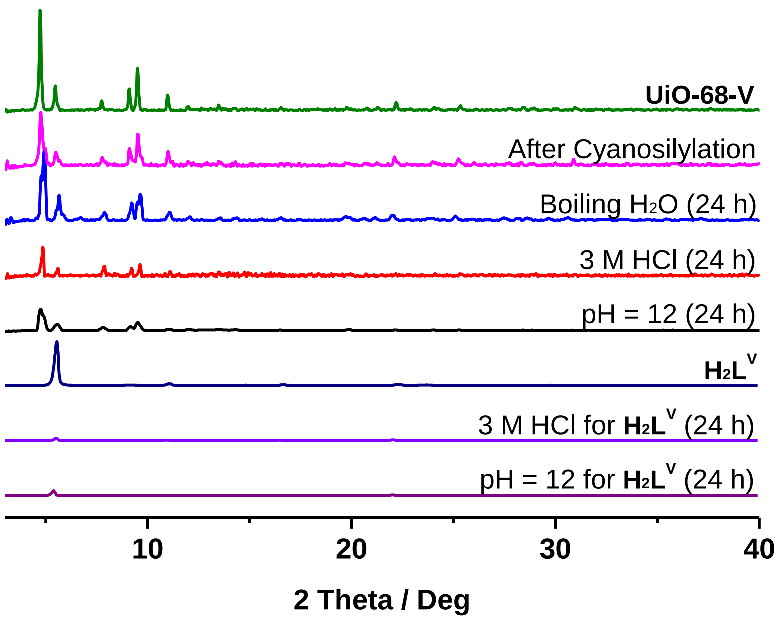
UiO-68-V
After Cyanosilylation
Boiling H_2O (24 h)
3 M HCl (24 h)
pH = 12 (24 h)
H_2L^{V}
3 M HCl for H_2L^{V} (24 h)
pH = 12 for H_2L^{V} (24 h)
10
20
30
40
2 Theta / Deg

e)

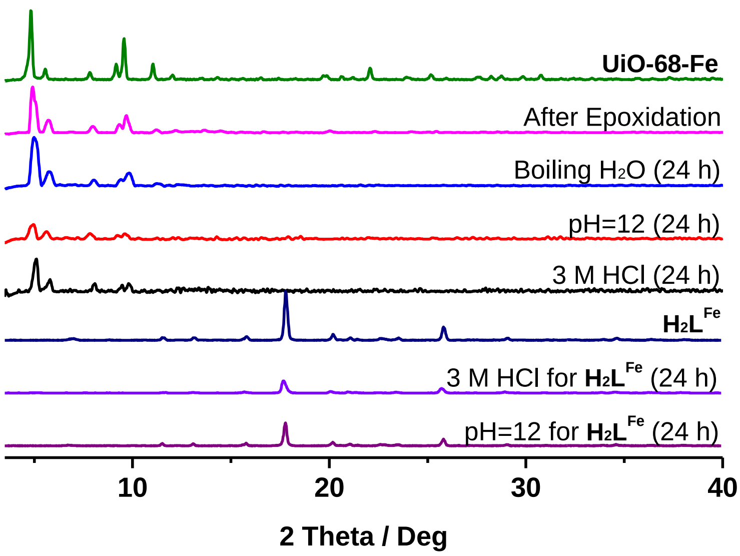

f) PXRD analysis of partially exchanged crystals by $H_2\mathbf{L}^{\mathbf{Cr}}$

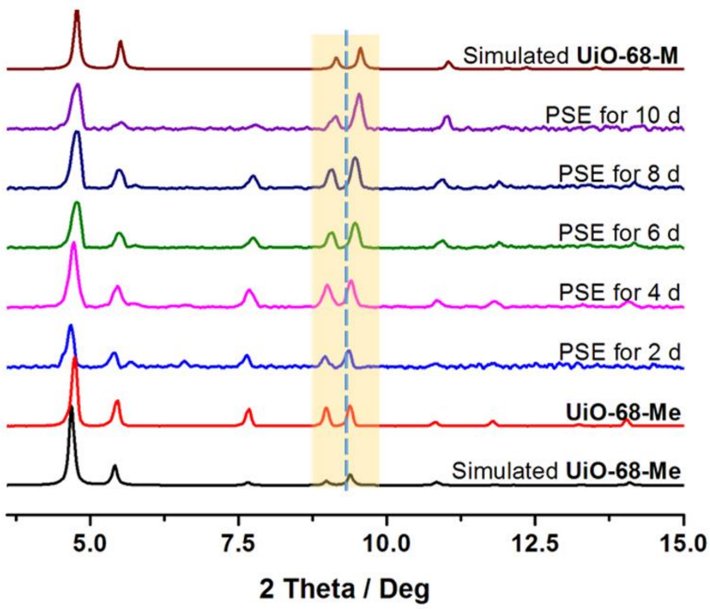

8. Figure S6. Residue weight percentage after treatment for 24 h in different solutions.

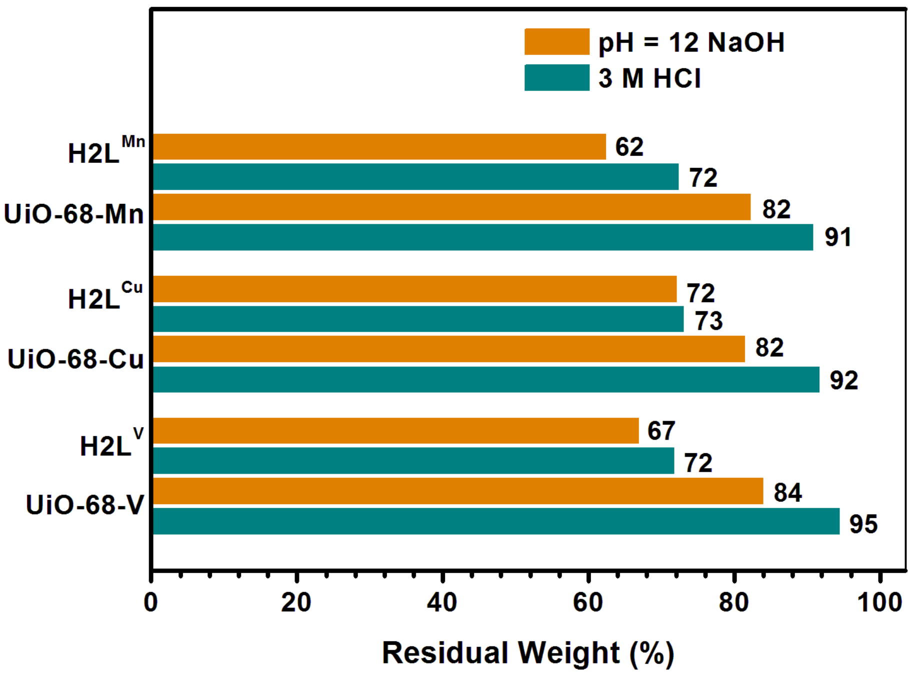

9. Figure S7. CD spectra

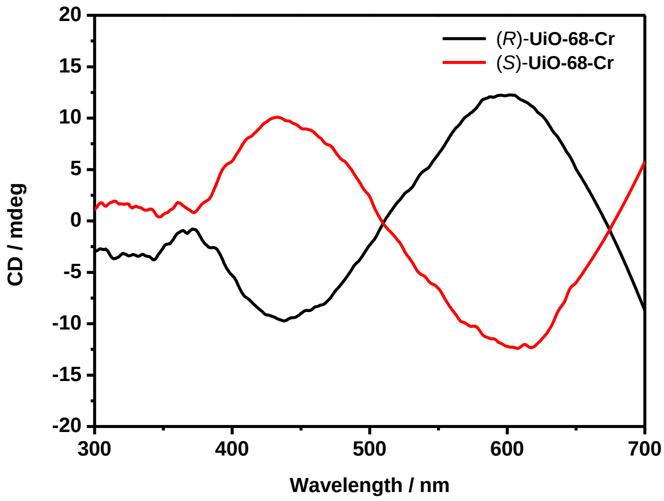

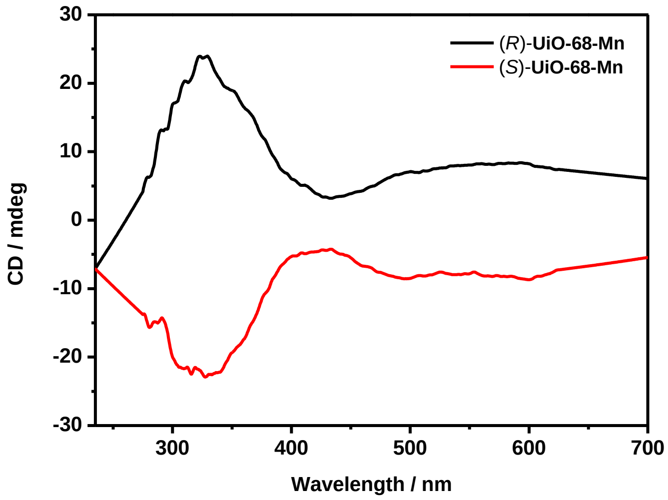

(R)-UiO-68-Mn
(S)-UiO-68-Mn
CD / mdeg
Wavelength / nm

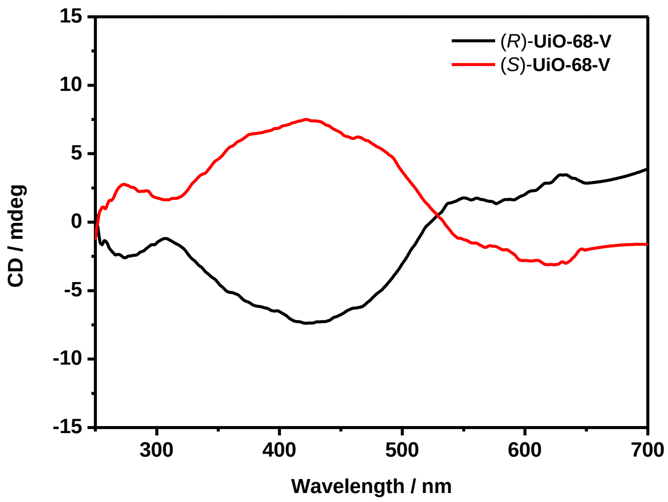

(R)-UiO-68-V
(S)-UiO-68-V
CD / mdeg
Wavelength / nm

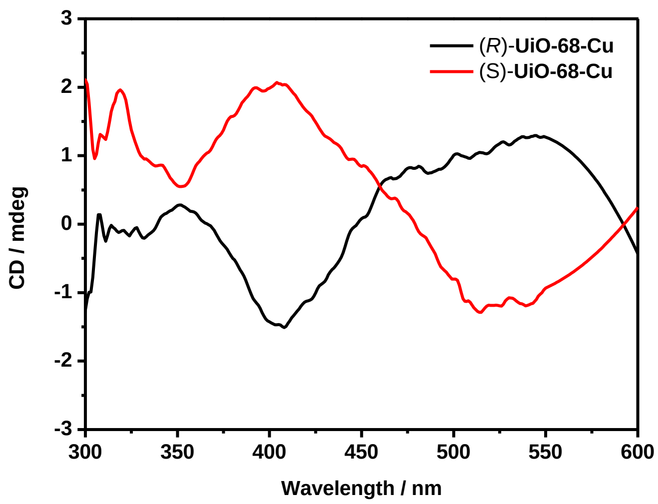

(R)-UiO-68-Cu
(S)-UiO-68-Cu
CD / mdeg
Wavelength / nm

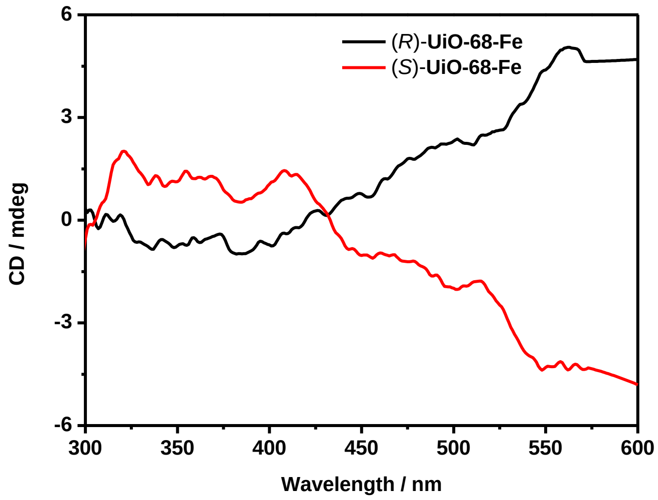

6
3
0
-3
-6
CD / mdeg
300
350
400
450
500
550
600
Wavelength / nm
(R)-UiO-68-Fe
(S)-UiO-68-Fe

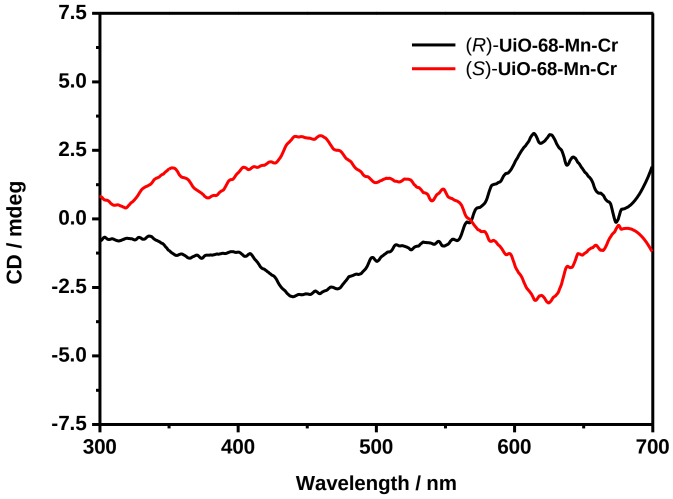

7.5
5.0
2.5
0.0
-2.5
-5.0
-7.5
CD / mdeg
300
400
500
600
700
Wavelength / nm
(R)-UiO-68-Mn-Cr
(S)-UiO-68-Mn-Cr

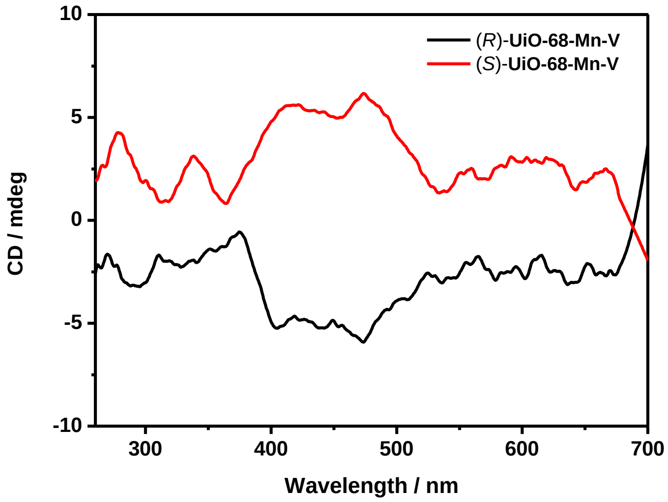

10
5
0
-5
-10
CD / mdeg
300
400
500
600
700
Wavelength / nm
(R)-UiO-68-Mn-V
(S)-UiO-68-Mn-V

10. Figure S8. TGA curves

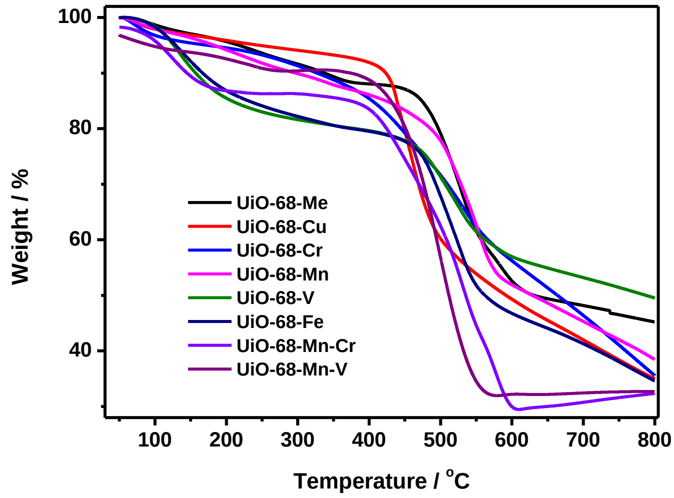

11. Figure S9. FT-IR spectra

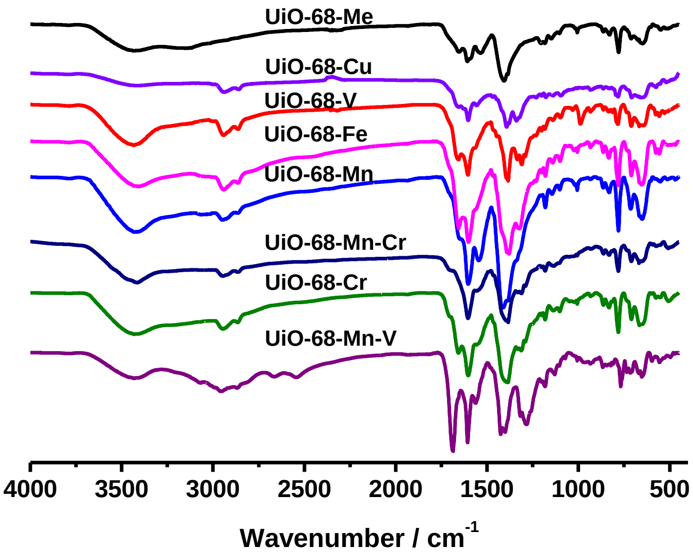

12. Figure S10. N_2 adsorption, Isotherm Log Plots and BET plots.

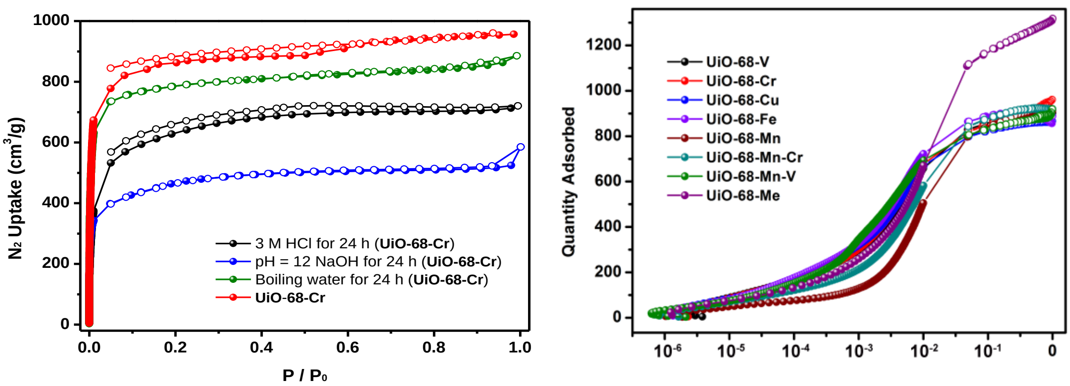

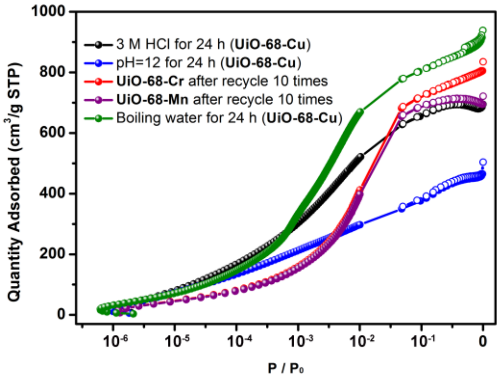
Quantity Adsorbed (cm³/g STP)
3 M HCl for 24 h (UiO-68-Cu)
pH=12 for 24 h (UiO-68-Cu)
UiO-68-Cr after recycle 10 times
UiO-68-Mn after recycle 10 times
Boiling water for 24 h (UiO-68-Cu)
P / P₀

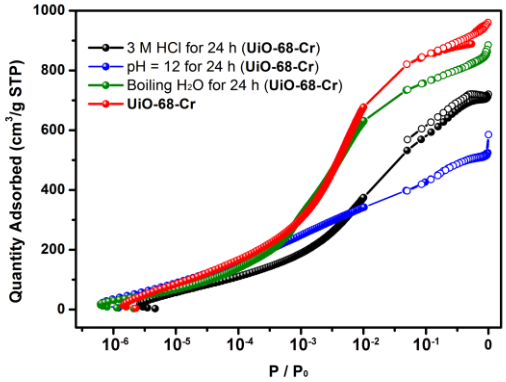
Quantity Adsorbed (cm³/g STP)
3 M HCl for 24 h (UiO-68-Cr)
pH = 12 for 24 h (UiO-68-Cr)
Boiling H₂O for 24 h (UiO-68-Cr)
UiO-68-Cr
P / P₀

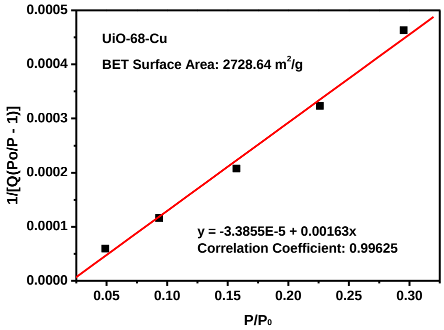
UiO-68-Cu
BET Surface Area: 2728.64 m²/g
y = -3.3855E-5 + 0.00163x
Correlation Coefficient: 0.99625
1/[Q(Po/P - 1)]
P/P₀

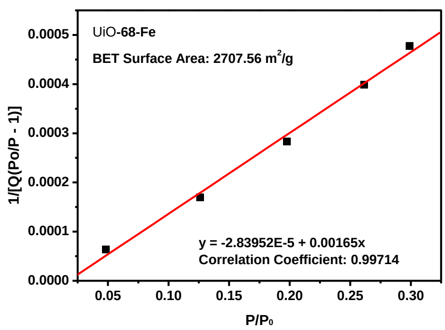
UiO-68-Fe
BET Surface Area: 2707.56 m²/g
y = -2.83952E-5 + 0.00165x
Correlation Coefficient: 0.99714
1/[Q(Po/P - 1)]
P/P₀

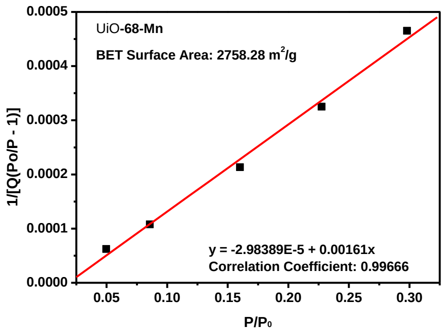
UiO-68-Mn
BET Surface Area: 2758.28 m²/g
y = -2.98389E-5 + 0.00161x
Correlation Coefficient: 0.99666
1/[Q(Po/P - 1)]
P/P₀

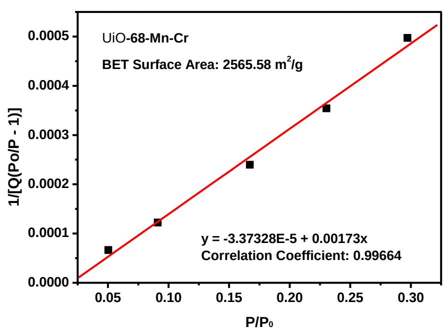
UiO-68-Mn-Cr
BET Surface Area: 2565.58 m²/g
y = -3.37328E-5 + 0.00173x
Correlation Coefficient: 0.99664
1/[Q(Po/P - 1)]
P/P₀

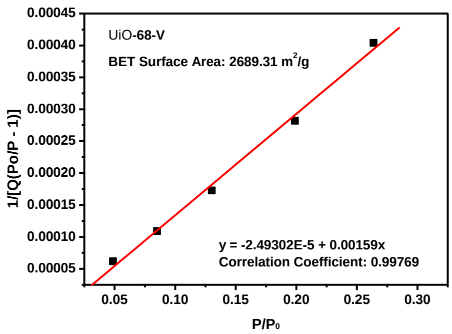
UiO-68-V
BET Surface Area: 2689.31 m²/g
y = -2.49302E-5 + 0.00159x
Correlation Coefficient: 0.99769
1/[Q(Po/P - 1)]
P/P₀

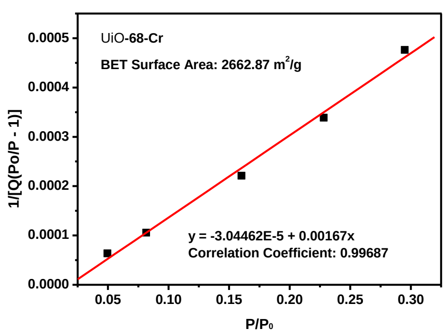
UiO-68-Cr
BET Surface Area: 2662.87 m²/g
y = -3.04462E-5 + 0.00167x
Correlation Coefficient: 0.99687
1/[Q(Po/P - 1)]
P/P₀

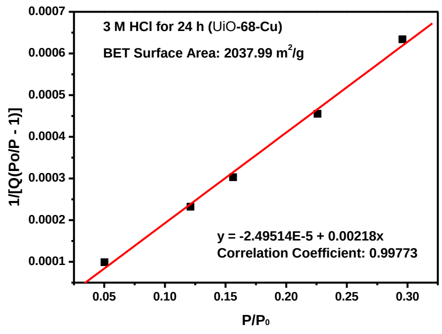
3 M HCl for 24 h (UiO-68-Cu)
BET Surface Area: 2037.99 m2/g
y = -2.49514E-5 + 0.00218x
Correlation Coefficient: 0.99773
1/[Q(Po/P - 1)]
P/P0

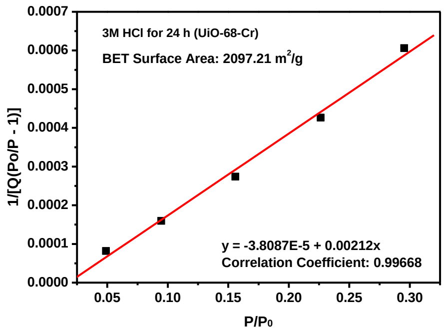
3M HCl for 24 h (UiO-68-Cr)
BET Surface Area: 2097.21 m2/g
y = -3.8087E-5 + 0.00212x
Correlation Coefficient: 0.99668
1/[Q(Po/P - 1)]
P/P0

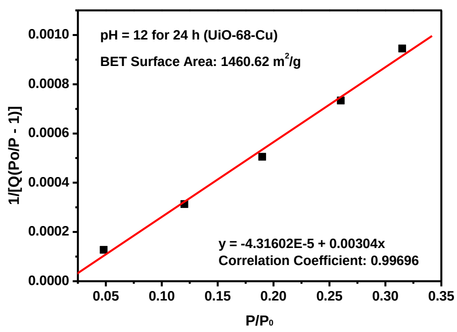
pH = 12 for 24 h (UiO-68-Cu)
BET Surface Area: 1460.62 m2/g
y = -4.31602E-5 + 0.00304x
Correlation Coefficient: 0.99696
1/[Q(Po/P - 1)]
P/P0

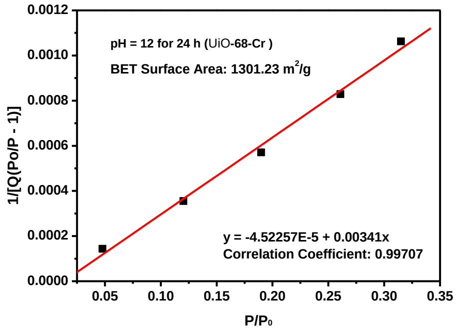
pH = 12 for 24 h (UiO-68-Cr)
BET Surface Area: 1301.23 m2/g
y = -4.52257E-5 + 0.00341x
Correlation Coefficient: 0.99707
1/[Q(Po/P - 1)]
P/P0

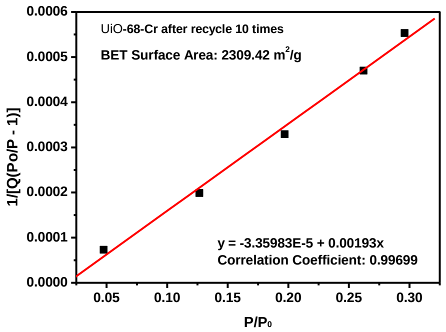
UiO-68-Cr after recycle 10 times
BET Surface Area: 2309.42 m2/g
y = -3.35983E-5 + 0.00193x
Correlation Coefficient: 0.99699
1/[Q(Po/P - 1)]
P/P0

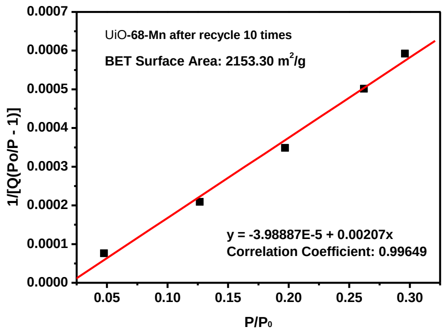
UiO-68-Mn after recycle 10 times
BET Surface Area: 2153.30 m2/g
y = -3.98887E-5 + 0.00207x
Correlation Coefficient: 0.99649
1/[Q(Po/P - 1)]
P/P0

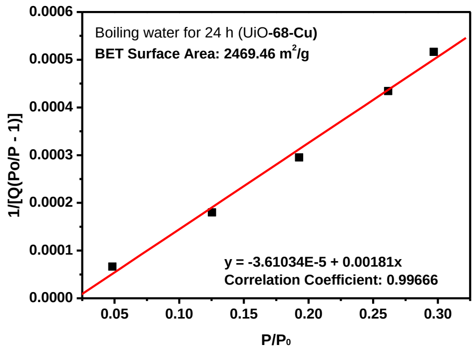
Boiling water for 24 h (UiO-68-Cu)
BET Surface Area: 2469.46 m2/g
y = -3.61034E-5 + 0.00181x
Correlation Coefficient: 0.99666
1/[Q(Po/P - 1)]
P/P0

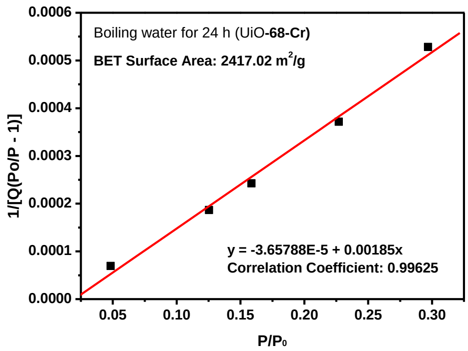
Boiling water for 24 h (UiO-68-Cr)
BET Surface Area: 2417.02 m2/g
y = -3.65788E-5 + 0.00185x
Correlation Coefficient: 0.99625
1/[Q(Po/P - 1)]
P/P0

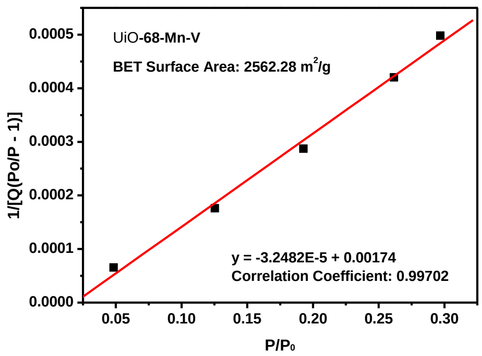

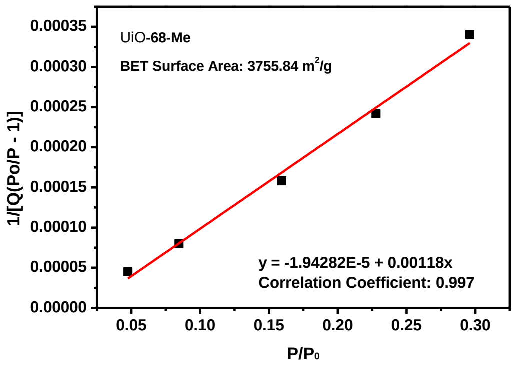

13. **Figure S11.** SEM / TEM images and EDS mappings

a) SEM images and particle size analysis

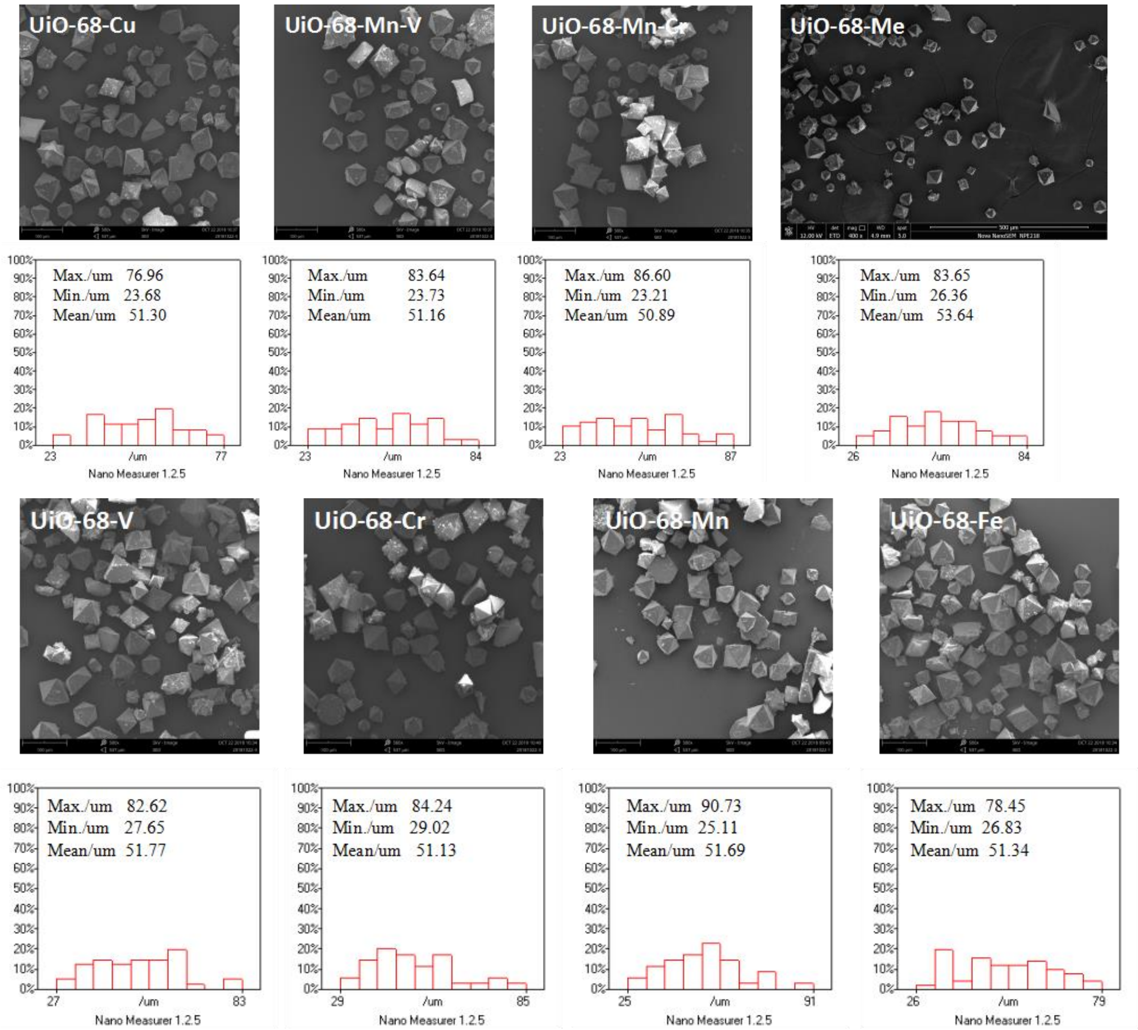

b) EDX mappings for the exchanged MOFs

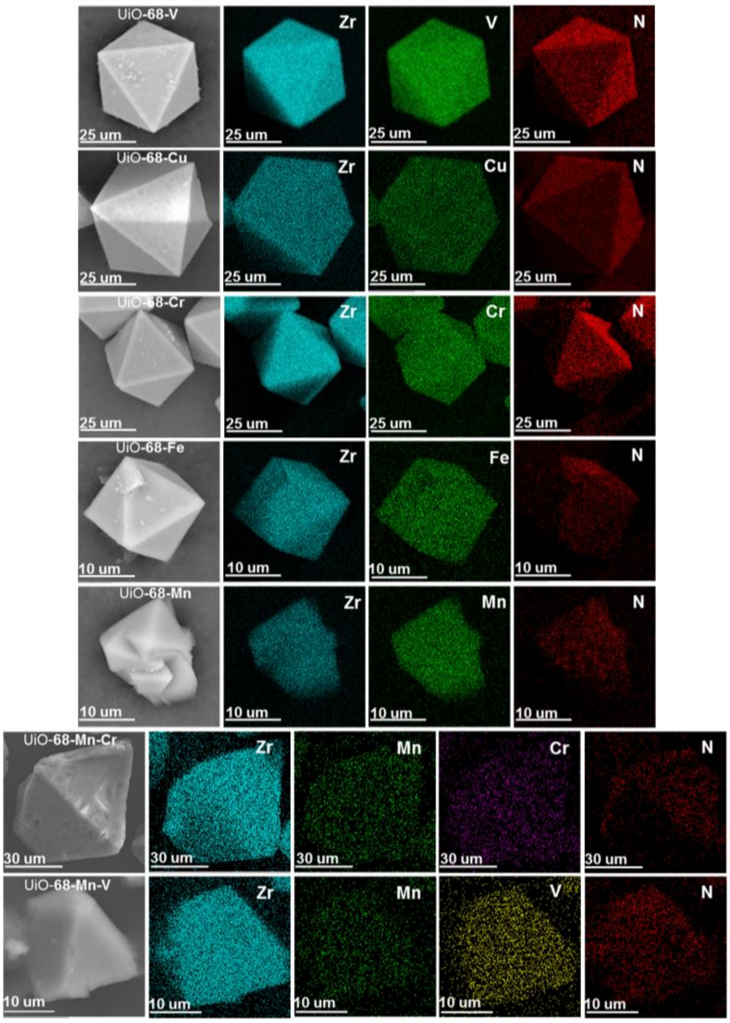

c) Cross-sectional SEM-EDX mappings during the PSE process for **UiO-68-Cr**

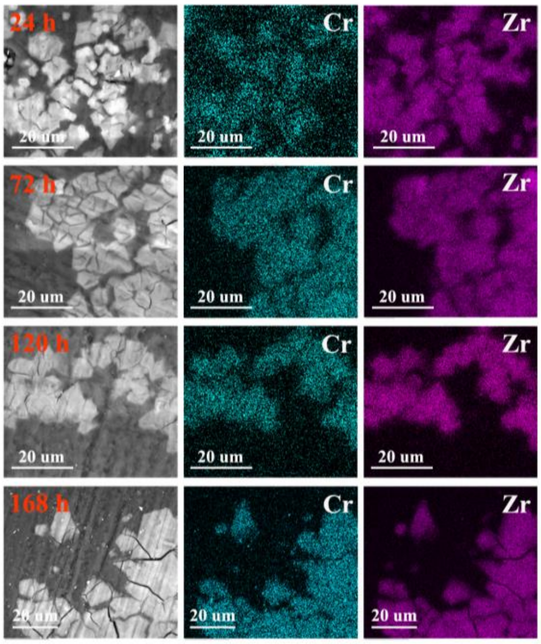

d) TEM-EDX mappings for the exchanged MOFs

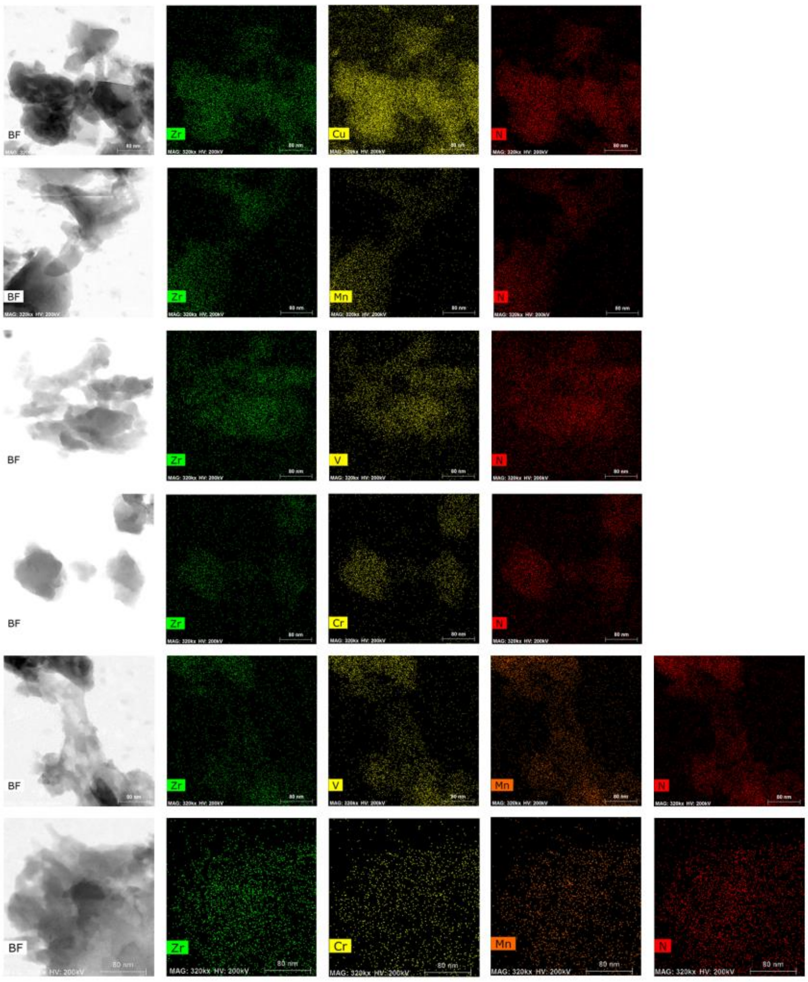

14. Figure S12 ^{1}H NMR Spectra

The activated **UiO-68-M** (5.0 mg) in nuclear magnetic tube were digested by HF(2 drops) in 0.5 mL DMSO-d_6 for 1 h, then collect the ^{1}H NMR.

(a) **UiO-68-Cu**

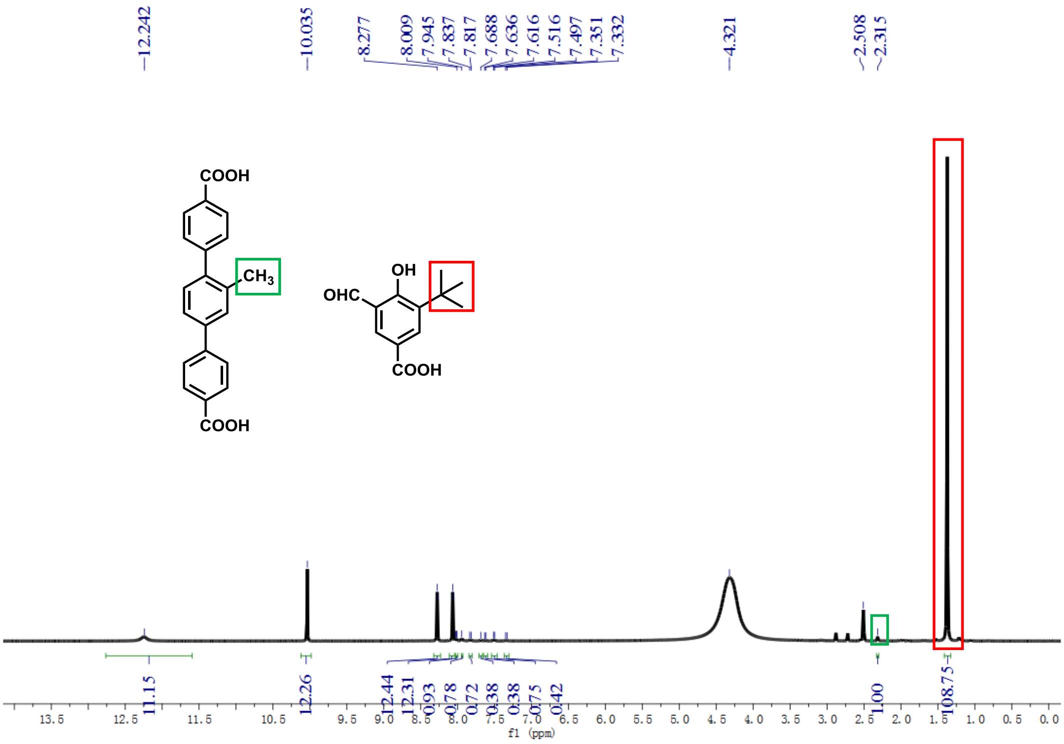

(b) UiO-68-Cr

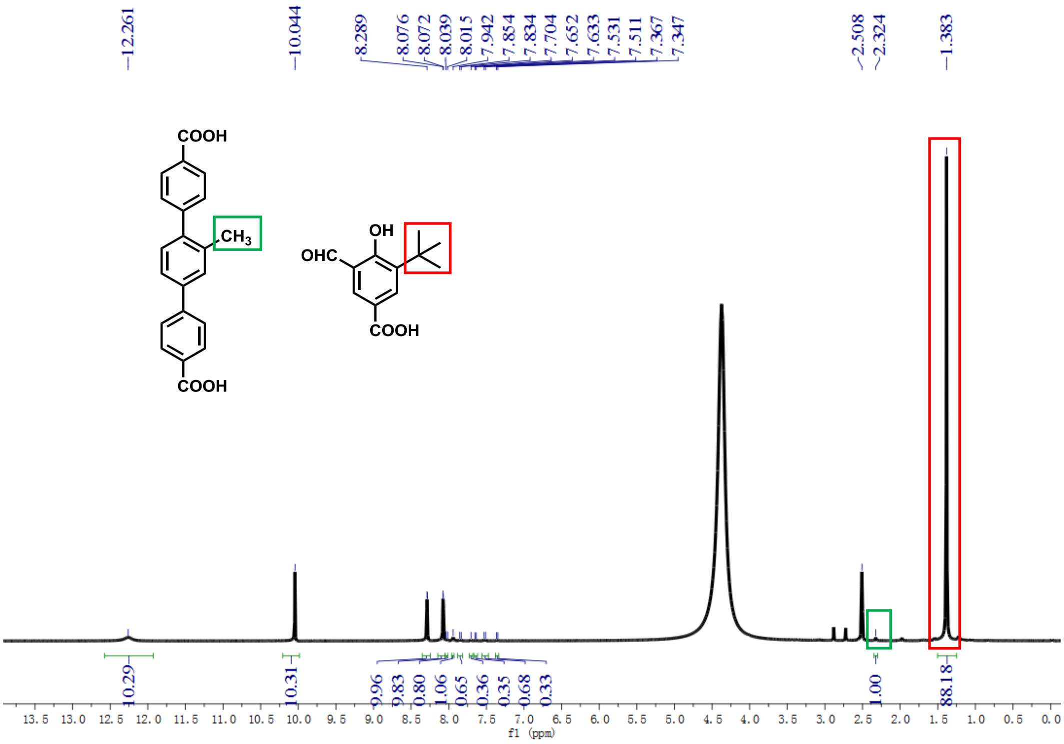

(c) UiO-68-Mn

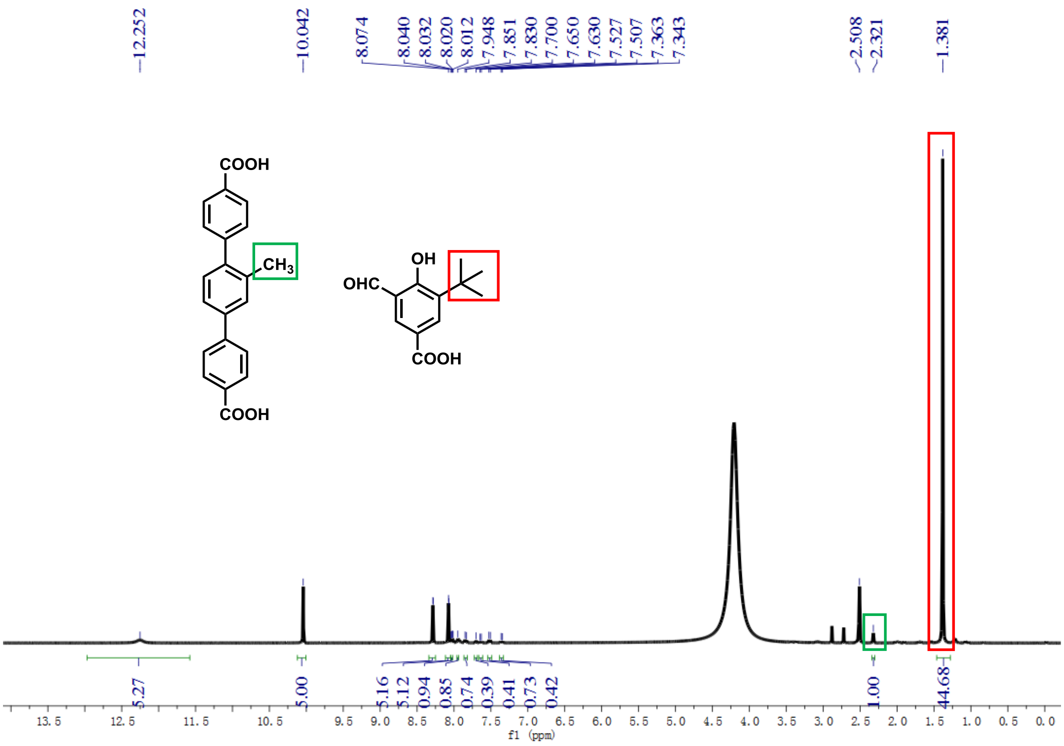

(d) UiO-68-V

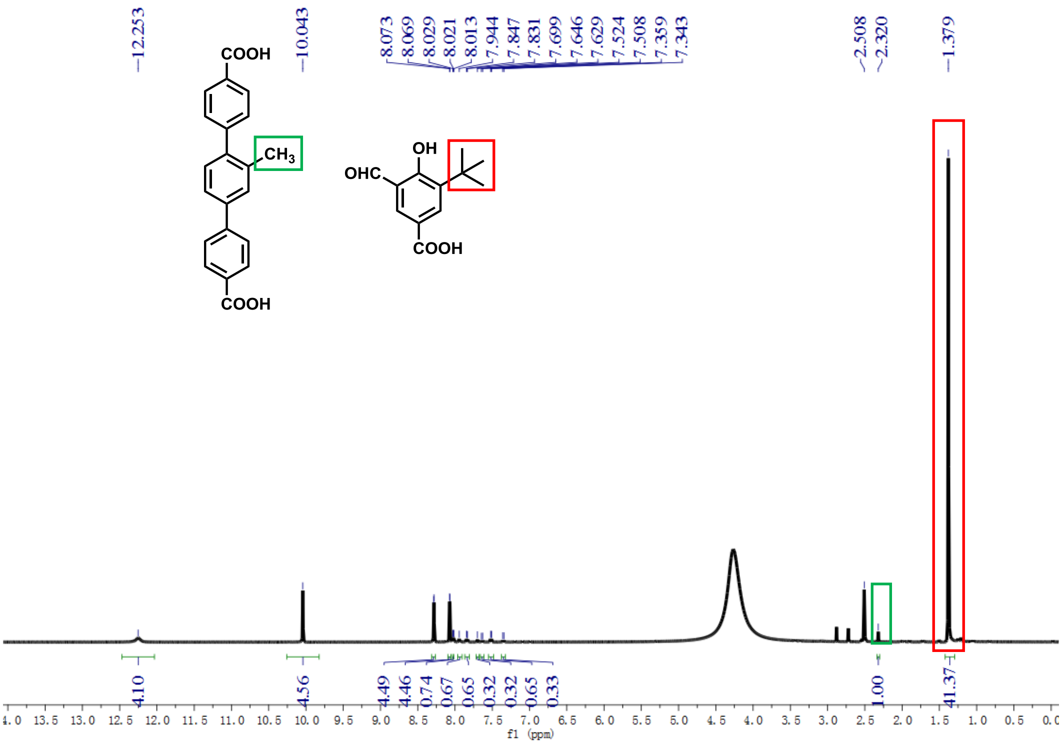

(e) UiO-68-Fe

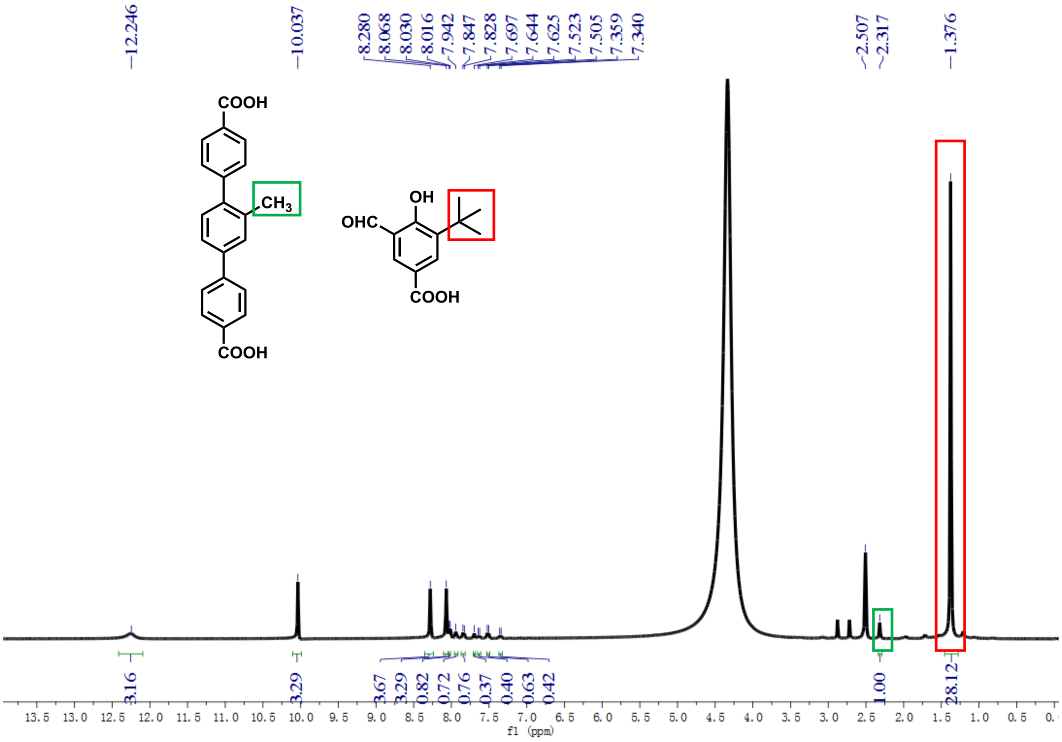

(f) UiO-68-Mn-Cr

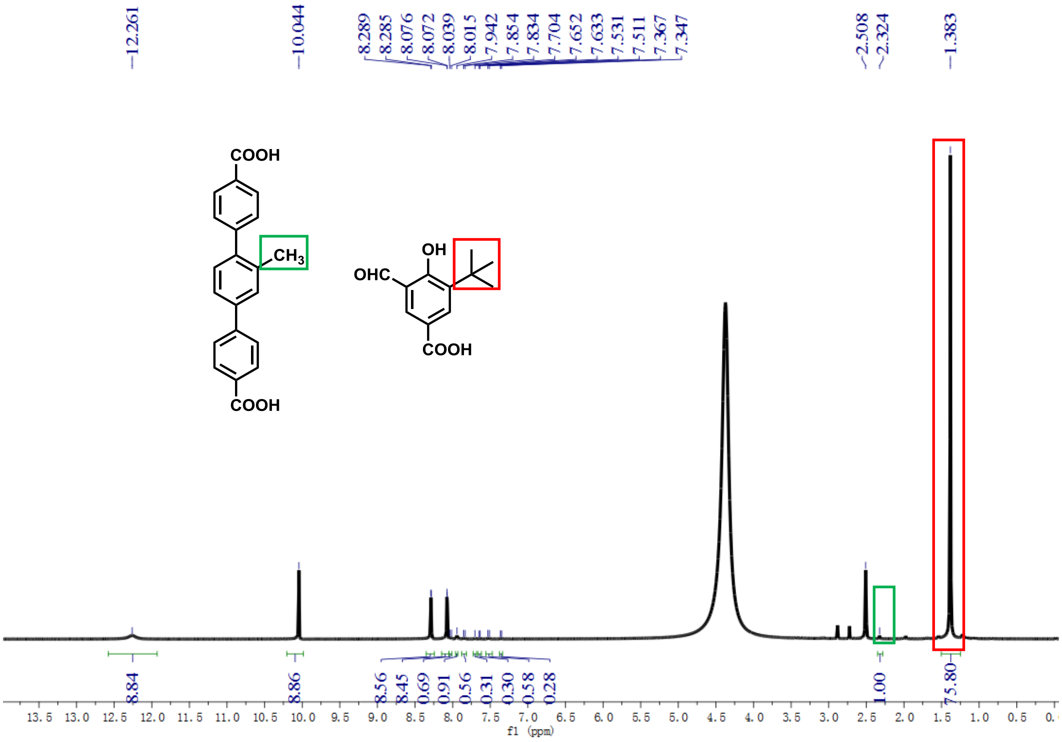

(g) UiO-68-Mn-V

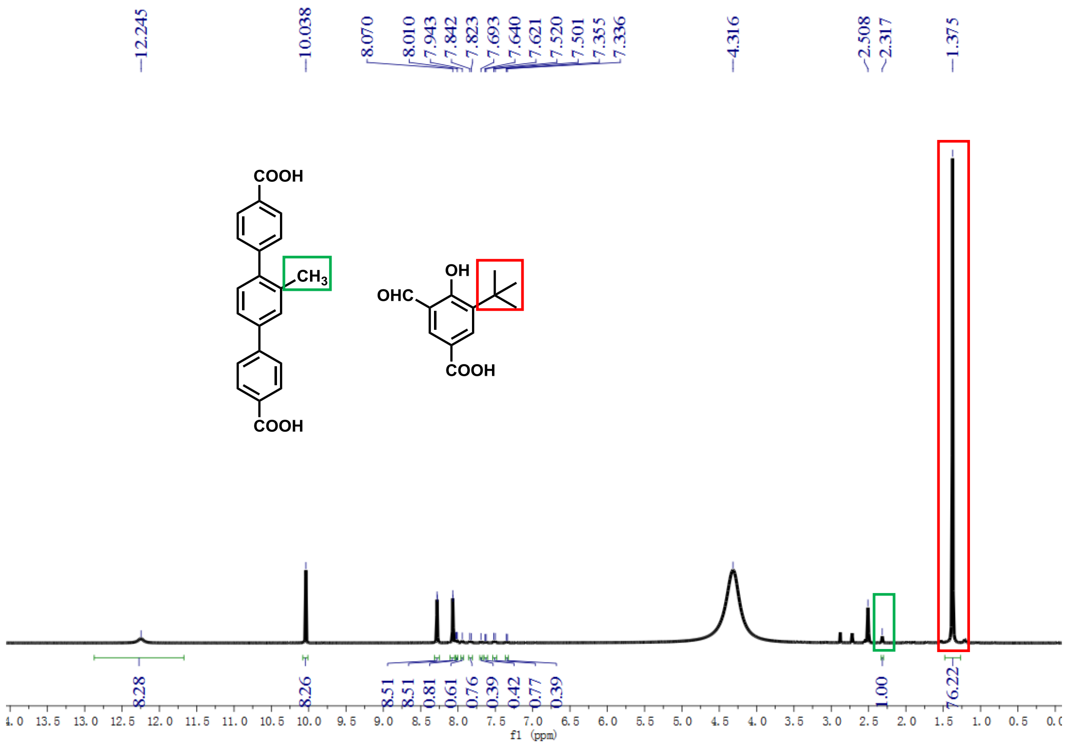

(h) [1]H NMR spectra showing the synthesis of **UiO-68-Cr** via PSE

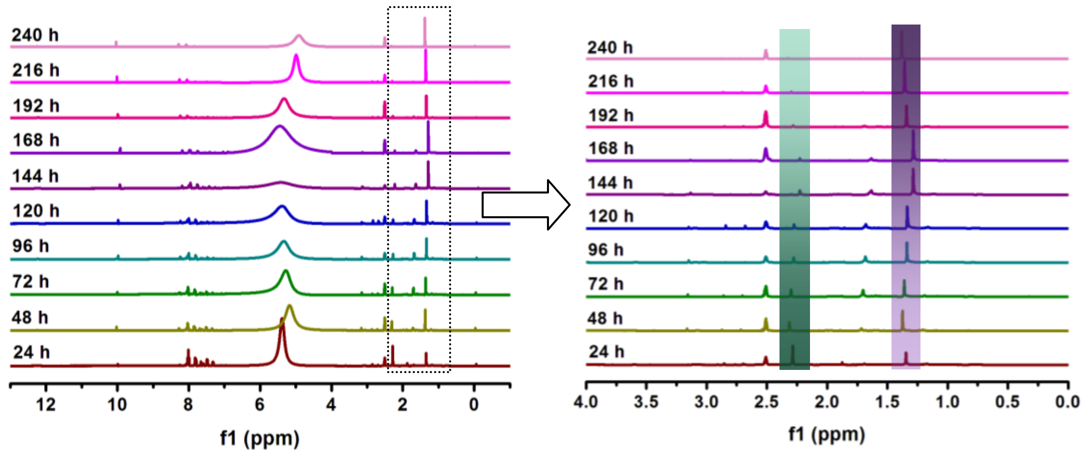

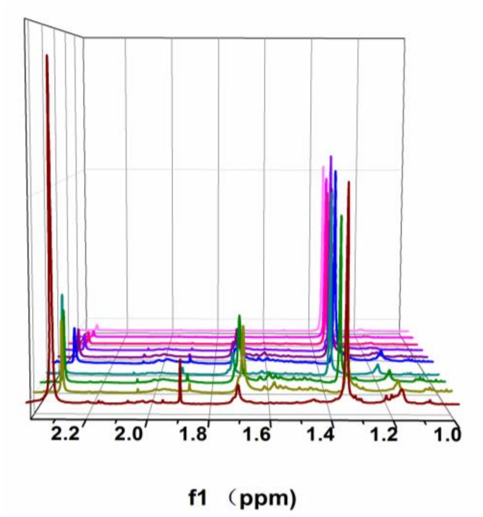

(i) ^{1}H NMR spectra of the solution during the PSE process of **UiO-68-Cr**. The solution was collected after exchanging, then large amount of water was added, adjusting the mixture to pH =2~3 by conc. HCl, stirred at 60 °C for 12 h to precipitate the 3-(*tert*-butyl)-5-formyl-4-hydroxybenzoic acid and H_2TPDC-Me, filter to get the solid, washing by H_2O then dried in 100 °C oven. The solid were then dissolved in DMSO-d_6 for ^{1}H NMR.

(a) **UiO-68-Cr**

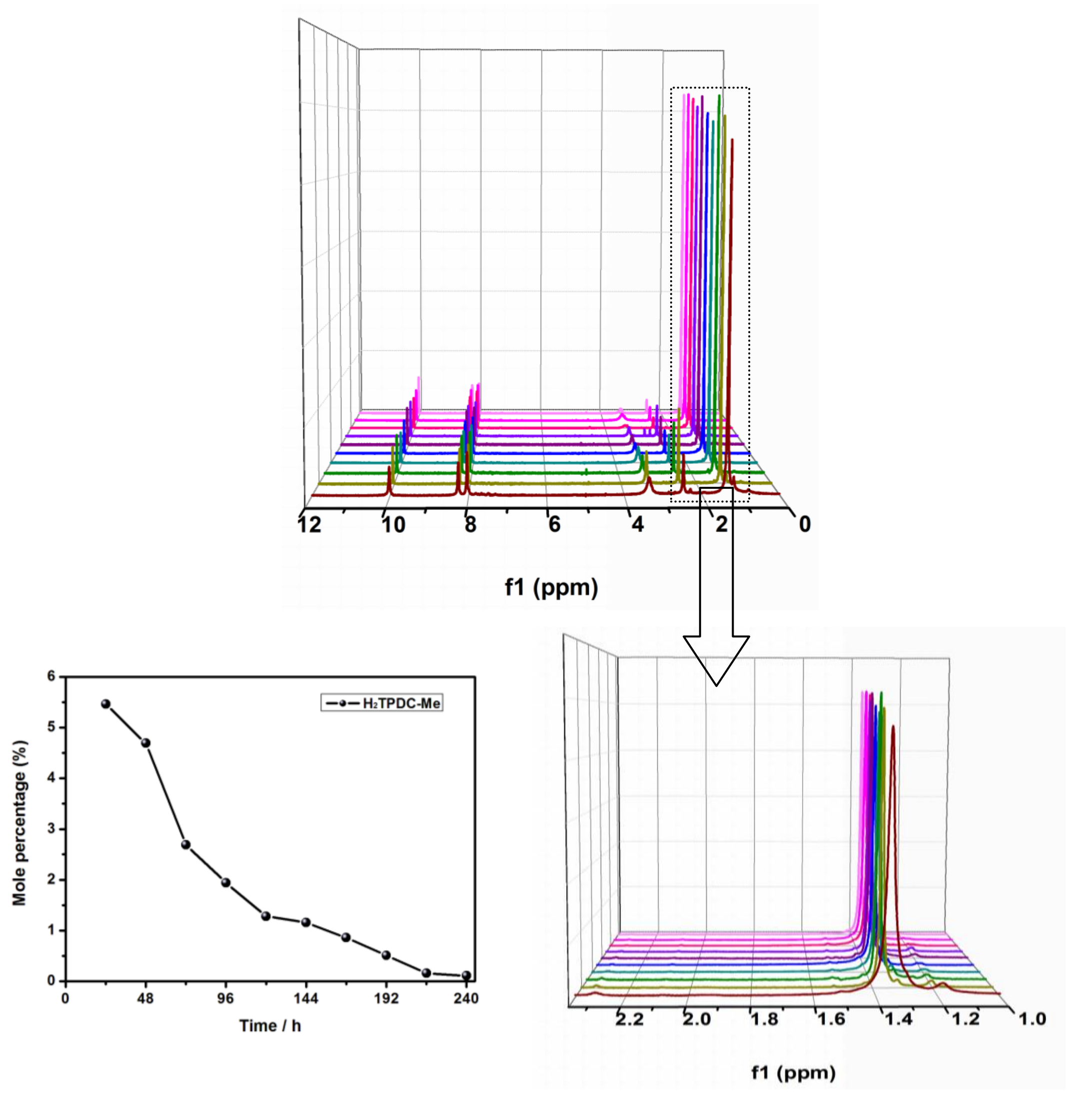

15. Table S4 ICP-OES results of **UiO-68-Cr** during the PSE process

Time (h)	Zr (wt %)	Cr (wt %)	Zr (mol %)	Cr (mol %)	Cr (mol %)/ Zr (mol %)	Exchange Ratio (%)
12	21.566	1.054	0.23642	0.02027	0.08573	8.5
24	15.939	1.889	0.17473	0.03633	0.2079	20.8
48	15.405	3.22	0.16888	0.06192	0.36667	36.7
72	13.414	3.644	0.14705	0.07008	0.47655	47.6
96	12.974	3.761	0.14223	0.07233	0.50853	50.8
120	13.129	4.686	0.14393	0.09012	0.62612	62.6
144	13.971	6.023	0.15316	0.11583	0.75626	75.6
168	12.906	6.182	0.14148	0.11888	0.84028	84
192	12.939	6.589	0.14184	0.12671	0.89332	89.3
216	12.119	6.297	0.13285	0.1211	0.91149	91.1
240	11.703	6.189	0.12829	0.11902	0.92771	92.7

16. Tables S5-S13. Additional catalytic results

16.1 Table S5. Alkene epoxidation

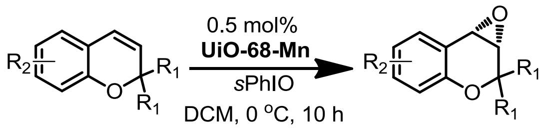

Entry	R_1	R_2	UiO-68-Mn	
			Conv. (%)[a]	ee (%)[b]
1	Me	H	91	88
2	-$(CH_2)_5$-	H	81	98
3	Me	6-Cl	88	90
4	Me	8-Cl	84	98
5	Me	8-Ph	78	82
6	Me	6-NO_2	80	96
7	Me	6-Me	85	83

[a] determined using ^{1}H NMR. [b]determined by HPLC.

16.2 Table S6. OKR reaction

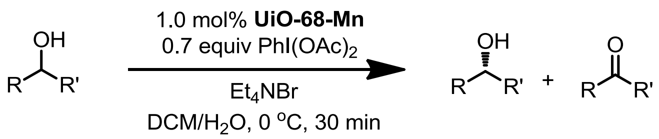

Entry	R	R’	UiO-68-Mn		
			Conv. (%)[a]	ee (%)[b]	k^c_{rel}
1	4-CF_3Ph	CH_3	59.8	99.7	30.6
2	Naphthalene	CH_3	50.1	80	21.4
3	Ph	CH_3	56.7	97	27.3
4	4-Br	CH_3	58.5	99.7	35.6
5	3-Br	CH_3	52.8	94	30.4

[a] determined using ^{1}H NMR. [b]determined by HPLC. [c]k_{el} = ln[(1-c)(1-ee)]/ln[(1-c)(1+ee)], where ee is the enantiomeric excess of the alcohol and c is the conversion of the alcohol.

16.3 Table S7. Alkene epoxidation

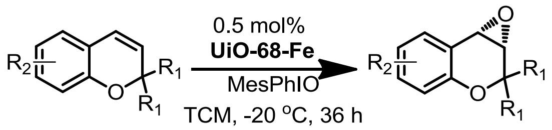

Entry	R_1	R_2	UiO-68-Fe	
			Conv. (%)[a]	ee (%)[b]
1	Me	H	84	86
2	$-(CH_2)_5-$	H	87	97
3	Me	$6-NO_2$	84	93
4	Me	8-Cl	80	90
5	Me	6-Me	85	84

[a]determined using ^{1}H NMR. [b]determined by HPLC.

16.4 Table S8. Asymmetric cyanation reaction

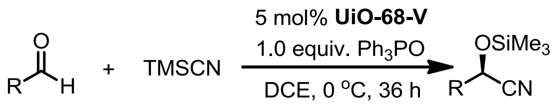

Entry	R	Conv. (%)[a]	ee (%)[b]
1	C_6H_5	85	82
2	$4-MeC_6H_4$	89	81
3	Thiophene	83	87
4	$4-MeOC_6H_4$	84	84
5	$4-BrC_6H_4$	80	80

[a]determined using ^{1}H NMR. [b]determined by HPLC.

16.5 Table S9. Aminolysis of trans-stilbene oxide with anilines

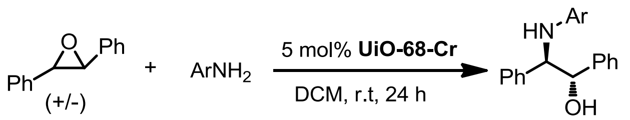

Entry	Ar	Conv. (%)[a]	ee (%)[b]
1	Ph	86 (trace)[c]	80
2	*o*-MeC_6H_4	87	84
3	*o*-EtC_6H_4	85	80
4	(2-Et-6-Me) C_6H_4	87 (trace)[c]	99
5	*p*-IC_6H_4	90 (trace)[c]	97
6	4-OMe	87	93

[a]determined using ^{1}H NMR base on anilines. [b]determined by HPLC. [c]Catalyzed by **UiO-68-Me** for both 24 h and 48 h.

16.6 Table S10. Alkene epoxidation

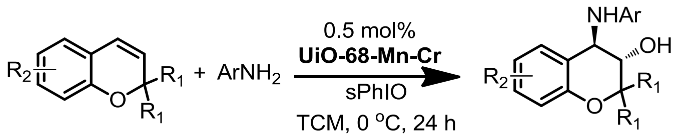

Entry	R_1	R_2	Ar	UiO-68-Mn-Cr	
				Conv. (%)[a]	ee (%)[b]
1	Me	H	Ph	85	80
2	Me	H	2-OMePh	83	82
3	Me	H	4-OMePh	82	87
4	Me	H	4-OEtPh	80	82
5	Me	H	4-Cl	80	96
6	Me	H	4-MePh	82	84
7	Me	H	2-Et-6-MePh	81	99.5
8	Me	6-Me	Ph	84	86
9	Me	6-Cl	Ph	80	88

[a] determined using ^{1}H NMR. [b]determined by HPLC.

16.7 Table S11. Recycle experiments of epoxidation reactions

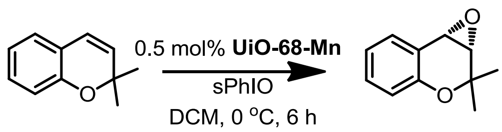

Run	Conv. (%)[a]	ee (%)[b]
1	86	88
2	85	88
3	85	88
4	84	88
5	85	88
6	84	85
7	82	86
8	84	88
9	83	88
10	83	88

[a]determined using ^{1}H NMR. [b]determined by HPLC.

16.8 Table S12. Recycle experiments of Alcohol OKR

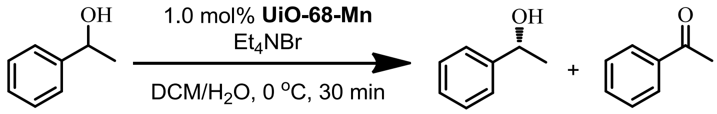

Run	Conv. (%)[a]	ee (%)[b]	k_{rel}
1	56.7	97	27.3
2	56.1	96	26.9
3	55.9	96	27.7
4	56.5	96	26.1
5	56.3	94	25.4
6	55.6	94	26.6
7	55.4	94	26.6
8	55.0	93	24.5
9	55.7	94	26.2
10	55.3	94	25.4

[a]determined using ^{1}H NMR. [b]determined by HPLC.

16.9 Table S13. Recycle experiments of Aminolysis of trans-Stilbene Oxide

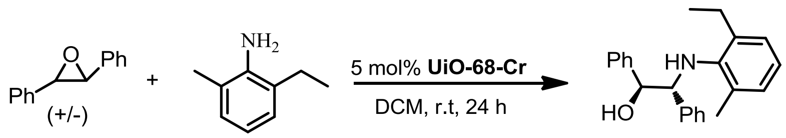

Run	Conv. (%)[a]	ee (%)[b]
1	87	99.5
2	87	98
3	86	99.5
4	85	98
5	85	98
6	86	96
7	85	96
8	85	97
9	86	97
10	85	96

[a]determined using ^{1}H NMR. [b]determined by HPLC.

17. HPLC and NMR results of catalysis

17.1 Alkene Epoxidation

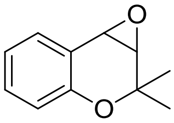

2,2-dimethyl-2,7b-dihydro-1aH-oxireno[2,3-c]chromene:

Enantiomeric excess was determined by HPLC with a chiralcel OD-H column (hexane/*i*-PrOH = 99/1, 1.0 mL/min, 230 nm), t $_{major}$ = 10.839 min, t $_{minor}$ = 13.943 min; ee = 88%, ^{1}H NMR[2] (400 MHz, $CDCl_3$) δ 7.32 (dd, *J* = 7.4, 1.7 Hz, 1H), 7.25 – 7.20 (m, 1H), 6.93 (td, *J* = 7.4, 1.1 Hz, 1H), 6.83 (d, *J* = 8.1 Hz, 1H), 3.90 (d, *J* = 4.4 Hz, 1H), 3.49 (d, *J* = 4.4 Hz, 1H), 1.58 (s, 3H), 1.23 (s, 3H).

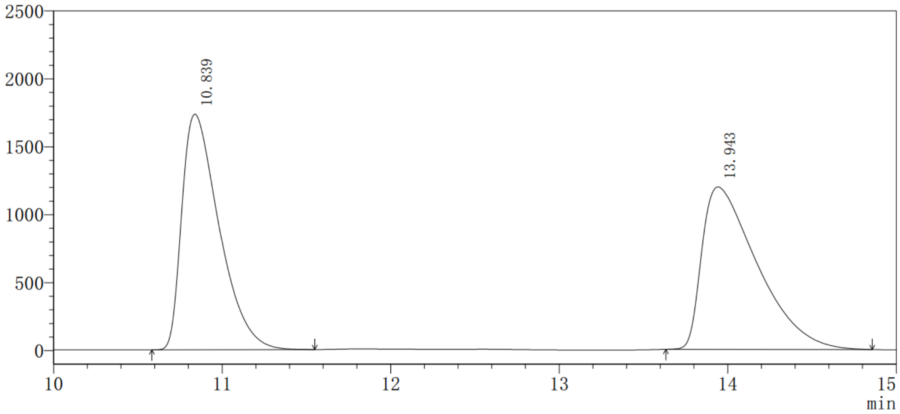

Detector:230nm

ID#	Start	End	Ret. Time	Height	Area	Area%
1	10.583	11.550	10.839	1734816	26701821	49.379
2	13.633	14.858	13.943	1196158	27373581	50.621
Total				2930974	54075401	100.000

Catalyzed by **UiO-68-Mn**

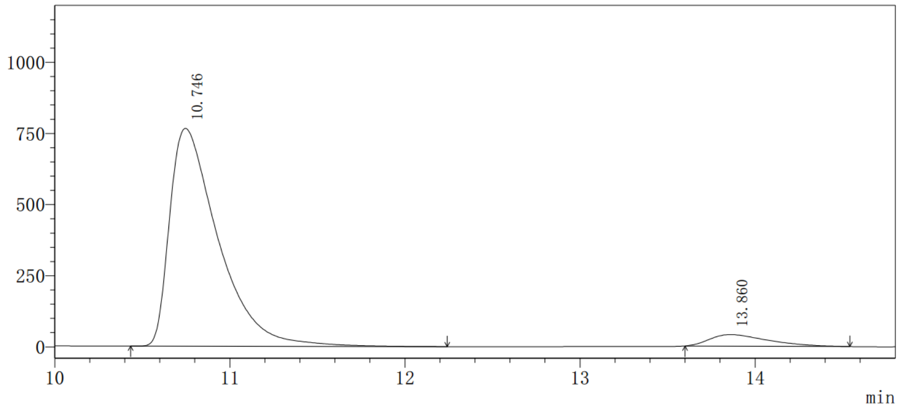

Detector:230nm

ID#	Start	End	Ret. Time	Height	Area	Area%
1	10.433	12.242	10.746	765478	14801715	94.058
2	13.600	14.542	13.860	40531	935047	5.942
Total				806009	15736762	100.000

Catalyzed by **UiO-68-Fe**

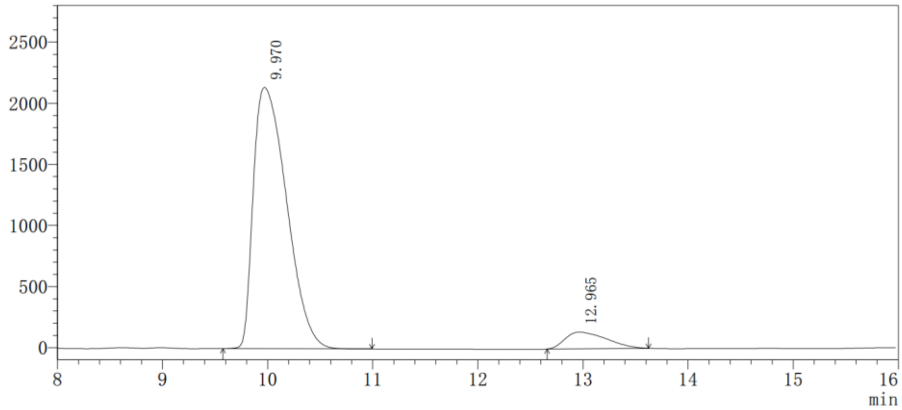

Detector: 230nm

ID#	Start	End	Ret. Time	Height	Area	Area%
1	9.575	10.992	9.970	2138281	47009849	92.684
2	12.658	13.625	12.965	136204	3710976	7.316
Total				2274485	50720825	100.000

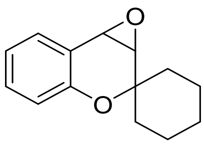

1a',7b'-dihydrospiro[cyclohexane-1,2'-oxireno[2,3-c]chromene]:

Enantiomeric excess was determined by HPLC with a chiralcel OD-H column (hexane/*i*-PrOH = 99/1, 1.0 mL/min, 230 nm), t $_{major}$ = 11.014 min, t $_{minor}$ = 18.381 min; ee = 97%, 1H NMR[2] (400 MHz, CDCl3) δ 7.33 (d, *J* = 7.4, 1.6 Hz, 1H), 7.26 – 7.22 (m, 1H), 6.92 (m, *J* = 7.4, 1.0 Hz, 1H), 6.85 (d, *J* = 8.1 Hz, 1H), 3.89 (d, *J* = 4.4 Hz, 1H), 3.48 (d, *J* = 4.4 Hz, 1H), 1.68 (ddd, *J* = 12.4, 11.1, 3.7 Hz, 6H), 1.61 (ddd, *J* = 16.5, 8.5, 4.8 Hz, 3H).

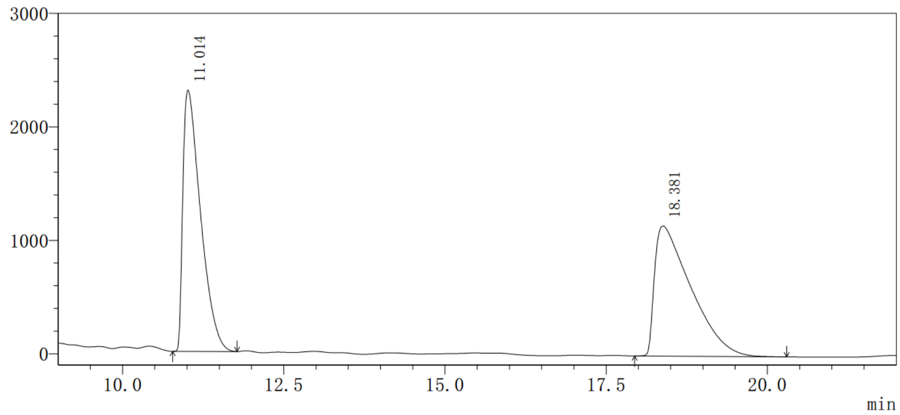

Detector:230nm

ID#	Start	End	Ret. Time	Height	Area	Area%
1	10.775	11.775	11.014	2302590	43930904	49.340
2	17.942	20.300	18.381	1148143	45106432	50.660
Total				3450733	89037336	100.000

Catalyzed by **UiO-68-Mn**

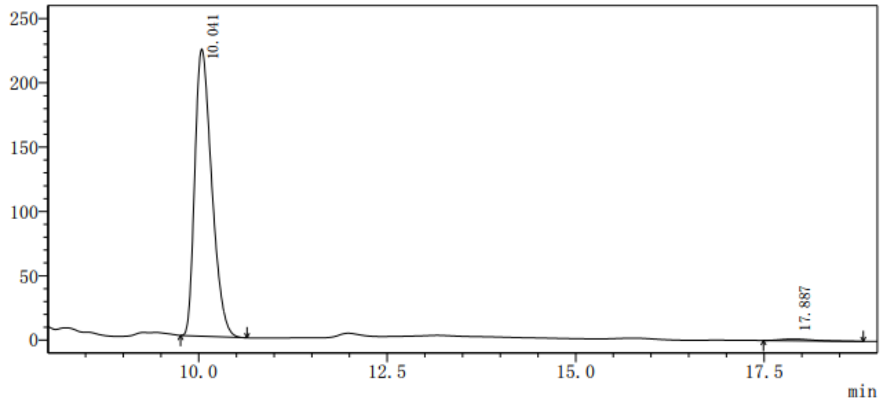

Detector:230nm

ID#	Start	End	Ret. Time	Height	Area	Area%
1	9.758	10.642	10.041	223200	3487411	98.893
2	17.492	18.817	17.887	1331	39035	1.107
Total				224531	3526447	100.000

Catalyzed by **UiO-68-Fe**

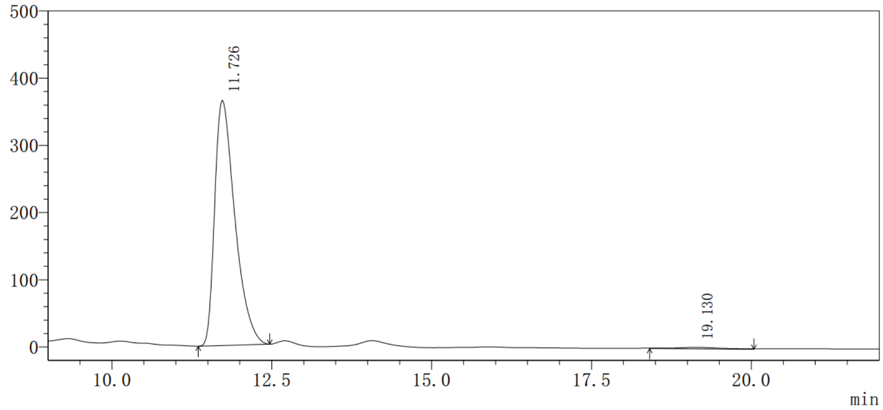

Detector:230nm

ID#	Start	End	Ret. Time	Height	Area	Area%
1	11.350	12.467	11.726	364769	8022306	98.611
2	18.408	20.042	19.130	2185	113033	1.389
Total				366954	8135339	100.000

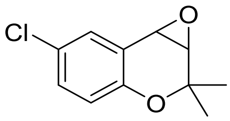

2,2-dimethyl-6-chloro-2,7b-dihydro-1aH-oxireno[2,3-c]chromene:

Enantiomeric excess was determined by HPLC with a chiralcel OD-H column (hexane/*i*-PrOH = 99/1, 1.0 mL/min, 230 nm), t $_{major}$ = 8.513 min, t $_{minor}$ = 10.443 min; ee = 90%, ^{1}H NMR[2] (400 MHz, $CDCl_3$) δ = 7.31 (d, *J* = 2.5, 1H), 7.18 (dd, *J* = 8.6, 2.6, 1H), 6.75 (d, *J* = 8.6, 1H), 3.86 (d, *J* = 4.2, 1H), 3.49 (d, *J* = 4.3, 1H), 1.25 (s, 3H), 1.24 (s, 3H).

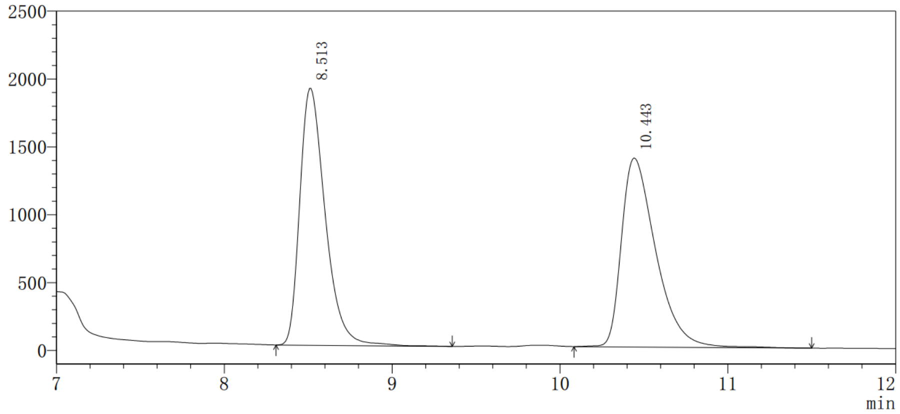

Detector:220nm

ID#	Start	End	Ret. Time	Height	Area	Area%
1	8.308	9.358	8.513	1892328	19970465	50.153
2	10.083	11.500	10.443	1392480	19848464	49.847
Total				3284808	39818929	100.000

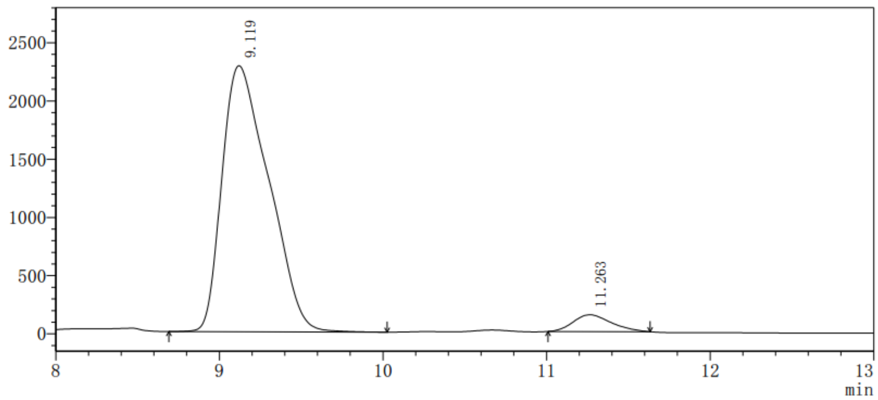

Detector: 230nm

ID#	Start	End	Ret. Time	Height	Area	Area%
1	8.692	10.025	9.119	2284694	45428131	95.094
2	11.008	11.633	11.263	144225	2343700	4.906
Total				2428919	47771831	100.000

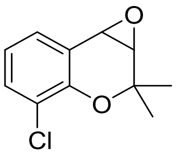

2,2-dimethyl-8-chloro-2,7b-dihydro-1aH-oxireno[2,3-c]chromene:
Enantiomeric excess was determined by HPLC with a chiralcel OD-H column (hexane/*i*-PrOH = 99/1, 1.0 mL/min, 230 nm), t_{major} = 9.109 min, t_{minor} = 13.020 min; ee = 98%, ^{1}H NMR[2] (400 MHz, $CDCl_3$) δ = 7.33 (dd, J = 8.0, 1.5, 1H), 7.25 (d, J = 1.5, 1H), 6.87 (t, J = 7.8, 1H), 3.91 (d, J = 4.4, 1H), 3.51 (d, J = 4.4, 1H), 1.66 (s, 3H), 1.27 (s, 3H).

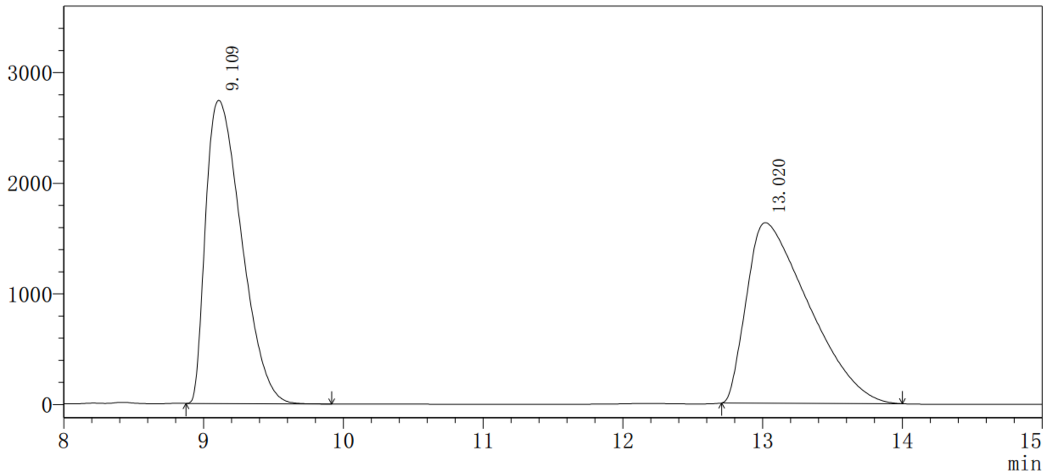

Detector:220nm

ID#	Start	End	Ret. Time	Height	Area	Area%
1	8.875	9.917	9.109	2740303	48832934	49.156
2	12.708	14.000	13.020	1630596	50510132	50.844
Total				4370899	99343066	100.000

Catalyzed by **UiO-68-Mn**

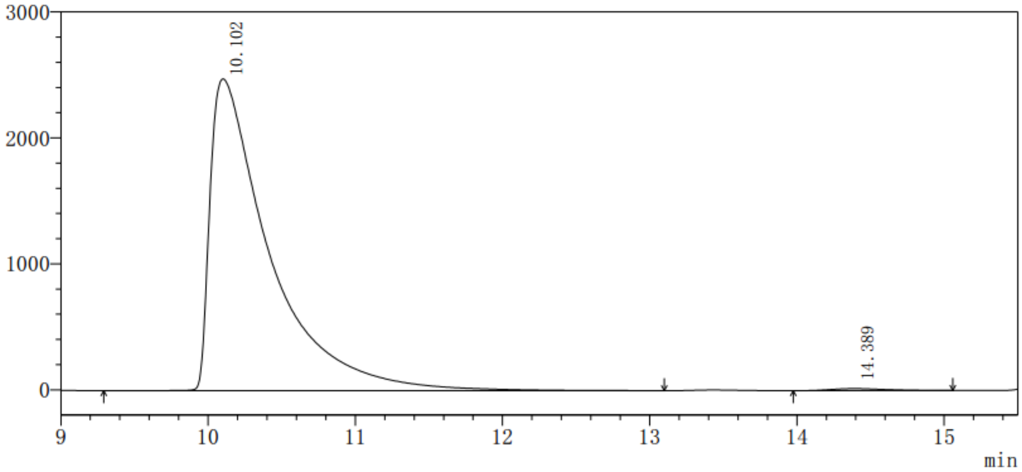

Detector: 220nm

ID#	Start	End	Ret. Time	Height	Area	Area%
1	9.292	13.100	10.102	2476213	69679263	99.410
2	13.975	15.058	14.389	16001	413859	0.590
Total				2492214	70093121	100.000

Catalyzed by **UiO-68-Fe**

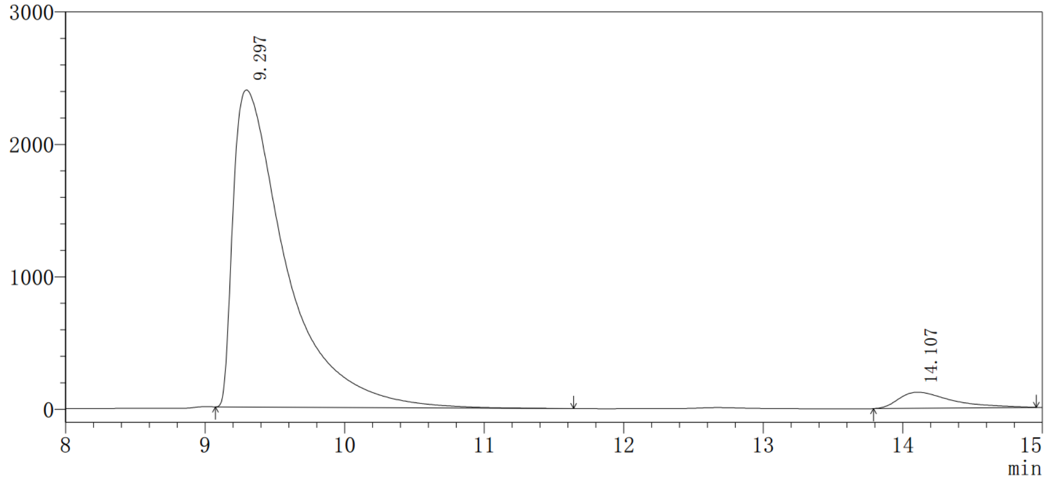

Detector: 230nm

ID#	Start	End	Ret. Time	Height	Area	Area%
1	9.075	11.642	9.297	2394643	63348873	95.152
2	13.792	14.958	14.107	121430	3227315	4.848
Total				2516072	66576189	100.000

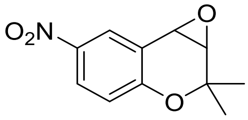

2,2-dimethyl-6-nitro-2,7b-dihydro-1aH-oxireno[2,3-c]chromene:

Enantiomeric excess was determined by HPLC with a chiralcel OD-H column (hexane/*i*-PrOH = 98/2, 1.0 mL/min, 230 nm), t_{major} = 18.130 min, t_{minor} = 22.760 min; ee = 96%,^{1}H NMR[2] (400 MHz, $CDCl_3$) δ 8.30 (d, *J* = 2.7 Hz, 1H), 8.12 (dd, *J* = 9.0, 2.8 Hz, 1H), 6.87 (d, *J* = 9.0 Hz, 1H), 3.99 (d, *J* = 4.3 Hz, 1H), 3.56 (d, *J* = 4.3 Hz, 1H), 1.60 (s, 3H), 1.30 (s, 3H).

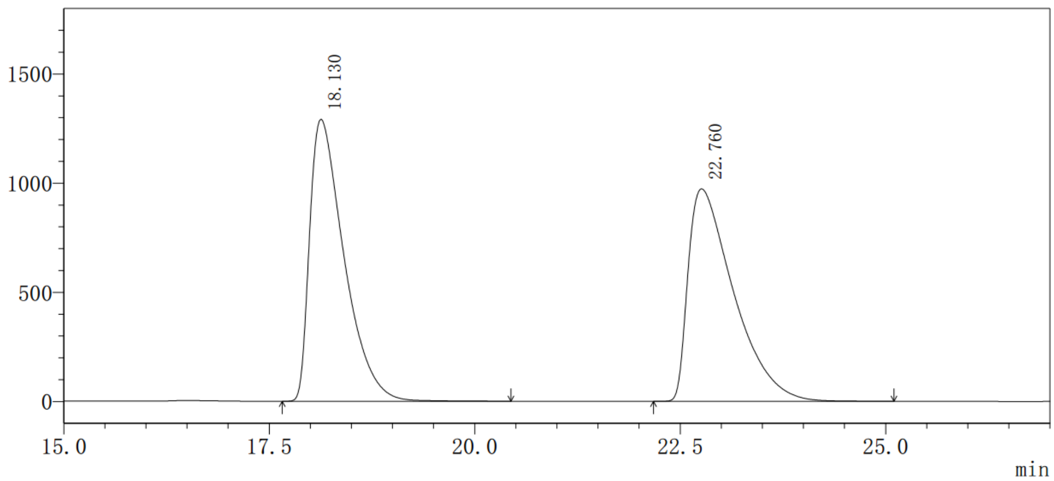

Detector:230nm

ID#	Start	End	Ret. Time	Height	Area	Area%
1	17.658	20.442	18.130	1291396	37651347	50.084
2	22.175	25.100	22.760	973106	37525551	49.916
Total				2264502	75176899	100.000

Catalyzed by **UiO-68-Mn**

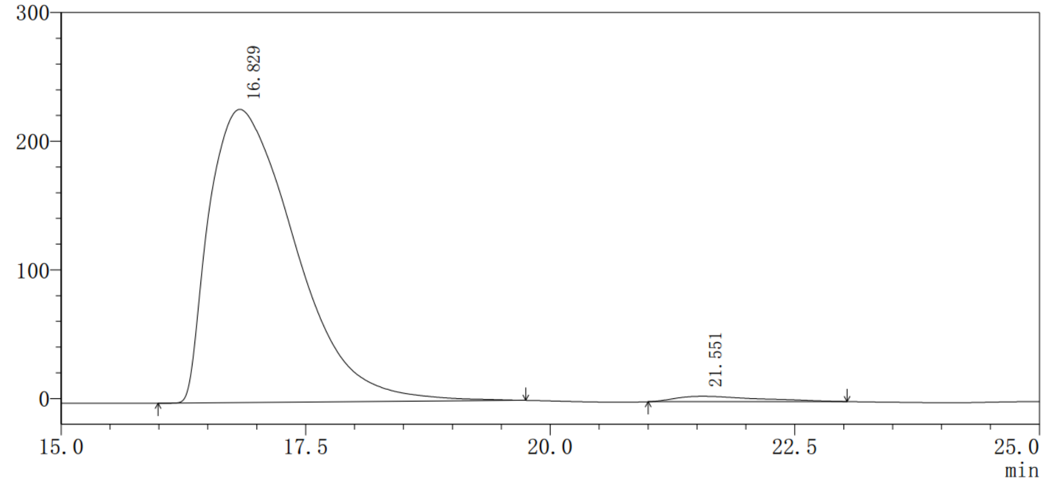

Detector:230nm

ID#	Start	End	Ret. Time	Height	Area	Area%
1	15.992	19.750	16.829	227966	13940916	98.230
2	21.000	23.033	21.551	4207	251172	1.770
Total				232174	14192088	100.000

Catalyzed by **UiO-68-Fe**

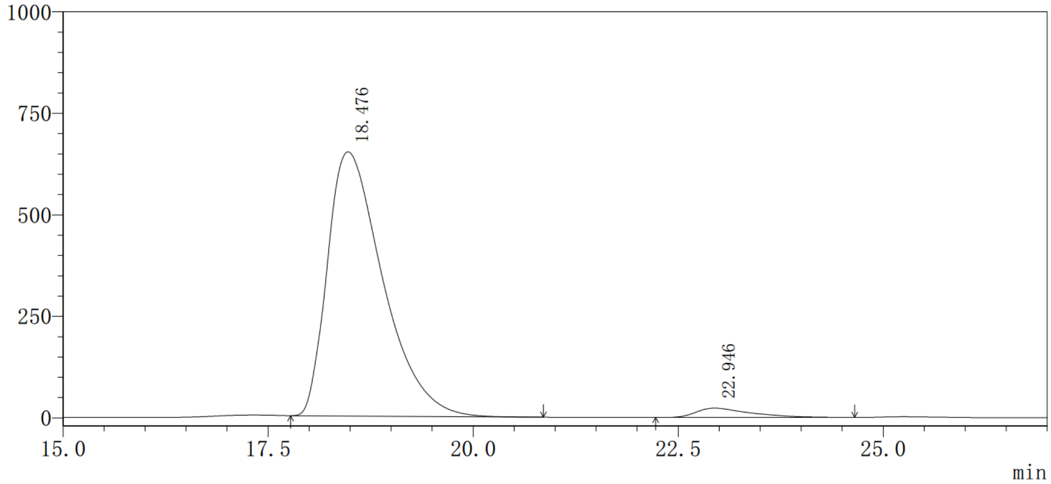

Detector: 230nm

ID#	Start	End	Ret. Time	Height	Area	Area%
1	17.775	20.858	18.476	650758	30592306	96.650
2	22.225	24.650	22.946	23074	1060299	3.350
Total				673833	31652605	100.000

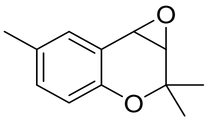

2,2-dimethyl-6-methyl-2,7b-dihydro-1aH-oxireno[2,3-c]chromene:

Enantiomeric excess was determined by HPLC with a chiralcel OD-H column (hexane/*i*-PrOH = 99/1, 1.0 mL/min, 230 nm), t $_{major}$ = 8.310 min, t $_{minor}$ = 12.586 min; ee = 83%, ^{1}H NMR[2] (400 MHz, $CDCl_3$) δ 7.15 (d, *J* = 2.2 Hz, 1H), 7.03 (dd, *J* = 8.5, 1.9 Hz, 1H), 6.72 (d, *J* = 8.2 Hz, 1H), 3.86 (d, *J* = 4.4 Hz, 1H), 3.47 (d, *J* = 4.4 Hz, 1H), 2.29 (s, 3H), 1.56 (s, 3H), 1.25 (s, 3H).

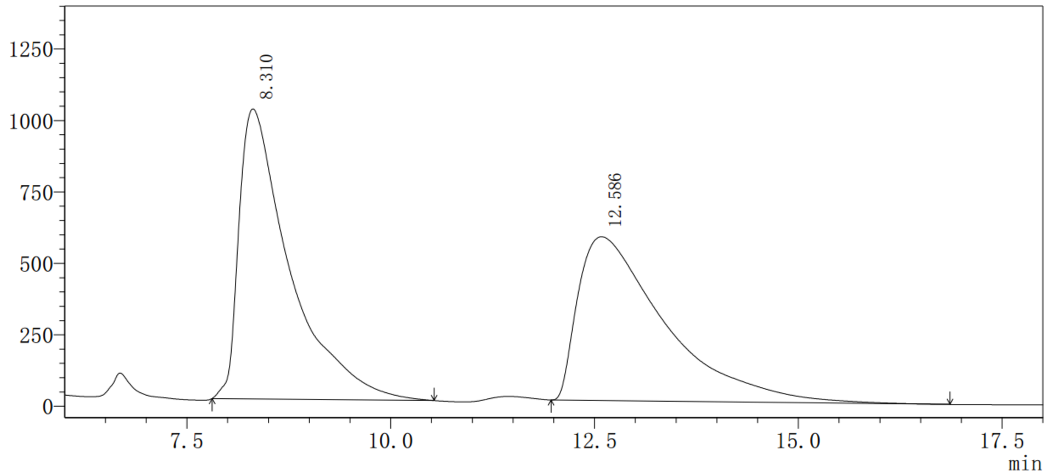

Detector:220nm

ID#	Start	End	Ret. Time	Height	Area	Area%
1	7.808	10.533	8.310	1015082	44011042	50.746
2	11.967	16.858	12.586	573419	42717218	49.254
Total				1588500	86728260	100.000

Catalyzed by **UiO-68-Mn**

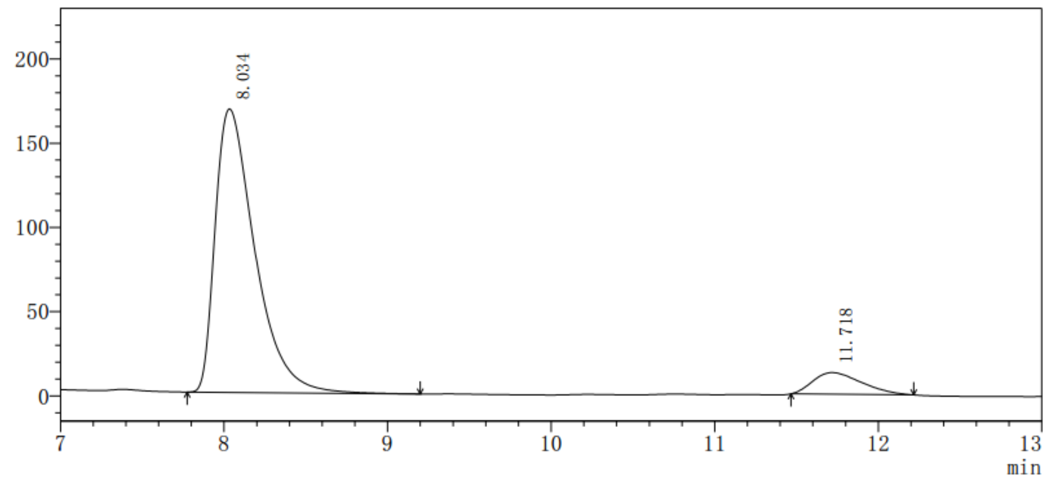

Detector: 220nm

ID#	Start	End	Ret. Time	Height	Area	Area%
1	7.775	9.200	8.034	168403	2831671	91.435
2	11.467	12.217	11.718	12822	265251	8.565
Total				181225	3096923	100.000

Catalyzed by **UiO-68-Fe**

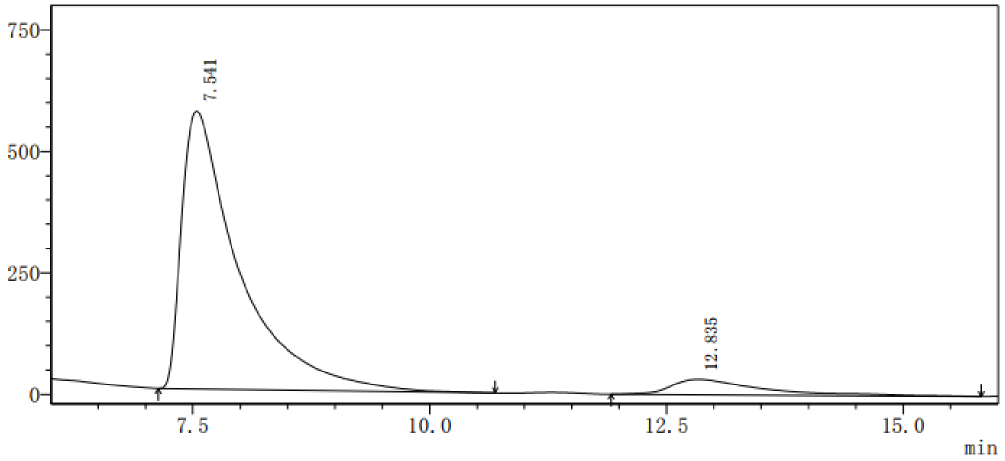

Detector:220nm

ID#	Start	End	Ret. Time	Height	Area	Area%
1	7.133	10.692	7.541	571849	24157782	91.993
2	11.917	15.825	12.835	31674	2102788	8.007
Total				603522	26260570	100.000

17.2 Alcohol OKR

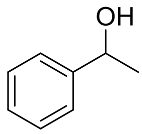

Phenethyl alcohol:

Enantiomeric excess was determined by HPLC with a chiralcel OD-H column (hexane/*i*-PrOH = 95/5, 1.0 mL/min, 220 nm), t $_{major}$ = 8.073 min, t $_{minor}$ = 9.563 min; ee = 99.1%.

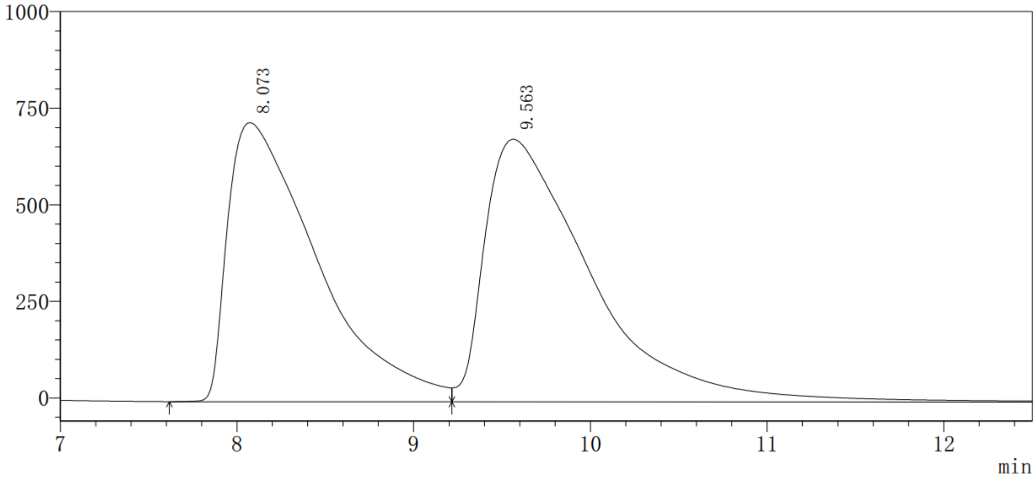

Detector:220nm

ID#	Start	End	Ret. Time	Height	Area	Area%
1	7.617	9.217	8.073	722353	25411357	46.943
2	9.217	16.050	9.563	679650	28721109	53.057
Total				1402003	54132466	100.000

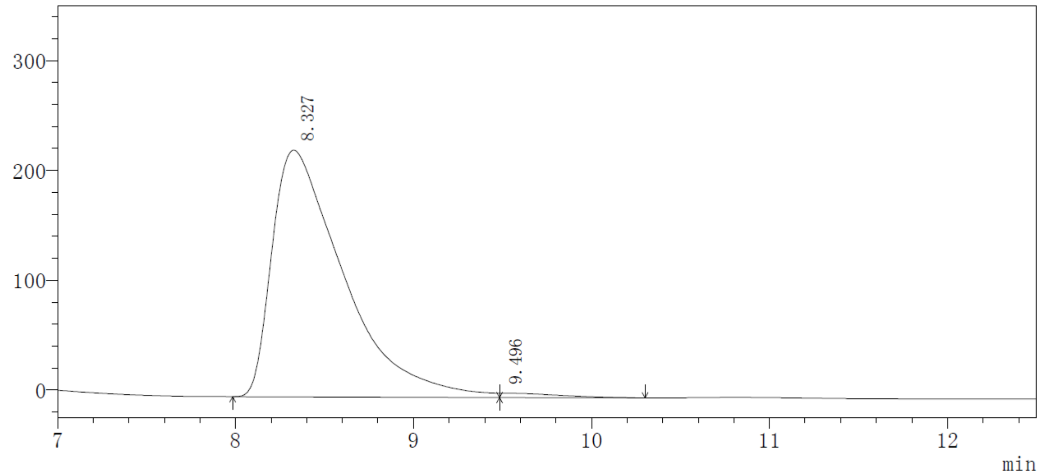

Detector:220nm

ID#	Start	End	Ret. Time	Height	Area	Area%
1	7.983	9.483	8.327	224588	6285843	98.671
2	9.483	10.300	9.496	3844	84696	1.329
Total				228432	6370539	100.000

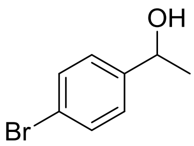

1-(4-Bromophenyl)ethanol:

Enantiomeric excess was determined by HPLC with a chiralcel OD-H column (hexane/*i*-PrOH = 95/5, 1.0 mL/min, 230 nm), t $_{major}$ = 9.041 min, t $_{minor}$ = 8.222 min; ee = 99.7%.

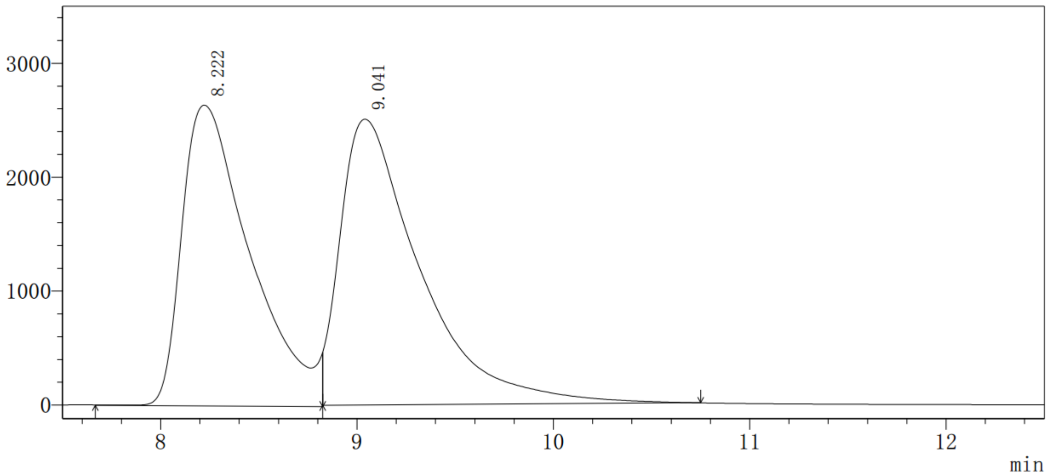

Detector:220nm

ID#	Start	End	Ret. Time	Height	Area	Area%
1	7.667	8.825	8.222	2639565	64090884	47.514
2	8.825	10.750	9.041	2508190	70798459	52.486
Total				5147755	134889343	100.000

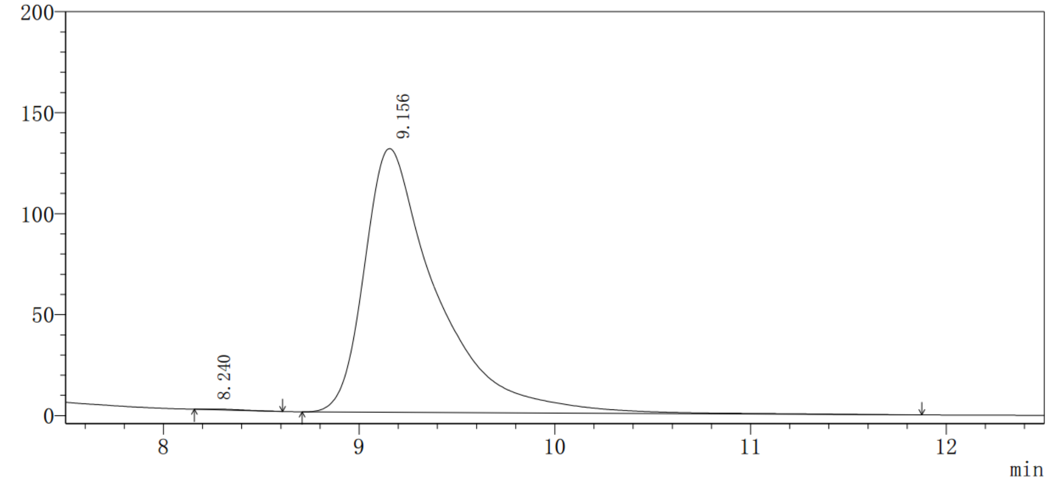

Detector:220nm

ID#	Start	End	Ret. Time	Height	Area	Area%
1	8.158	8.608	8.240	241	3866	0.114
2	8.708	11.875	9.156	130634	3387756	99.886
Total				130875	3391622	100.000

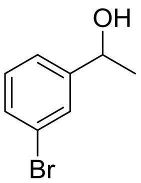

1-(3-Bromophenyl)ethanol:

Enantiomeric excess was determined by HPLC with a chiralcel OD-H column (hexane/*i*-PrOH = 98/2, 1.0 mL/min, 220 nm), t $_{major}$ = 17.389 min, t $_{minor}$ = 15.316 min; ee = 94%.

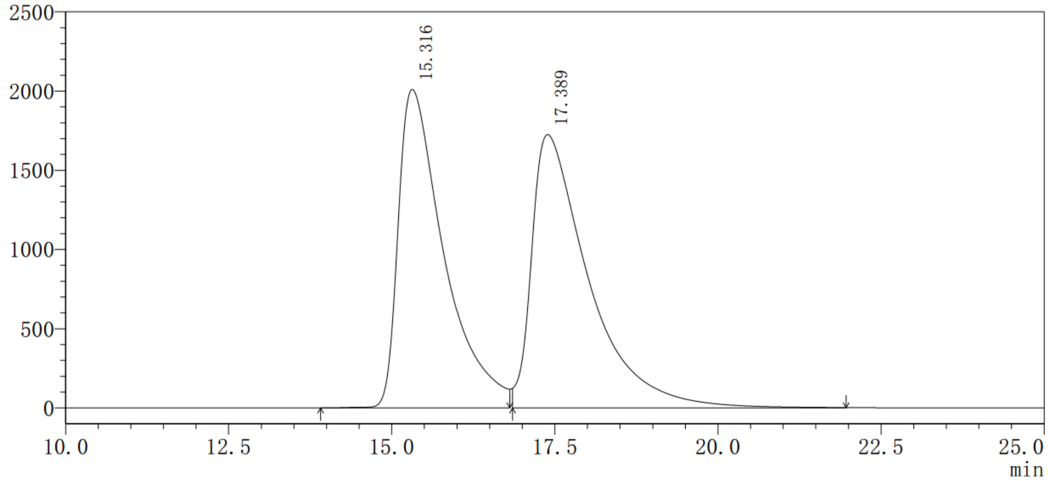

Detector:220nm

ID#	Start	End	Ret. Time	Height	Area	Area%
1	13.908	16.808	15.316	2011214	97891300	48.195
2	16.850	21.967	17.389	1725731	105221688	51.805
Total				3736945	203112988	100.000

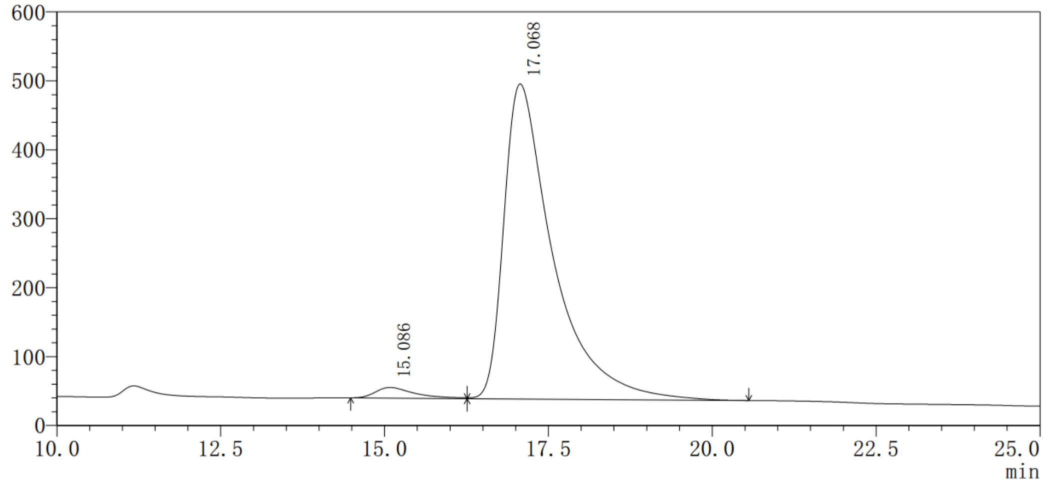

Detector:220nm

ID#	Start	End	Ret. Time	Height	Area	Area%
1	14.483	16.258	15.086	15449	649148	2.642
2	16.258	20.558	17.068	457057	23922009	97.358
Total				472506	24571157	100.000

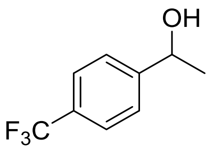

1-(3-Fluorophenyl)ethanol:

Enantiomeric excess was determined by HPLC with a chiralcel OJ-H column (hexane/*i*-PrOH = 99/1, 0.8 mL/min, 220 nm), t $_{major}$ = 29.220 min, t $_{minor}$ = 26.319 min; ee = 99.7%.

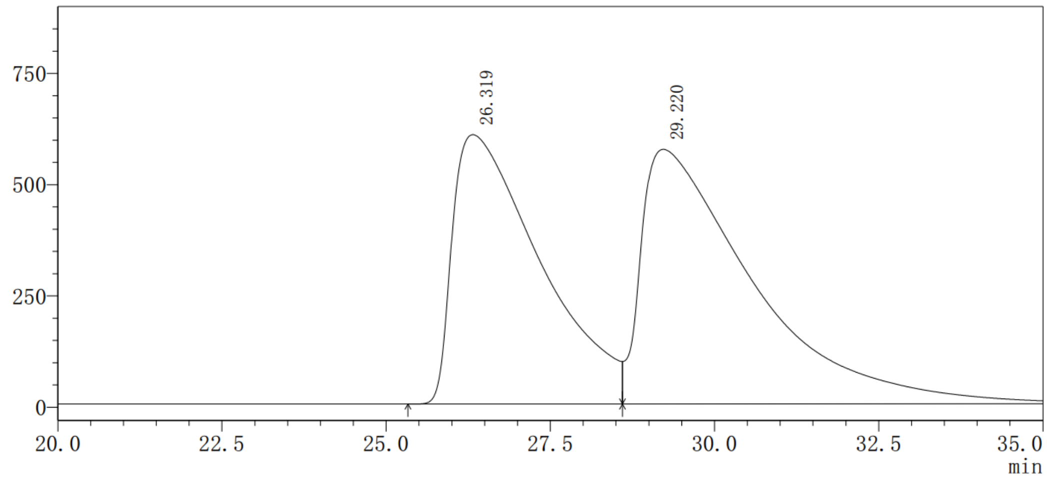

Detector:220nm

ID#	Start	End	Ret. Time	Height	Area	Area%
1	25.333	28.600	26.319	605359	56202476	45.104
2	28.600	38.267	29.220	572228	68402927	54.896
Total				1177587	124605404	100.000

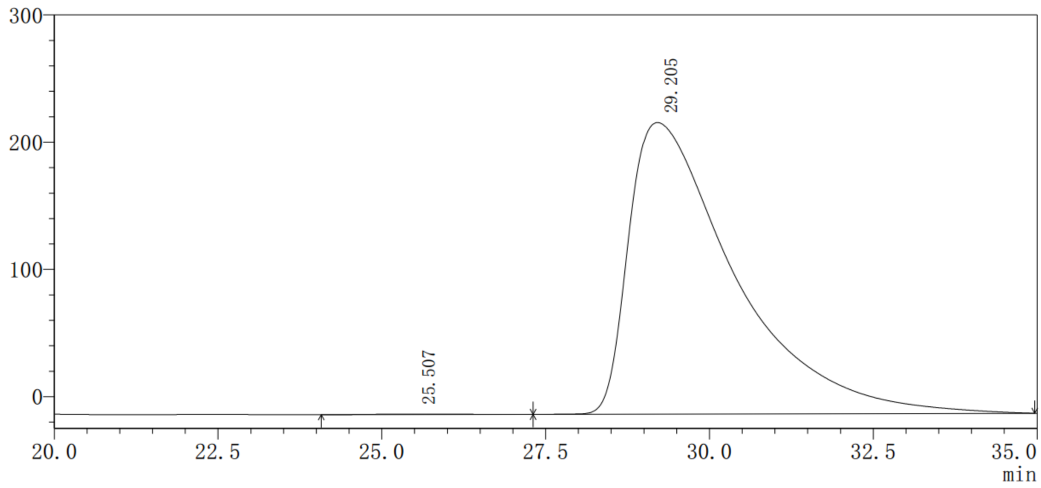

Detector:220nm

ID#	Start	End	Ret. Time	Height	Area	Area%
1	24.075	27.308	25.507	434	38516	0.149
2	27.308	34.967	29.205	229252	25880240	99.851
Total				229686	25918755	100.000

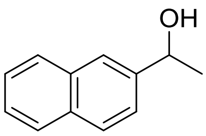

1-(2-Naphthyl)ethanol:

Enantiomeric excess was determined by HPLC with a chiralcel OJ-H column (hexane/*i*-PrOH = 90/10, 0.8 mL/min, 250 nm), t $_{major}$ = 16.687 min, t $_{minor}$ = 21.609 min; ee = 80%.

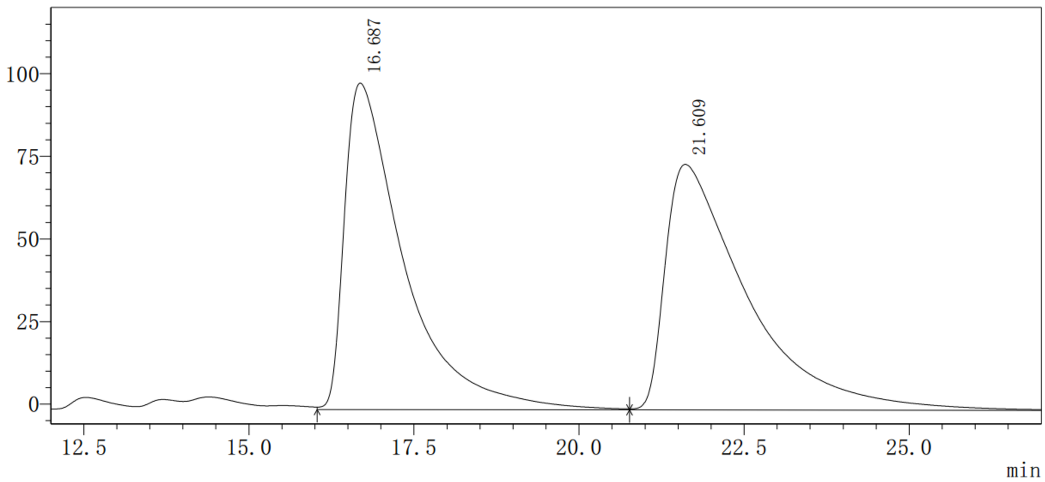

Detector:250nm

ID#	Start	End	Ret. Time	Height	Area	Area%
1	16.033	20.767	16.687	98790	6210786	49.054
2	20.767	28.500	21.609	74318	6450343	50.946
Total				173108	12661130	100.000

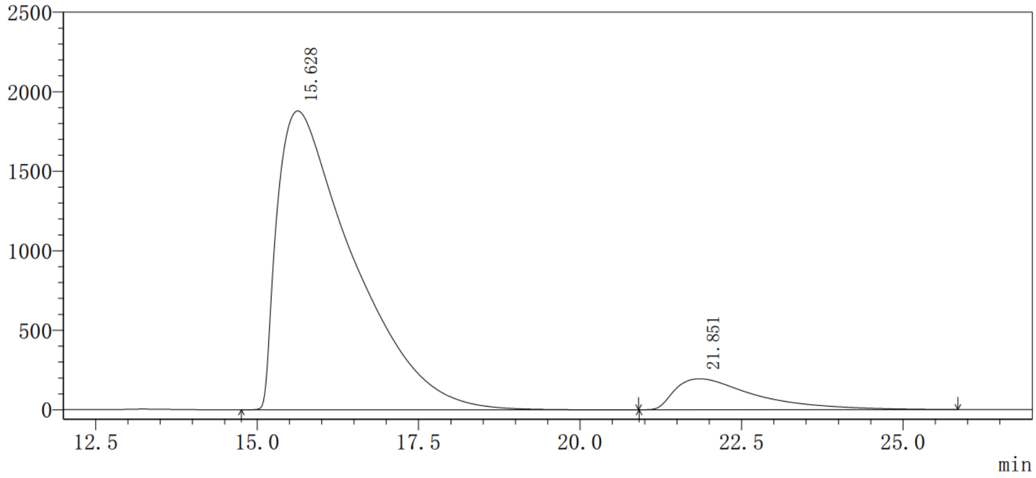

Detector:250nm

ID#	Start	End	Ret. Time	Height	Area	Area%
1	14.758	20.908	15.628	1879399	154609015	90.074
2	20.917	25.850	21.851	194520	17038047	9.926
Total				2073920	171647061	100.000

17.3 Cyanosilylation of aldehydes

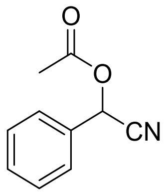

Enantiomeric excess was determined by HPLC with a chiralcel OD-H column (hexane/*i*-PrOH = 95/5, 1.0 mL/min, 230 nm), t $_{major}$ = 9.246 min, t $_{minor}$ = 8.212 min; ee = 82%, ^{1}HNMR ($CDCl_3$) δ: 0.23 (s, 9H), 5.44 (s, 1H), 7.25-7.57 (m, 5H).

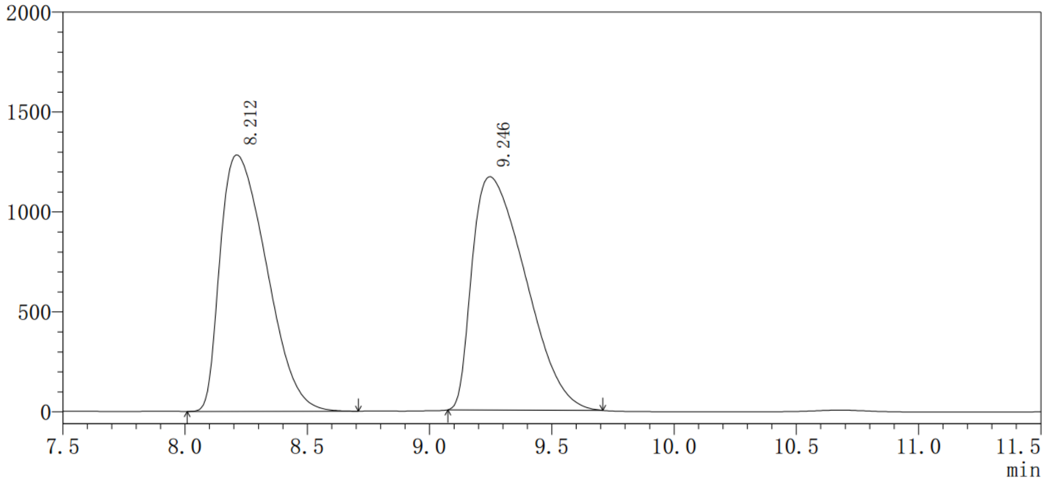

Detector:220nm

ID#	Start	End	Ret. Time	Height	Area	Area%
1	8.008	8.708	8.212	1283346	16899476	48.714
2	9.075	9.708	9.246	1167006	17791732	51.286
Total				2450351	34691208	100.000

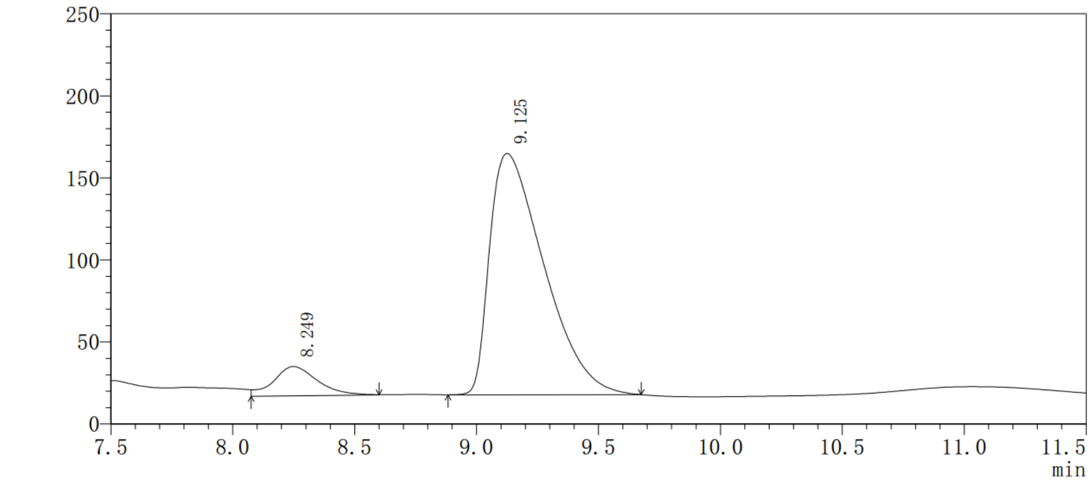

Detector:230nm

ID#	Start	End	Ret. Time	Height	Area	Area%
1	8.075	8.600	8.249	17931	224793	8.964
2	8.883	9.675	9.125	147229	2282979	91.036
Total				165160	2507772	100.000

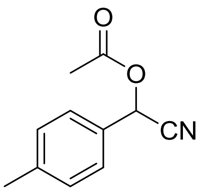

Enantiomeric excess was determined by HPLC with a chiralcel OD-H column (hexane/*i*-PrOH = 95/5, 1.0 mL/min, 230 nm), t $_{major}$ = 9.203 min, t $_{minor}$ = 6.988 min; ee = 81%, ^{1}H NMR ($CDCl_3$) δ: 0.27 (s, 9H), 3.81 (s, 3H), 5.43 (s, 1H), 6.91-6.94 (m, 2H), 7.35-7.40 (m, 2H).

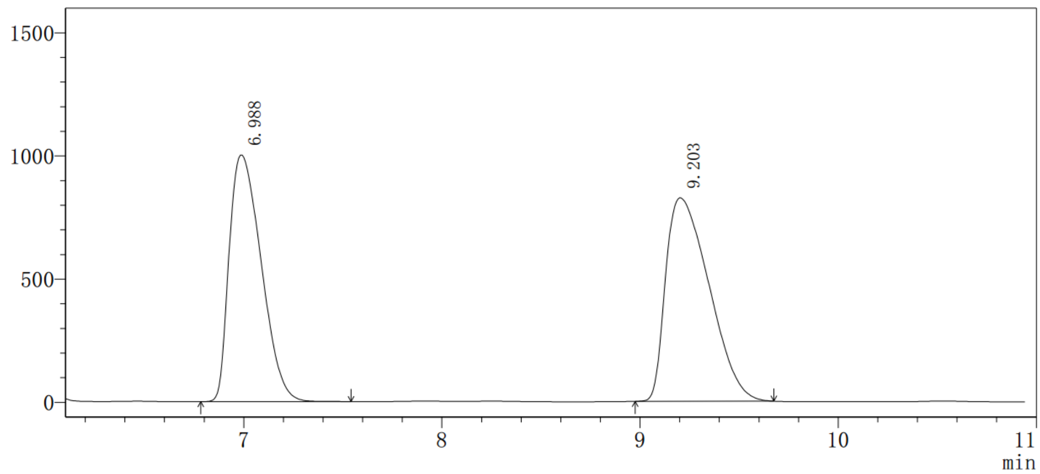

Detector:230nm

ID#	Start	End	Ret. Time	Height	Area	Area%
1	6.783	7.542	6.988	1000714	11253875	47.224
2	8.975	9.675	9.203	826057	12576805	52.776
Total				1826770	23830680	100.000

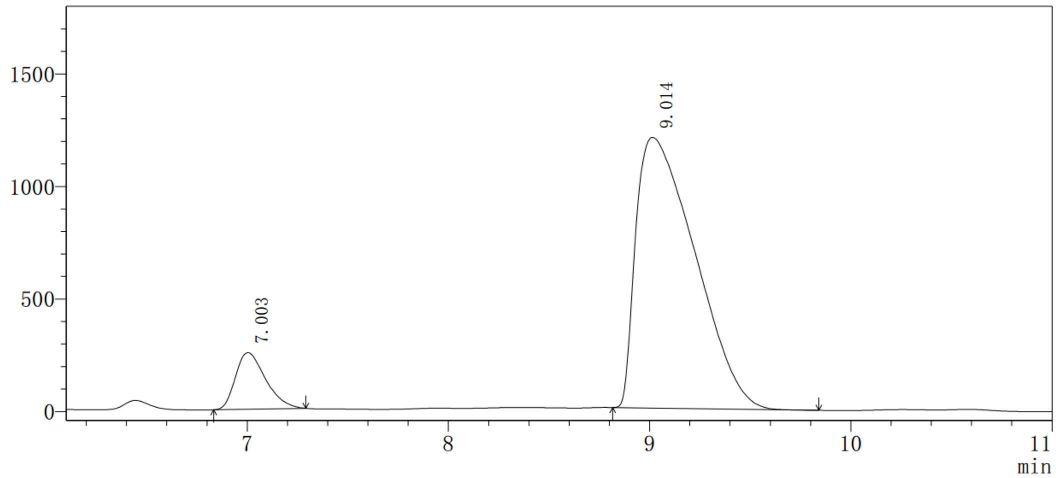

Detector:230nm

ID#	Start	End	Ret. Time	Height	Area	Area%
1	6.833	7.292	7.003	251777	2622778	9.650
2	8.817	9.842	9.014	1203145	24556224	90.350
Total				1454922	27179002	100.000

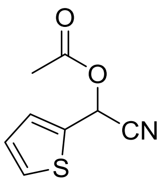

Enantiomeric excess was determined by HPLC with a chiralcel AD-H column (hexane/*i*-PrOH = 95/5, 1.0 mL/min, 230 nm), t $_{major}$ = 10.044 min, t $_{minor}$ = 9.028 min; ee = 87%, ^{1}H NMR ($CDCl_3$) δ: 0.24 (s, 9H), 5.73 (s, 1H), 7.00 (d, 1H), 7.19 (d, 1H), 7.37 (d, 1H).

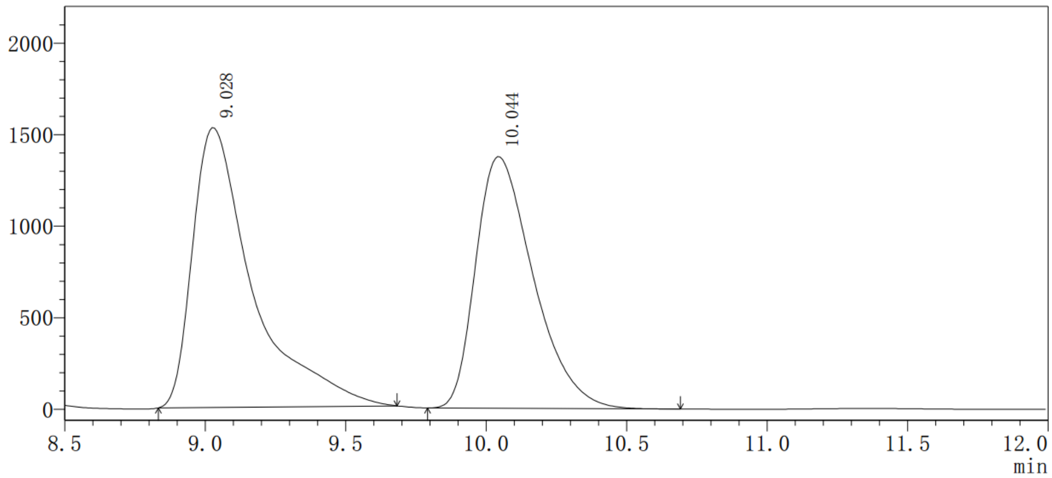

Detector:230nm

ID#	Start	End	Ret. Time	Height	Area	Area%
1	8.833	9.683	9.028	1528001	22678401	53.631
2	9.792	10.692	10.044	1374539	19607725	46.369
Total				2902540	42286126	100.000

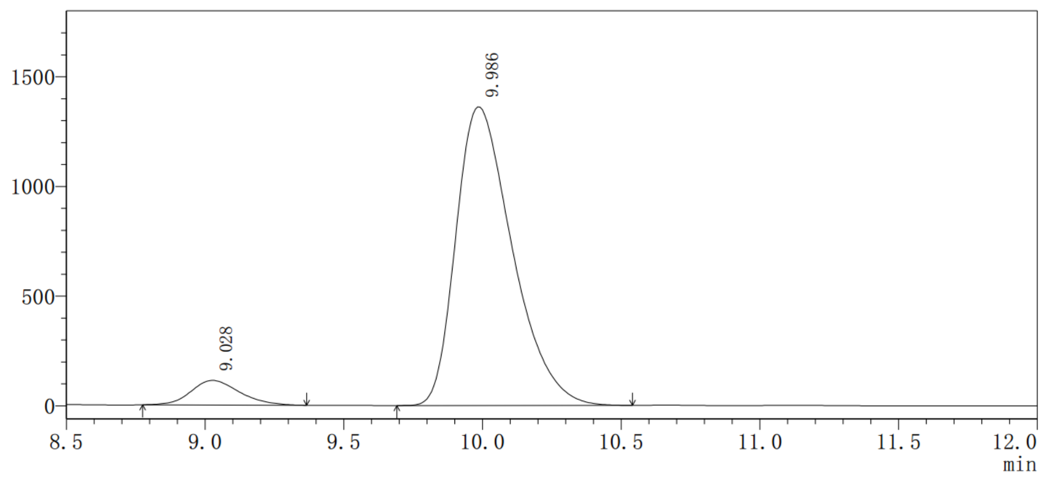

Detector:230nm

ID#	Start	End	Ret. Time	Height	Area	Area%
1	8.775	9.367	9.028	112087	1366258	6.630
2	9.692	10.542	9.986	1361572	19239655	93.370
Total				1473659	20605913	100.000

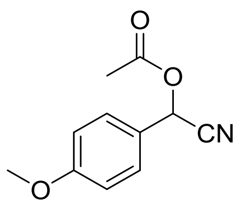

Enantiomeric excess was determined by HPLC with a chiralcel OD-H column (hexane/*i*-PrOH = 95/5, 1.0 mL/min, 230 nm), t $_{major}$ = 12.605 min, t $_{minor}$ = 10.610 min; ee = 84%, ^{1}H NMR ($CDCl_3$) δ: 0.21 (s, 9H), 3.82 (s, 3H), 5.44 (s, 1H), 6.91-6.94 (m, 2H), 7.37-7.40 (m, 2H).

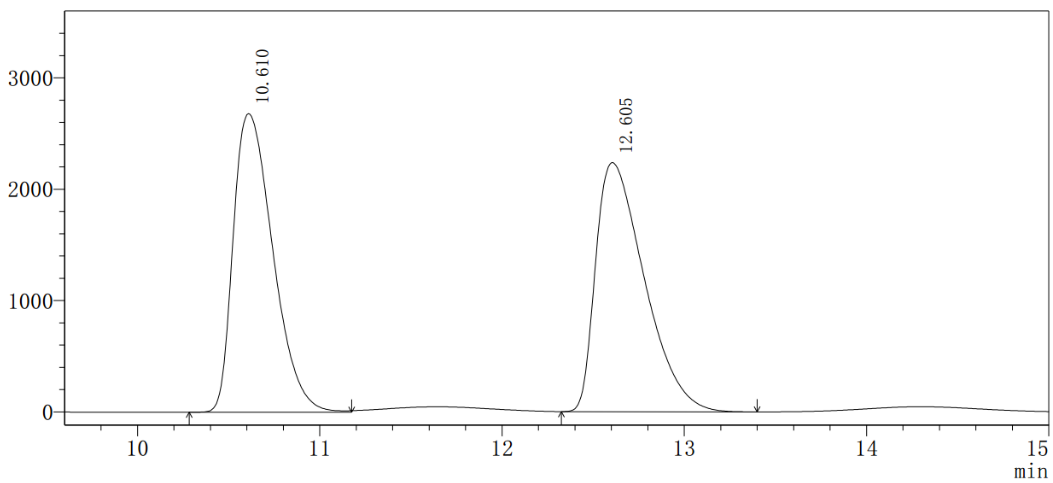

Detector:230nm

ID#	Start	End	Ret. Time	Height	Area	Area%
1	10.283	11.175	10.610	2683503	40628846	49.394
2	12.325	13.400	12.605	2237311	41626243	50.606
Total				4920814	82255088	100.000

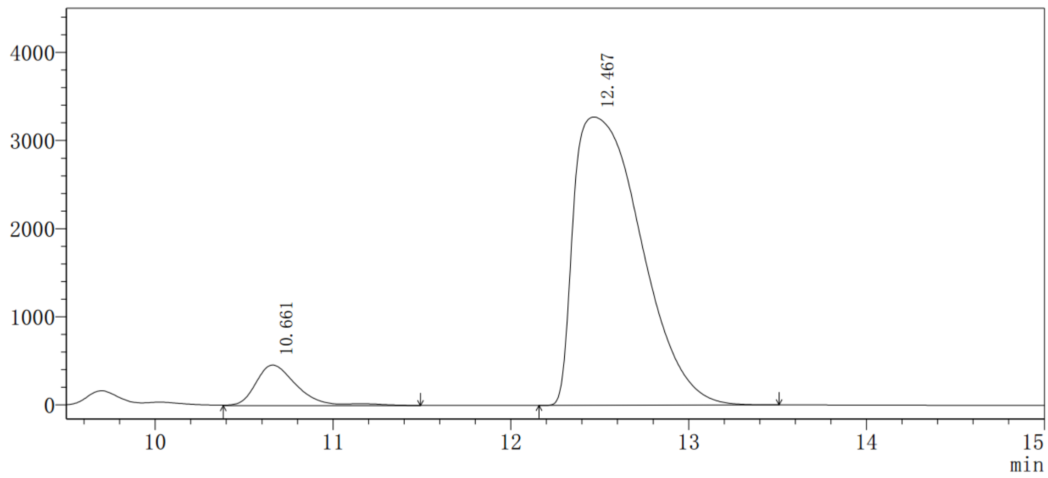

Detector:230nm

ID#	Start	End	Ret. Time	Height	Area	Area%
1	10.383	11.492	10.661	462124	7590622	8.063
2	12.158	13.508	12.467	3271463	86549716	91.937
Total				3733587	94140338	100.000

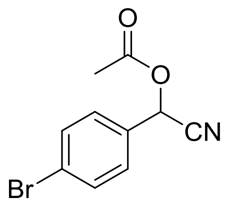

Enantiomeric excess was determined by HPLC with a chiralcel OD-H column (hexane/*i*-PrOH = 95/5, 1.0 mL/min, 230 nm), t $_{major}$ = 13.494 min, t $_{minor}$ = 10.344 min; ee = 80%, ^{1}H NMR ($CDCl_3$) δ: 0.24 (s, 9H), 5.51 (s, 1H), 7.40-7.49(m, 4H).

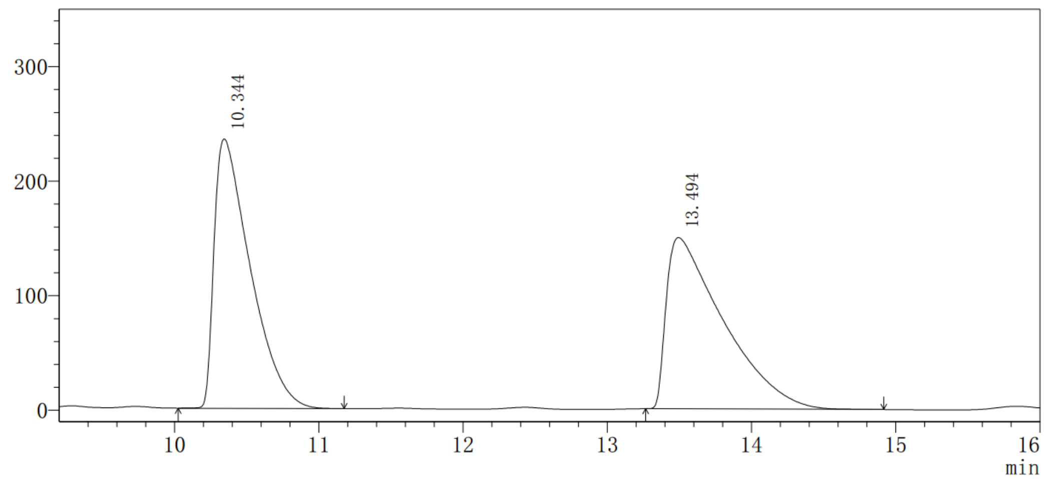

Detector:250nm

ID#	Start	End	Ret. Time	Height	Area	Area%
1	10.025	11.175	10.344	235112	4096944	49.936
2	13.267	14.917	13.494	149454	4107497	50.064
Total				384566	8204440	100.000

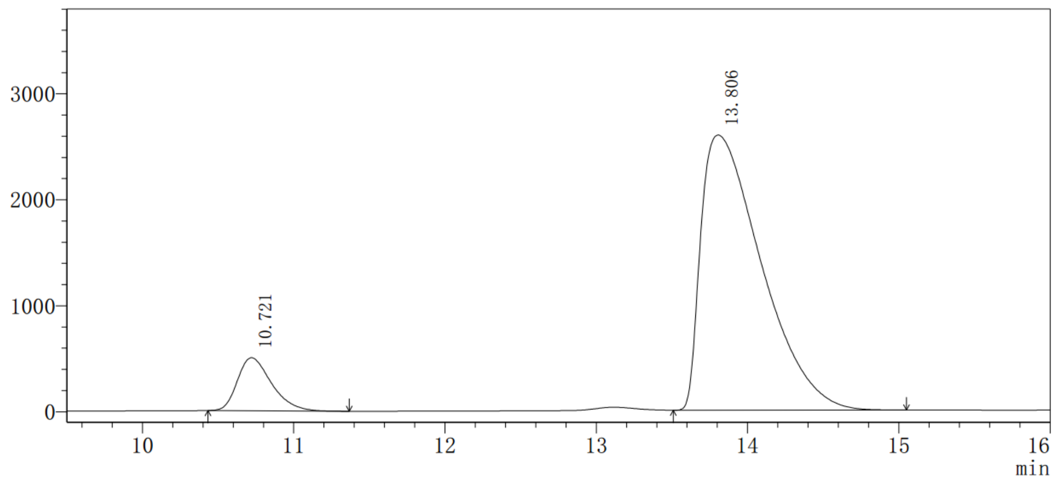

Detector:230nm

ID#	Start	End	Ret. Time	Height	Area	Area%
1	10.433	11.367	10.721	500509	7841845	9.792
2	13.508	15.050	13.806	2596438	72240259	90.208
Total				3096948	80082104	100.000

17.4 Aminolysis of trans-Stilbene Oxide

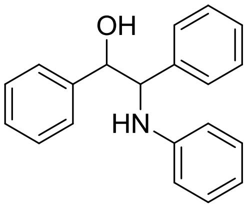

1,2-diphenyl-2-(phenylamino)ethanol: Enantiomeric excess was determined by HPLC with a chiralcel AD-H column (hexane/*i*-PrOH = 90/10, 0.75 mL/min, 250 nm), t $_{major}$ = 15.565 min, t $_{minor}$ = 19.390 min; ee= 81 %. ^{1}H NMR (400 MHz, $CDCl_3$) δ 7.33 – 7.20 (m, 7H), 7.17 – 7.11 (m, 2H), 7.12 (s, 2H), 6.91 – 6.82 (m, 2H), 6.45 (dd, *J* = 8.8, 2.3 Hz, 2H), 5.05 (d, *J* = 4.9 Hz, 1H), 4.65 (d, *J* = 4.9 Hz, 1H), 4.12 (d, *J* = 158.0 Hz, 1H).

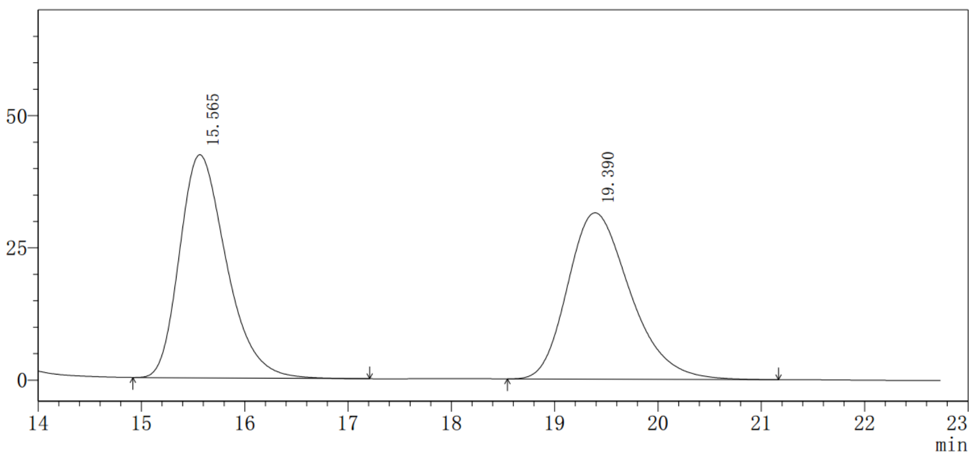

Detetor: 250nm

ID#	Start	End	Ret. Time	Height	Area	Area%
1	14.917	17.208	15.565	42200	1331751	50.125
2	18.542	21.167	19.390	31462	1325132	49.875
Total				73661	2656883	100.000

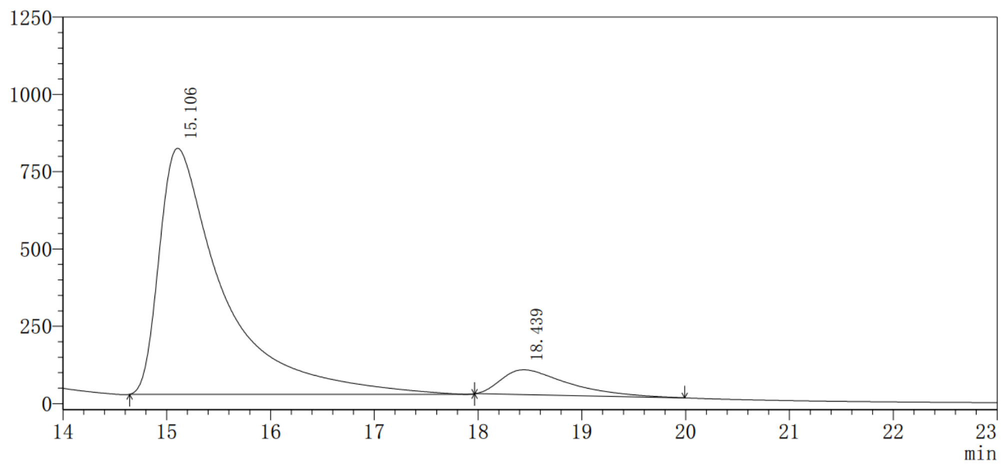

Detector:250nm

ID#	Start	End	Ret. Time	Height	Area	Area%
1	14.642	17.967	15.106	796215	34398910	90.458
2	17.967	19.992	18.439	80538	3628772	9.542
Total				876754	38027682	100.000

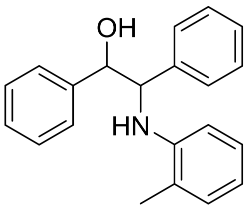

2-((4-methylphenyl)amino)-1,2-diphenylethanol:

Enantiomeric excess was determined by HPLC with a chiralcel AD-H column (hexane/*i*-PrOH = 95/5, 1.0 mL/min, 250 nm), t $_{major}$ = 18.086 min, t $_{minor}$ = 21.627 min; ee = 84%. ^{1}H NMR (400 MHz, $CDCl_3$) δ 7.35 – 7.23 (m, 6H), 7.22 – 7.12 (m, 4H), 7.01 (d, *J* = 7.3 Hz, 1H), 6.91 (t, *J* = 8.2 Hz, 1H), 6.60 (t, *J* = 7.4 Hz, 1H), 6.34 (d, *J* = 7.7 Hz, 1H), 5.04 (d, *J* = 4.7 Hz, 1H), 4.67 (d, *J* = 5.3Hz, 1H), 4.25 (s, 1H), 2.38 (s, 1H), 2.12 (s, 3H).

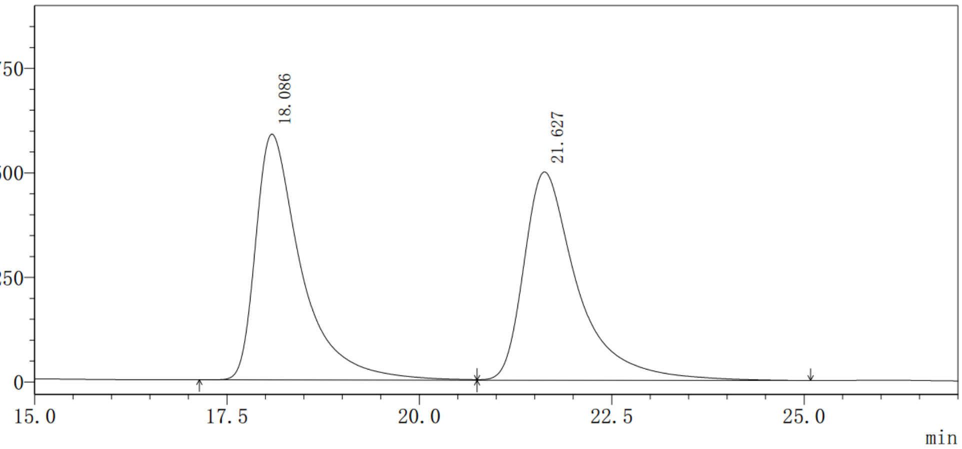

Detector:250nm

ID#	Start	End	Ret. Time	Height	Area	Area%
1	17.142	20.750	18.086	588021	24320375	50.051
2	20.750	25.083	21.627	498302	24271256	49.949
Total				1086323	48591632	100.000

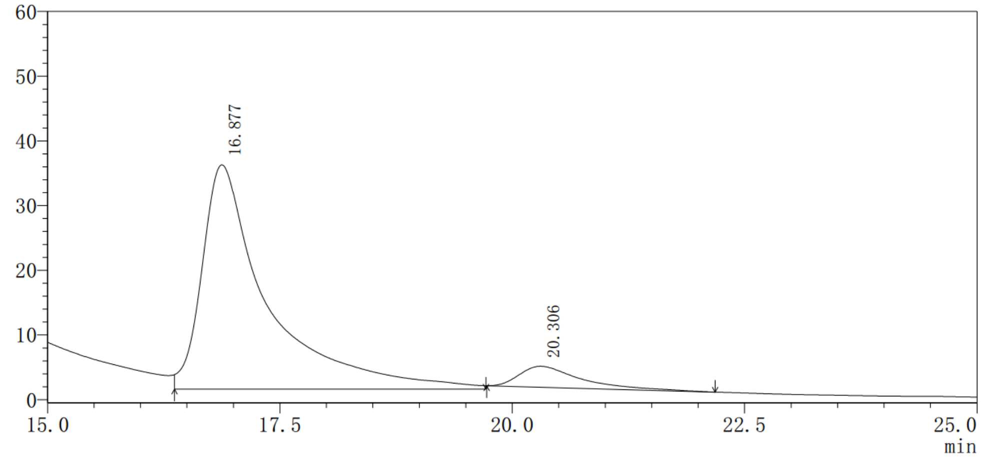

Detector:250nm

ID#	Start	End	Ret. Time	Height	Area	Area%
1	16.367	19.717	16.877	34688	1710756	91.959
2	19.725	22.183	20.306	3236	149586	8.041
Total				37924	1860342	100.000

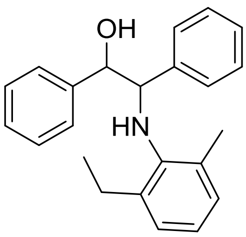

2-((2-methyl-6-ethylphenyl)amino)-1,2-diphenylethanol: Enantiomeric excess was determined by HPLC with a chiralcel OD-H column (hexane/*i*-PrOH = 90/10, 1.0 mL/min, 250 nm), t $_{major}$ = 9.615 min, t $_{minor}$ = 9.008 min; ee = 99%. ^{1}H NMR (400 MHz, $CDCl_3$) δ 7.27 – 7.15 (m, 6H), 7.07 – 6.92 (m, 6H), 6.84 (t, *J* = 7.5 Hz, 1H), 5.10 (d, 1H), 4.39 (d, *J* = 4.1 Hz, 1H), 2.65 – 2.48 (m, 2H), 2.20 (s, *J* = 3.1 Hz, 3H), 1.19 (t, *J* = 7.5 Hz, 3H).

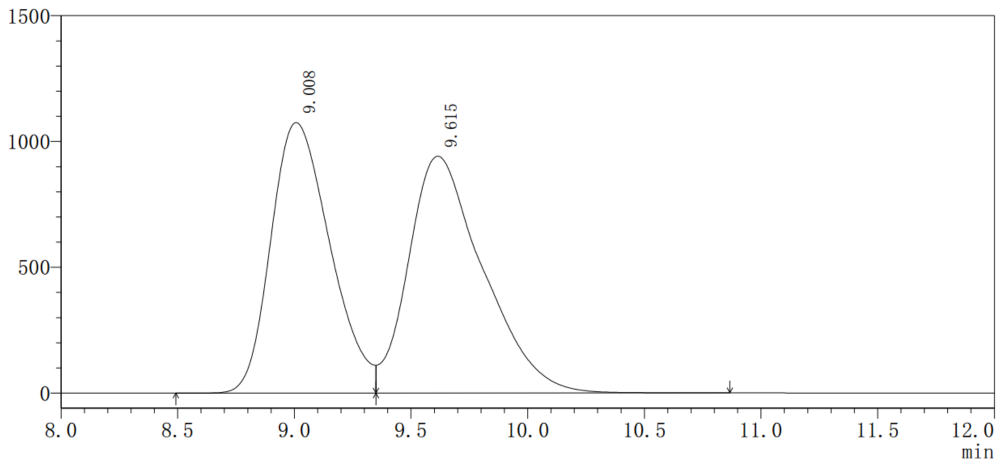

Detector:250nm

ID#	Start	End	Ret. Time	Height	Area	Area%
1	8.492	9.350	9.008	1075691	18991416	47.634
2	9.350	10.867	9.615	941632	20878276	52.366
Total				2017323	39869691	100.000

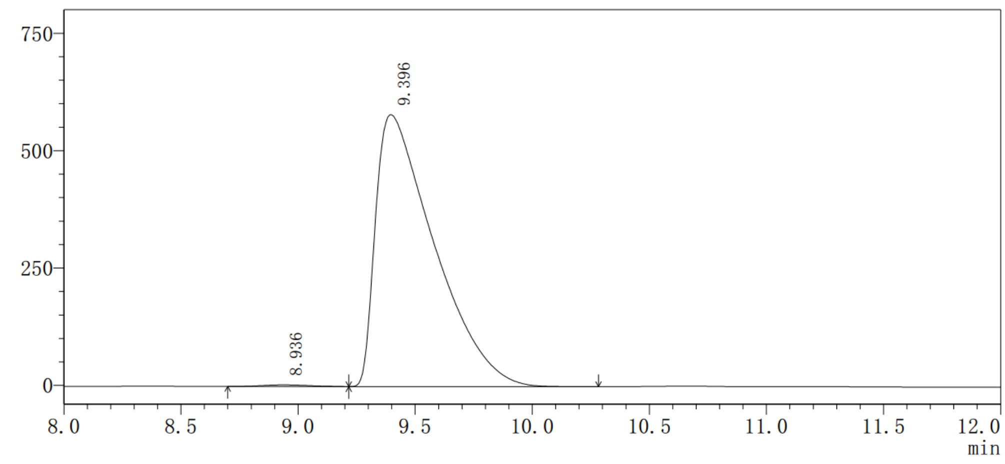

Detector:250nm

ID#	Start	End	Ret. Time	Height	Area	Area%
1	8.700	9.217	8.936	3396	47385	0.468
2	9.217	10.283	9.396	579122	10083628	99.532
Total				582519	10131013	100.000

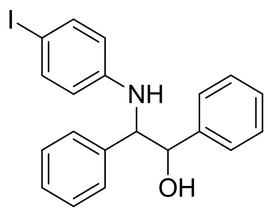

2-((4-iodophenyl)amino)-1,2-diphenylethanol:

Enantiomeric excess was determined by HPLC with a chiralcel OD-H column (hexane/*i*-PrOH = 90/10, 1.0 mL/min, 250 nm), t $_{major}$ = 19.274 min, t $_{minor}$ = 15.657 min; ee = 96%. ^{1}H NMR (400 MHz, $CDCl_3$) δ 7.33 – 7.27 (m, 5H), 7.27 – 7.20 (m, 3H), 7.11 – 7.03 (m, 4H), 6.30 – 6.26 (m, 2H), 5.06 (d, 1H), 4.59 (d, *J* = 4.8 Hz, 1H).

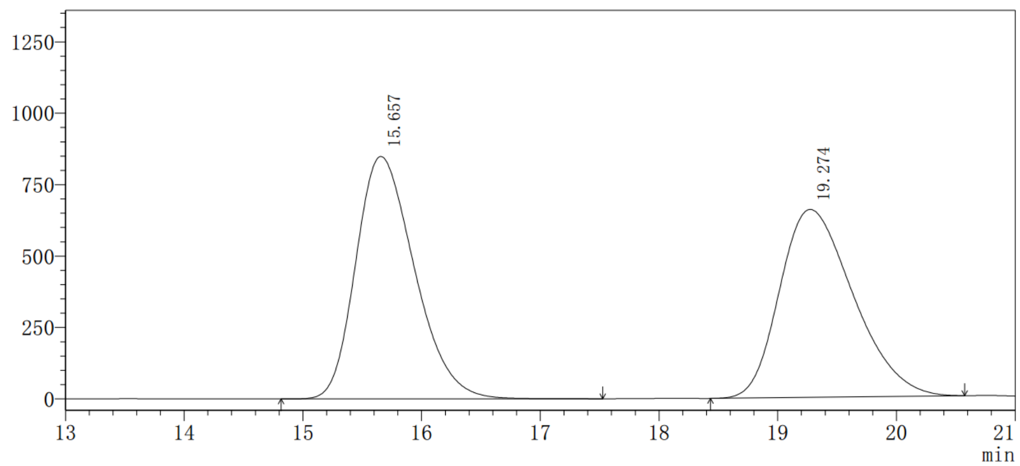

Detector:250nm

ID#	Start	End	Ret. Time	Height	Area	Area%
1	14.817	17.525	15.657	848813	29159597	50.659
2	18.433	20.575	19.274	658034	28400741	49.341
Total				1506848	57560338	100.000

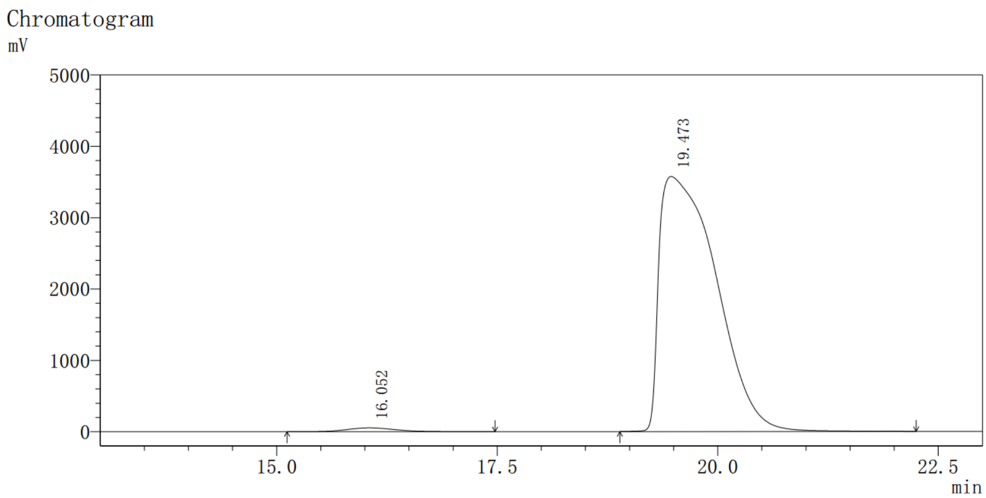

Detector:250nm

ID#	Start	End	Ret. Time	Height	Area	Area%
1	15.117	17.475	16.052	54004	2066423	1.267
2	18.892	22.250	19.473	3575202	161018399	98.733
Total				3629206	163084822	100.000

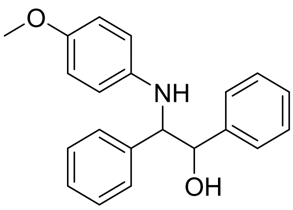

2-((4-methoxyphenyl)amino)-1,2-diphenylethanol:
Enantiomeric excess was determined by HPLC with a chiralcel OD-H column (hexane/*i*-PrOH = 90/10, 1.0 mL/min, 250 nm), t $_{major}$ = 23.115 min, t $_{minor}$ = 19.676 min; ee = 93%. ^{1}H NMR (400 MHz, $CDCl_3$) δ 7.30 – 7.21 (m, 6H), 7.13 (dd, *J* = 7.2, 2.4 Hz, 2H), 7.09 (dd, *J* = 6.9, 2.8 Hz, 2H), 6.70 – 6.61 (m, 2H), 6.52 – 6.42 (m, 2H), 5.03 (t, *J* = 5.2 Hz, 1H), 4.60 (d, *J* = 5.0 Hz, 1H), 4.15(s, 1H), 3.67 (s, 3H).

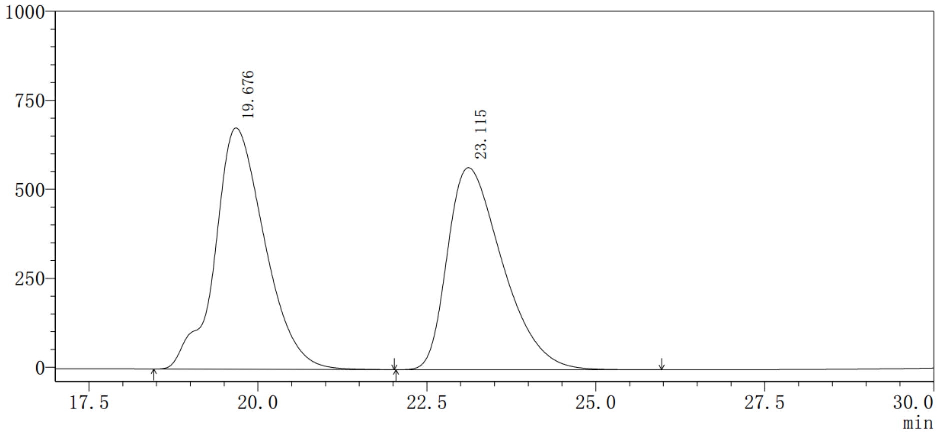

Detector:250nm

ID#	Start	End	Ret. Time	Height	Area	Area%
1	18.458	22.017	19.676	678176	34959190	52.025
2	22.042	25.975	23.115	567819	32237371	47.975
Total				1245996	67196561	100.000

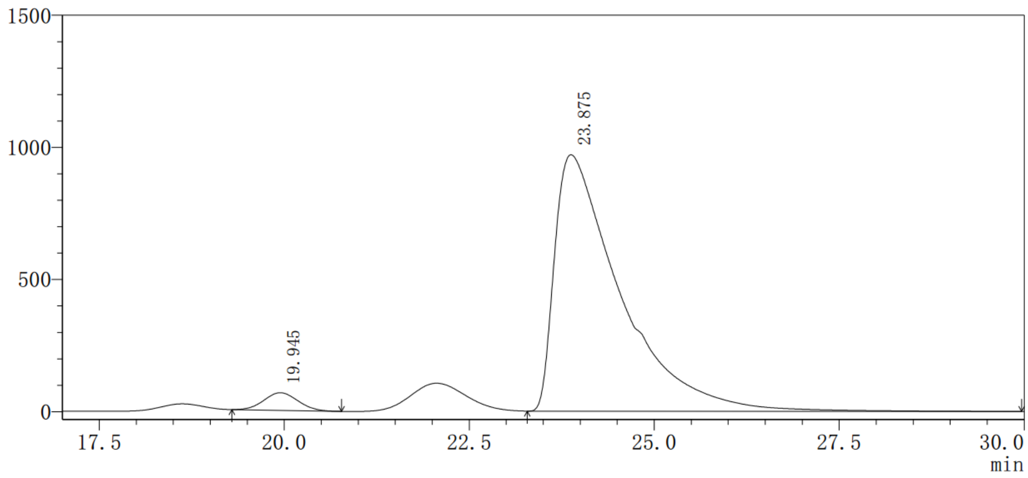

Detector:250nm

ID#	Start	End	Ret. Time	Height	Area	Area%
1	19.292	20.775	19.945	66664	2137226	3.433
2	23.283	29.967	23.875	970587	60110026	96.567
Total				1037250	62247252	100.000

17.5 Alkene epoxidation/epoxide aminolysis

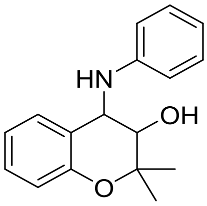

2,2-dimethyl-4-(phenylamino)chroman-3-ol:

Enantiomeric excess was determined by HPLC with a chiralcel AD-H column (hexane/*i*-PrOH = 95/5, 1.0 mL/min, 250 nm), t $_{major}$ = 17.357 min, t $_{minor}$ = 19.986 min; ee = 80%, ^{1}H NMR (400 MHz, $CDCl_3$) δ 7.23 (dd, *J* = 20.5, 12.1 Hz, 4H), 6.87 – 6.79 (m, 5H), 4.56 (d, *J* = 9.0 Hz, 1H), 3.72 (d, *J* = 9.0 Hz, 1H), 2.61 (s, 1H), 1.56 (s, 3H), 1.37 (s, 3H).

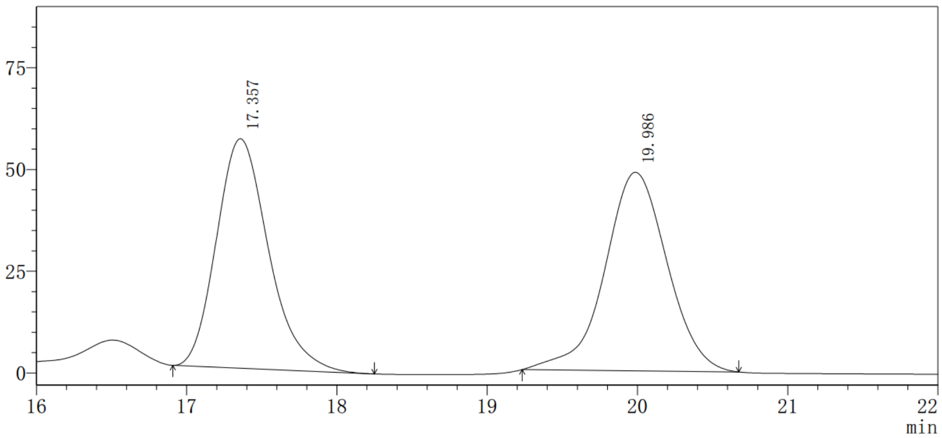

Detector:250nm

ID#	Start	End	Ret. Time	Height	Area	Area%
1	16.908	18.250	17.357	56392	1360415	49.155
2	19.233	20.675	19.986	48788	1407211	50.845
Total				105180	2767626	100.000

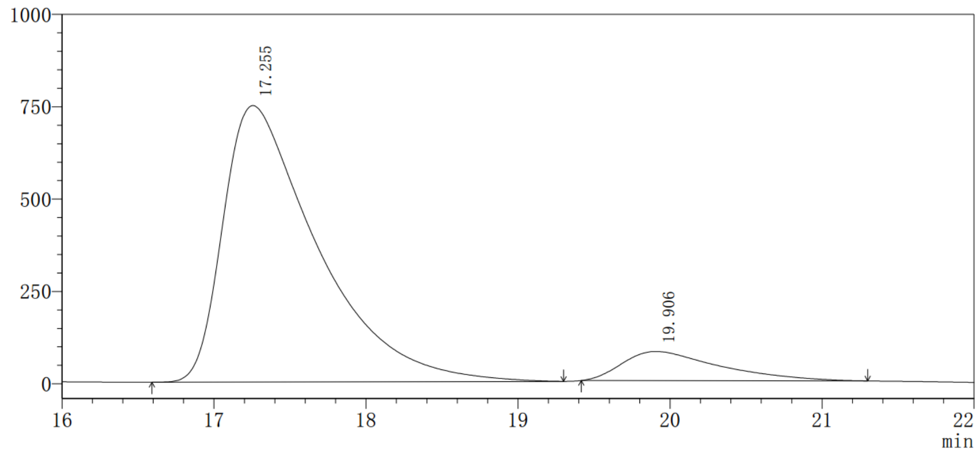

Detector:250nm

ID#	Start	End	Ret. Time	Height	Area	Area%
1	16.592	19.300	17.255	748420	32319403	90.208
2	19.417	21.300	19.906	78960	3508231	9.792
Total				827380	35827633	100.000

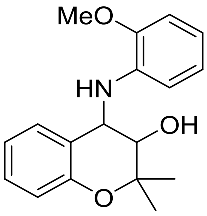

2,2-dimethyl-4-(o-methoxyl-phenylamino)chroman-3-ol:
Enantiomeric excess was determined by HPLC with a chiralcel AD-H column (hexane/*i*-PrOH = 95/5, 1.0 mL/min, 220 nm), t $_{major}$ = 13.578 min, t $_{minor}$ = 11.461 min; ee = 82%, ^{1}H NMR ($CDCl_3$) δ: 7.28-7.16 (m, 3H), 6.72~6.95 (m, 5H), 4.57 (d, *J* = 8Hz, 1H), 3.88 (s, 3H), 3.73 (d, *J* = 8 Hz, 1H), 2.74 (s, 1H), 1.53 (s, 3H), 1.29 (s, 3H).

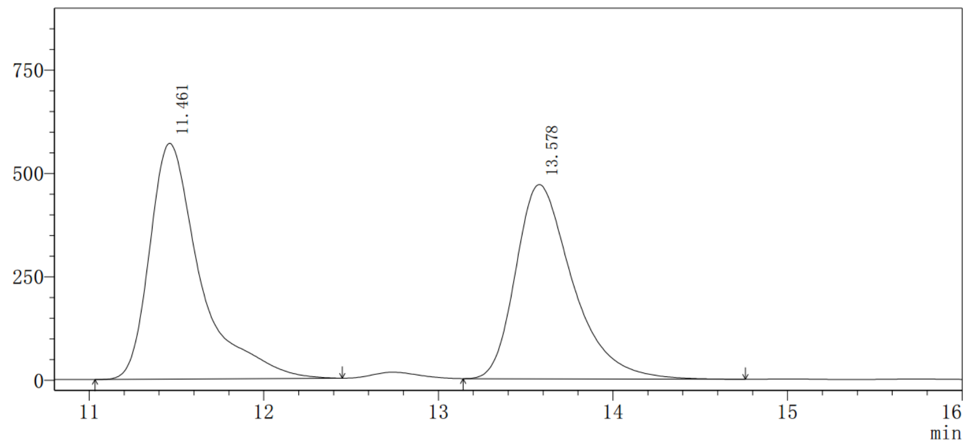

Detector:250nm

ID#	Start	End	Ret. Time	Height	Area	Area%
1	11.033	12.450	11.461	570692	11503559	51.862
2	13.142	14.758	13.578	470204	10677745	48.138
Total				1040895	22181304	100.000

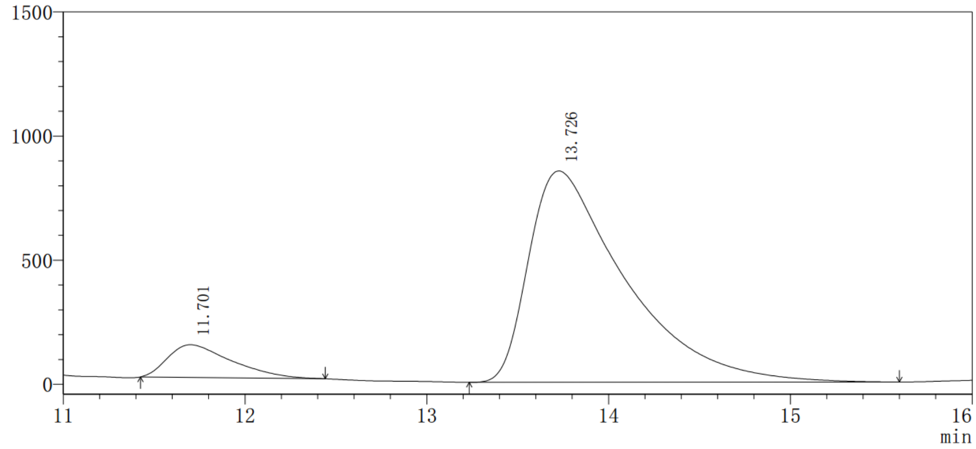

Detector:230nm

ID#	Start	End	Ret. Time	Height	Area	Area%
1	11.425	12.442	11.701	131678	3199752	9.213
2	13.233	15.600	13.726	851534	31532336	90.787
Total				983212	34732089	100.000

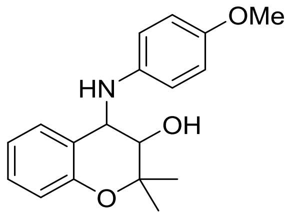

2,2-dimethyl-4-(*p*-methoxyl-phenylamino)chroman-3-ol:

Enantiomeric excess was determined by HPLC with a chiralcel AD-H column (hexane/*i*-PrOH = 90/10, 1.0 mL/min, 250 nm), t_{major} = 19.469 min, t_{minor} = 16.984 min; ee = 87%, ^{1}H NMR (400 MHz, $CDCl_3$) δ 7.31 – 7.08 (m, 2H), 6.89 – 6.72 (m, 5H), 4.42 (d, *J* = 9.2 Hz, 1H), 3.78 (s, 3H), 3.65 (d, *J* = 9.2 Hz, 1H), 2.78 (s, 1H), 1.52 (s, 3H), 1.33 (s, 3H).

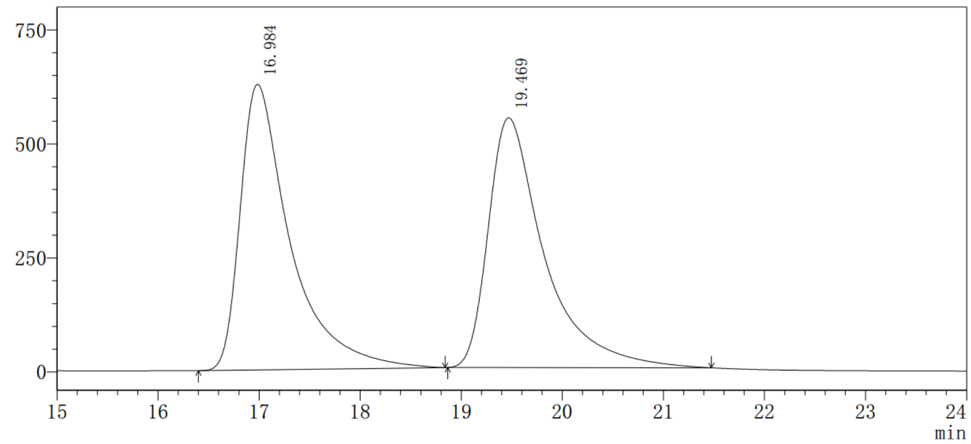

Detector:250nm

ID#	Start	End	Ret. Time	Height	Area	Area%
1	16.400	18.842	16.984	626080	21508807	50.466
2	18.867	21.475	19.469	547523	21111786	49.534
Total				1173603	42620592	100.000

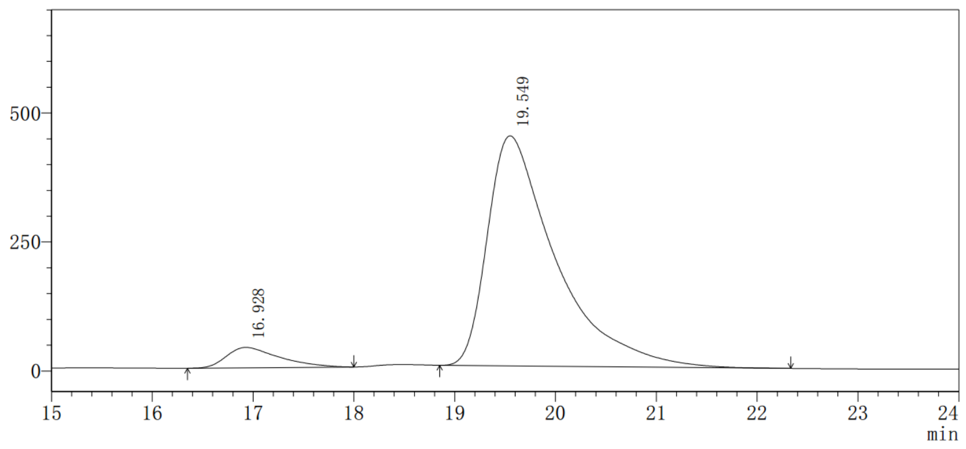

Detector:250nm

ID#	Start	End	Ret. Time	Height	Area	Area%
1	16.350	18.000	16.928	39596	1438093	6.403
2	18.850	22.333	19.549	446028	21021399	93.597
Total				485624	22459492	100.000

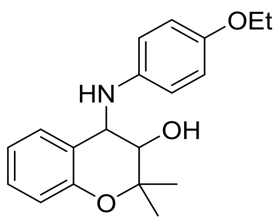

2,2-dimethyl-4-(*p*-ethoxyl-phenylamino)chroman-3-ol

Enantiomeric excess was determined by HPLC with a chiralcel AD-H column (hexane/*i*-PrOH = 90/10, 1.0 mL/min, 250 nm), t $_{major}$ = 19.464 min, t $_{minor}$ = 14.551 min; ee = 82%， ^{1}H NMR ($CDCl_3$) δ: 6.70~7.36 (m, 8H), 4.60 (d, *J* = 8Hz, 1H), 4.06 (m, 2H), 3.74 (d, *J* = 8 Hz, 1H), 2.80 (s, 1H), 1.54 (s, 3H), 1.43 (t, *J* = 8 Hz, 3H), 1.38 (s, 3H).

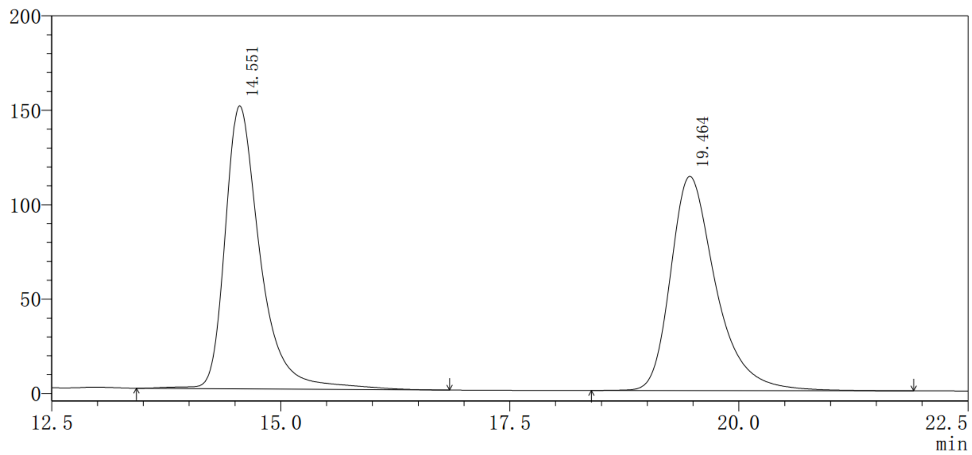

Detector:250nm

ID#	Start	End	Ret. Time	Height	Area	Area%
1	13.425	16.842	14.551	149913	4001554	50.583
2	18.392	21.908	19.464	113478	3909333	49.417
Total				263391	7910887	100.000

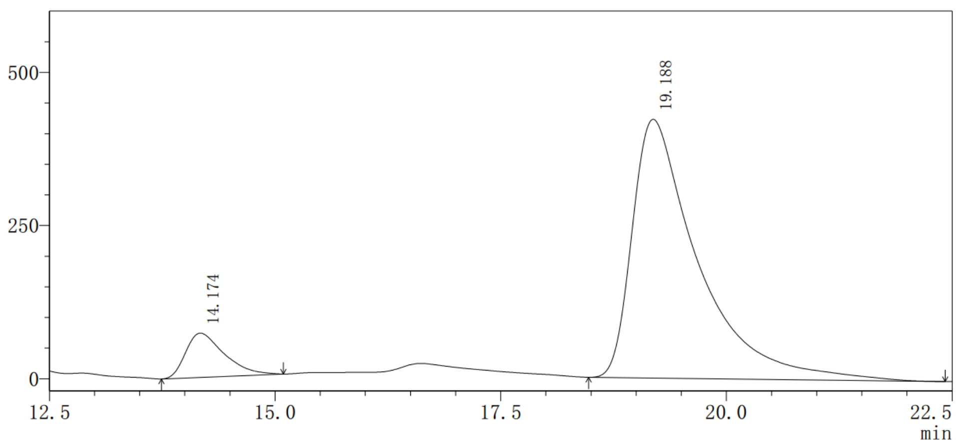

Detector:250nm

ID#	Start	End	Ret. Time	Height	Area	Area%
1	13.742	15.092	14.174	72275	2144827	9.067
2	18.475	22.425	19.188	422311	21511781	90.933
Total				494586	23656607	100.000

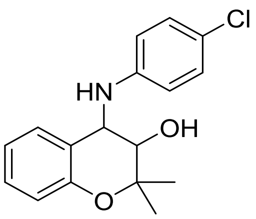

2,2-dimethyl-4-(*p*-chlorophenylamino)chroman-3-ol

Enantiomeric excess was determined by HPLC with a chiralcel OD-H column (hexane/*i*-PrOH = 95/5, 1.0 mL/min, 250 nm), t $_{major}$ = 22.833 min, t $_{minor}$ = 24.469 min; ee = 96%， ^{1}H NMR ($CDCl_3$) δ: 6.70~7.22 (m, 9H), 4.46 (d, *J* = 8 Hz, 1H), 3.84 (br, 1H), 3.56 (d, *J* = 4 Hz, 1H), 2.55 (br, 1H), 1.50 (s, 3H), 1.33 (s, 3H).

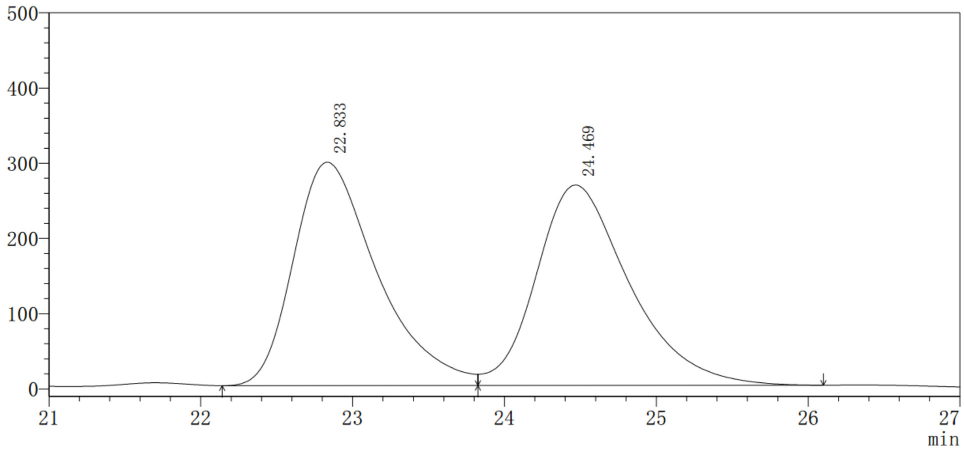

Detector:250nm

ID#	Start	End	Ret. Time	Height	Area	Area%
1	22.142	23.825	22.833	297006	11429881	50.142
2	23.825	26.100	24.469	266341	11365113	49.858
Total				563347	22794994	100.000

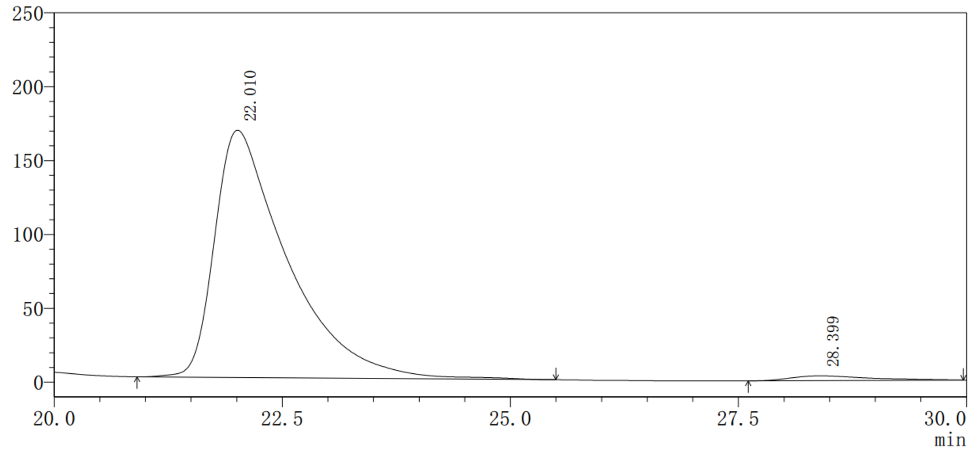

Detector:250nm

ID#	Start	End	Ret. Time	Height	Area	Area%
1	20.908	25.500	22.010	167425	9295320	97.936
2	27.608	29.967	28.399	3240	195893	2.064
Total				170666	9491213	100.000

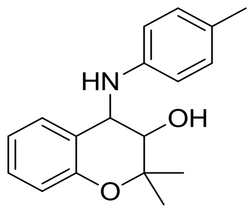

2,2-dimethyl-4-(p-tolylamino)chroman-3-ol

Enantiomeric excess was determined by HPLC with a chiralcel AD-H column (hexane/*i*-PrOH = 95/5, 1.0 mL/min, 250 nm), t $_{major}$ = 17.638 min, t $_{minor}$ = 20.693 min; ee = 84%, ^{1}H NMR ($CDCl_3$) δ: 6.72-7.30 (m, 8H), 4.47(d, *J* = 8 Hz, 1H), 3.70 (br, 1H), 3.65 (d, *J* = 8 Hz, 1H), 2.72 (br, 1H), 2.29 (s, 3H), 1.53 (s, 3H), 1.34 (s, 3H).

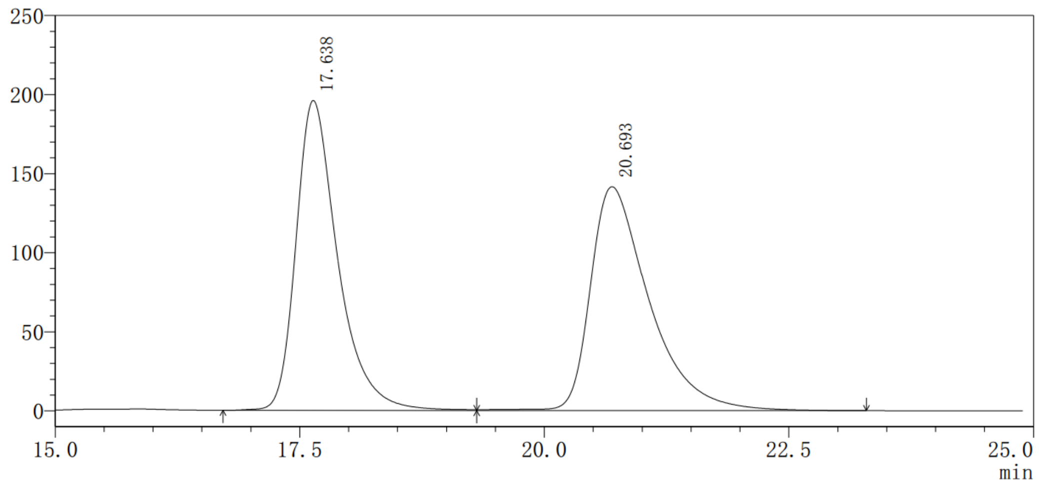

Detector:250nm

ID#	Start	End	Ret. Time	Height	Area	Area%
1	16.717	19.308	17.638	195977	5835191	49.666
2	19.308	23.292	20.693	141552	5913689	50.334
Total				337529	11748880	100.000

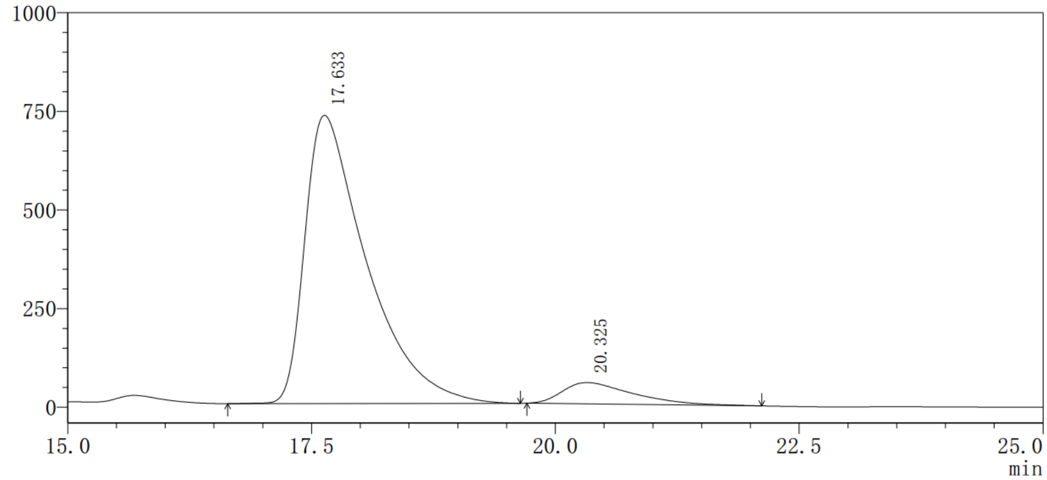

Detector:250nm

ID#	Start	End	Ret. Time	Height	Area	Area%
1	16.642	19.642	17.633	730831	32176164	92.196
2	19.708	22.117	20.325	53972	2723537	7.804
Total				784803	34899701	100.000

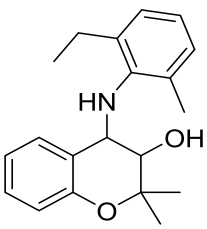

2,2-dimethyl-4-(2-Methyl-6-Ehtyl-phenylamino)chroman-3-ol

Enantiomeric excess was determined by HPLC with a chiralcel AD-H column (hexane/*i*-PrOH = 95/5, 1.0 mL/min, 250 nm), t $_{major}$ = 5.197 min, t $_{minor}$ = 6.754 min; ee = 99.5%， ^{1}H NMR ($CDCl_3$) δ: 6.86~7.54 (m, 7H), 4.49 (d, *J* = 12 Hz, 1H), 3.80 (d, *J* = 12 Hz, 1H), 3.50 (br, 2H), 2.75 (q, *J* = 8 Hz, 2H), 2.42 (s, 3H), 1.53 (s, 3H), 1.26~1.32 (m, 6H).

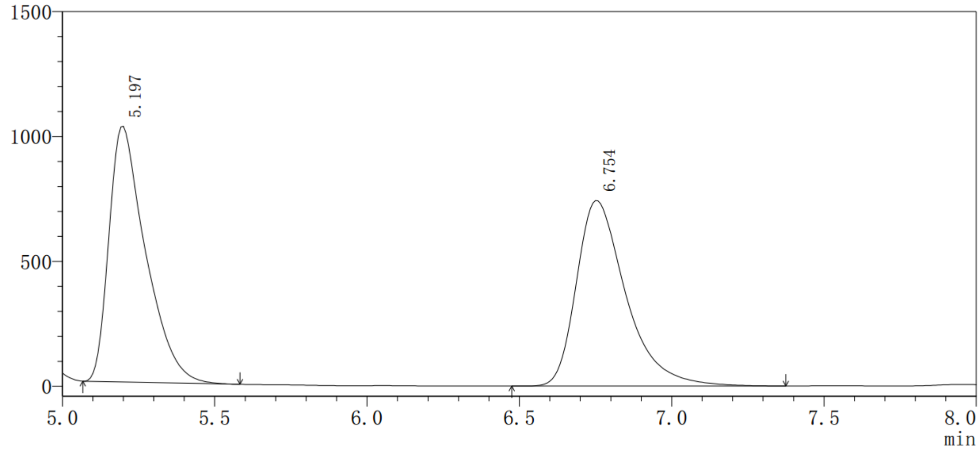

Detector:250nm

ID#	Start	End	Ret. Time	Height	Area	Area%
1	5.067	5.583	5.197	1024237	8602788	50.651
2	6.475	7.375	6.754	742930	8381621	49.349
Total				1767167	16984409	100.000

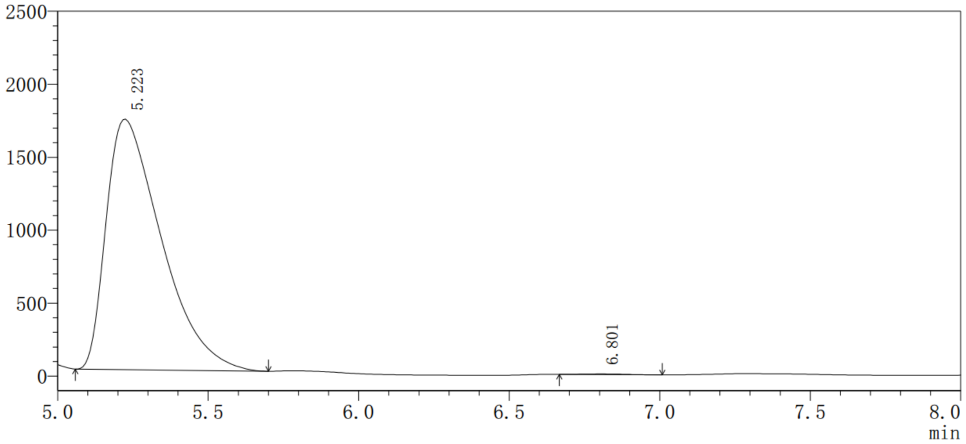

Detector:250nm

ID#	Start	End	Ret. Time	Height	Area	Area%
1	5.058	5.700	5.223	1717049	21957316	99.793
2	6.667	7.008	6.801	4582	45503	0.207
Total				1721631	22002818	100.000

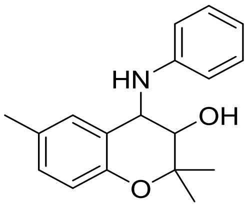

2,2-dimethyl-6-methyl-4-(phenylamino)chroman-3-ol

Enantiomeric excess was determined by HPLC with a chiralcel AD-H column (hexane/*i*-PrOH = 95/5, 1.0 mL/min, 250 nm), t $_{major}$ = 14.573 min, t $_{minor}$ = 17.357 min; ee = 86%， ^{1}H NMR ($CDCl_3$) δ: 6.72~7.26 (m, 8H), 4.48 (t, *J* = 8 Hz, 1H), 3.82 (br, 1H), 3.66 (d, *J* = 8 Hz, 1H), 2.52 (br, 1H), 2.20 (s, 3H), 1.50 (s, 3H), 1.33 (s, 3H).

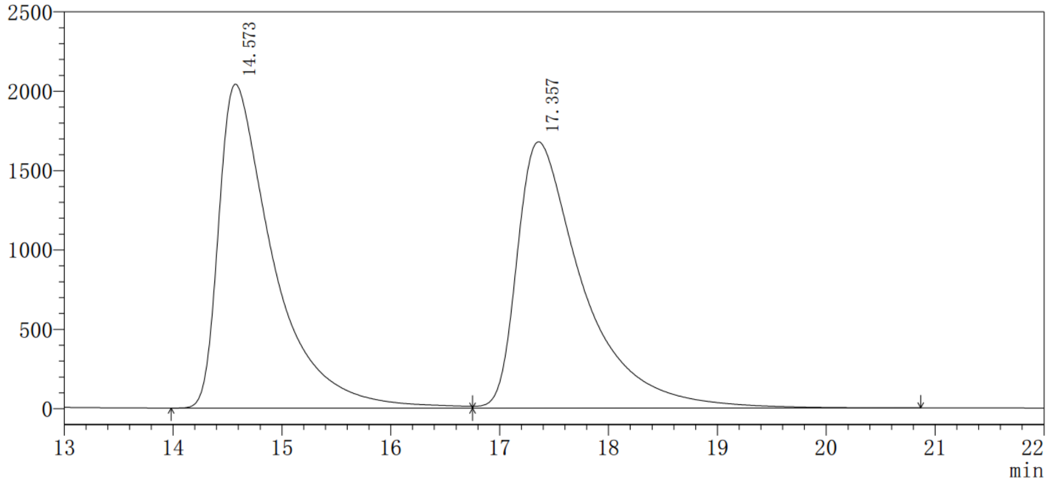

Detector:250nm

ID#	Start	End	Ret. Time	Height	Area	Area%
1	13.983	16.750	14.573	2040967	71140981	50.099
2	16.750	20.867	17.357	1677341	70861187	49.901
Total				3718308	142002168	100.000

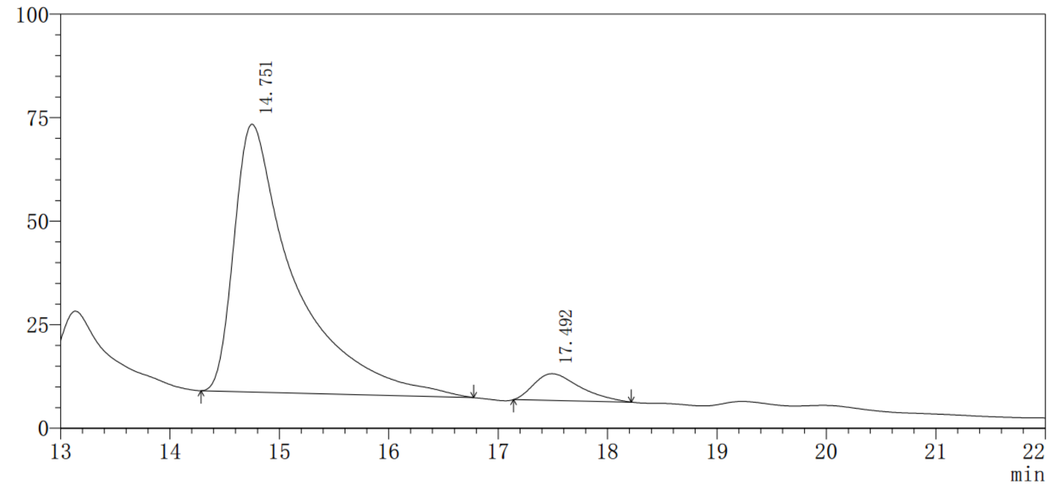

Detector:240nm

ID#	Start	End	Ret. Time	Height	Area	Area%
1	14.283	16.775	14.751	64681	2499394	92.983
2	17.142	18.217	17.492	6446	188632	7.017
Total				71127	2688026	100.000

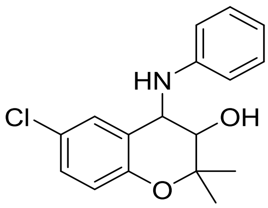

2,2-dimethyl-6-nitro-4-(phenylamino)chroman-3-ol

Enantiomeric excess was determined by HPLC with a chiralcel AD-H column (hexane/*i*-PrOH = 95/5, 1.0 mL/min, 250 nm), t $_{major}$ = 16.036 min, t $_{minor}$ = 21.961 min; ee = 87%， ^{1}H NMR ($CDCl_3$) δ: 6.76~7.26 (m, 8H), 4.48 (t, *J* = 12 Hz, 1H), 3.80 (br, 1H), 3.66 (d, *J* = 8 Hz, 1H), 2.54 (br, 1H), 1.50 (s, 3H), 1.32 (s, 3H).

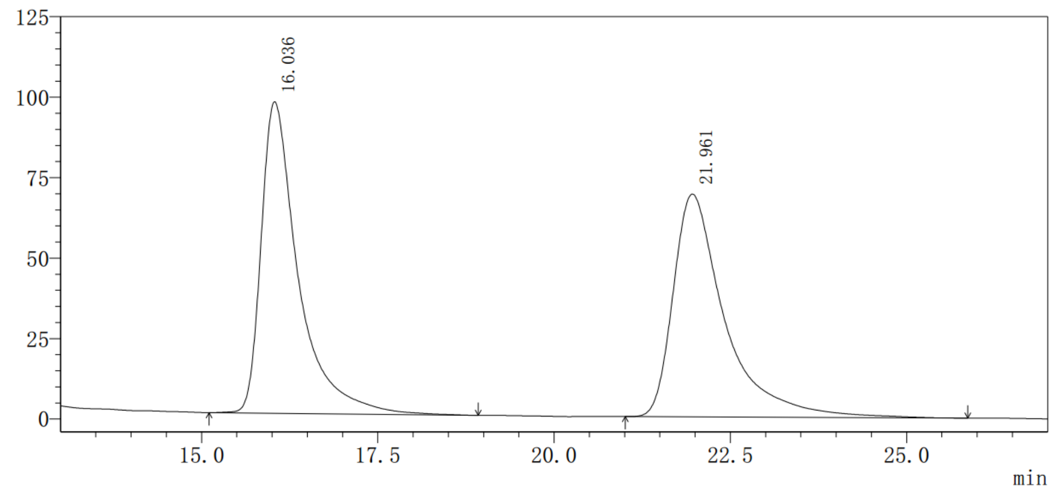

Detector:250nm

ID#	Start	End	Ret. Time	Height	Area	Area%
1	15.108	18.925	16.036	96796	3559388	50.140
2	21.008	25.867	21.961	69240	3539568	49.860
Total				166036	7098955	100.000

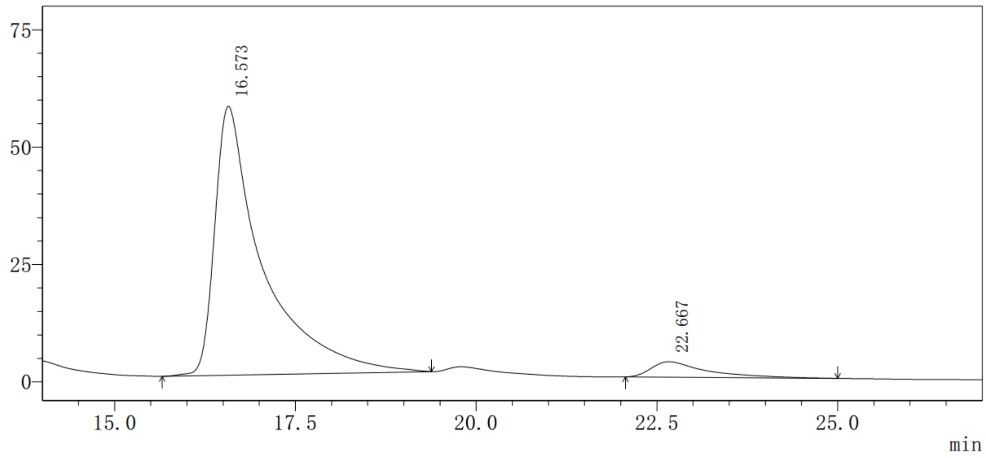

Detector:240nm

ID#	Start	End	Ret. Time	Height	Area	Area%
1	15.658	19.383	16.573	57258	2641384	93.747
2	22.067	25.000	22.667	3305	176170	6.253
Total				60563	2817554	100.000

17.6 Recycled experiments of alkene epoxidation by UiO-68-Mn

Run 1

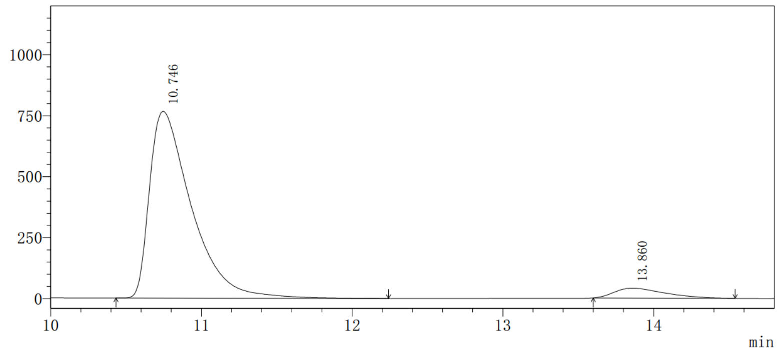

Detector:230nm

ID#	Start	End	Ret. Time	Height	Area	Area%
1	10.433	12.242	10.746	765478	14801715	94.058
2	13.600	14.542	13.860	40531	935047	5.942
Total				806009	15736762	100.000

Run 2

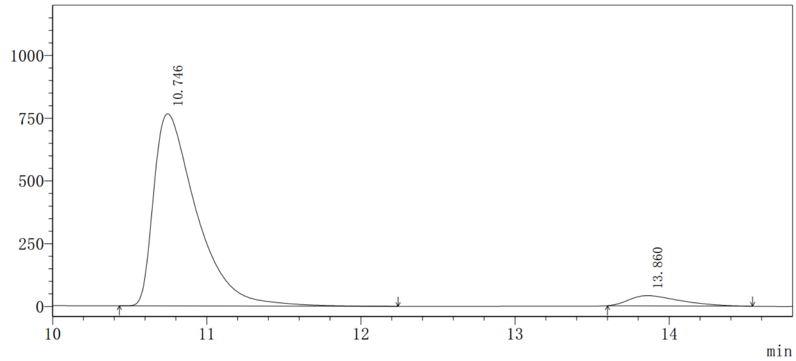

Detector:230nm

ID#	Start	End	Ret. Time	Height	Area	Area%
1	10.433	12.242	10.746	765478	14801715	94.058
2	13.600	14.542	13.860	40531	935047	5.942
Total				806009	15736762	100.000

Run 3

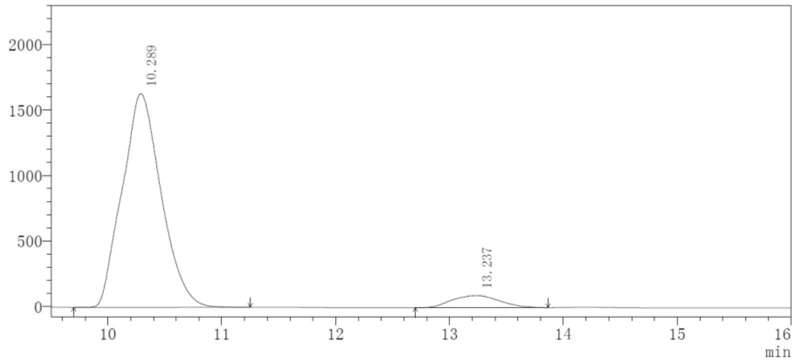

Detector:230nm

ID#	Start	End	Ret. Time	Height	Area	Area%
1	9.700	11.250	10.289	1632033	38861277	93.568
2	12.700	13.867	13.237	92185	2671182	6.432
Total				1724219	41532459	100.000

Run 4

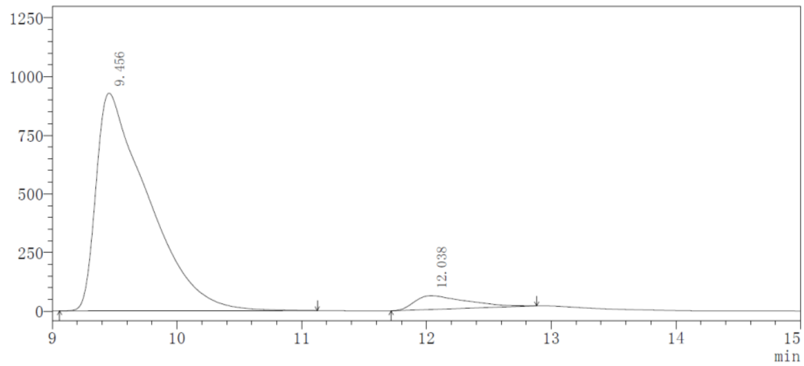

Detector:230nm

ID#	Start	End	Ret. Time	Height	Area	Area%
1	9.058	11.125	9.456	927333	26930795	94.060
2	11.717	12.883	12.038	58582	1700693	5.940
Total				985915	28631489	100.000

Run 5

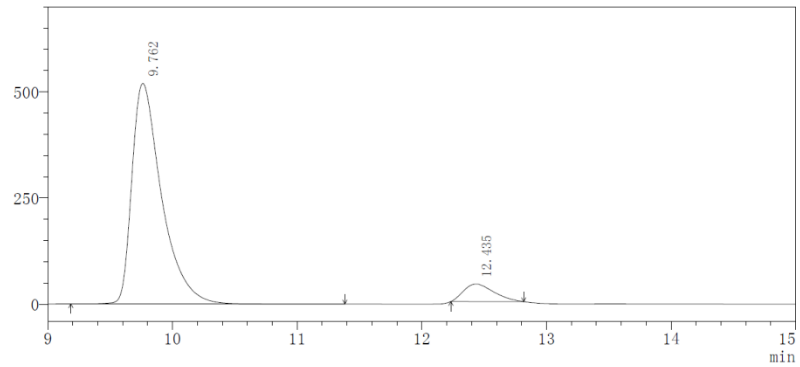

Detector:230nm

ID#	Start	End	Ret. Time	Height	Area	Area%
1	9.183	11.383	9.762	518581	8578228	92.483
2	12.233	12.817	12.435	41287	697218	7.517
Total				559868	9275445	100.000

Run 6

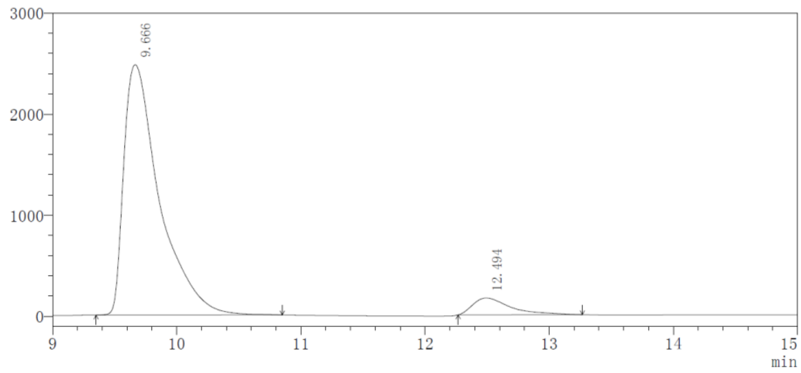

Detector:230nm

ID#	Start	End	Ret. Time	Height	Area	Area%
1	9.350	10.850	9.666	2478492	49577603	93.372
2	12.267	13.267	12.494	166878	3519525	6.628
Total				2645370	53097127	100.000

Run 7

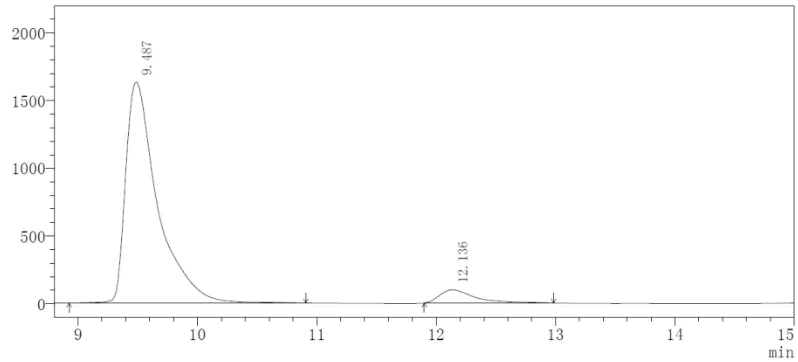

Detector:230nm

ID#	Start	End	Ret. Time	Height	Area	Area%
1	8.925	10.908	9.487	1630814	30293352	93.800
2	11.900	12.983	12.136	96789	2002217	6.200
Total				1727603	32295570	100.000

Run 8

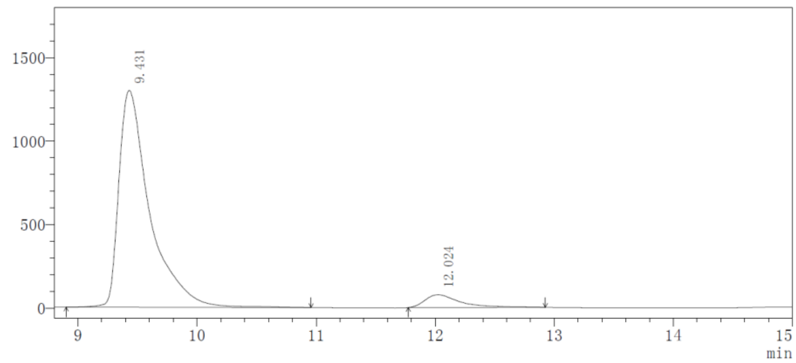

Detector:230nm

ID#	Start	End	Ret. Time	Height	Area	Area%
1	8.900	10.958	9.431	1298227	23411912	93.800
2	11.775	12.925	12.024	76365	1547376	6.200
Total				1374593	24959288	100.000

Run 9

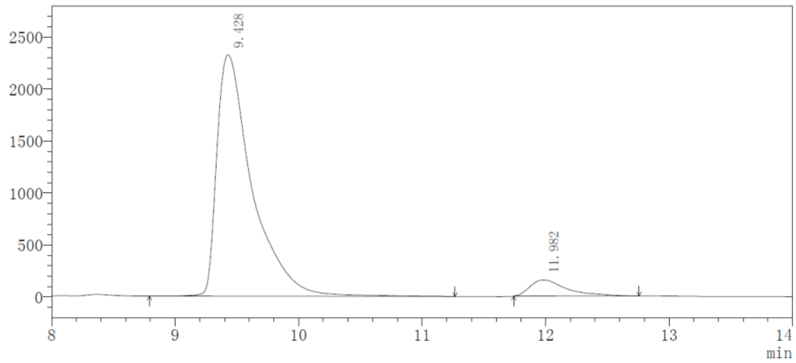

Detector: 230nm

ID#	Start	End	Ret. Time	Height	Area	Area%
1	8.792	11.267	9.428	2322894	46140494	93.551
2	11.742	12.758	11.982	156193	3180595	6.449
Total				2479087	49321089	100.000

Run 10

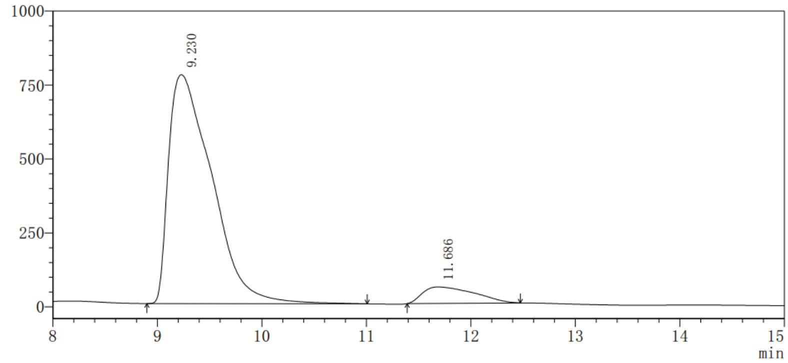

Detector: 230nm

ID#	Start	End	Ret. Time	Height	Area	Area%
1	8.900	11.008	9.230	774086	22259619	92.124
2	11.392	12.475	11.686	55436	1903126	7.876
Total				829523	24162745	100.000

17.7 Recycled experiments of Alcohol OKR by UiO-68-Mn

Run 1

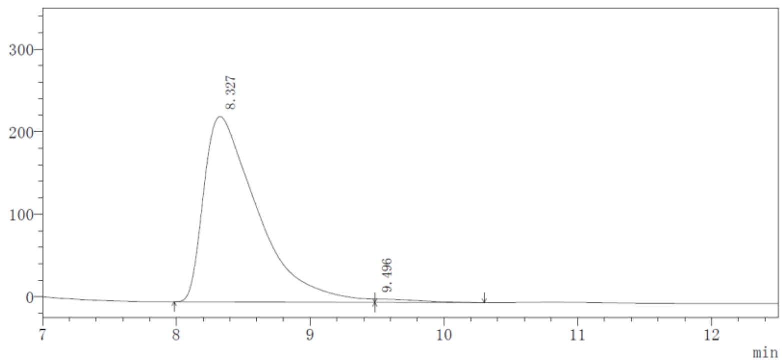

Detector: 220nm

ID#	Start	End	Ret. Time	Height	Area	Area%
1	7.983	9.483	8.327	224588	6285843	98.671
2	9.483	10.300	9.496	3844	84696	1.329
Total				228432	6370539	100.000

Run 2

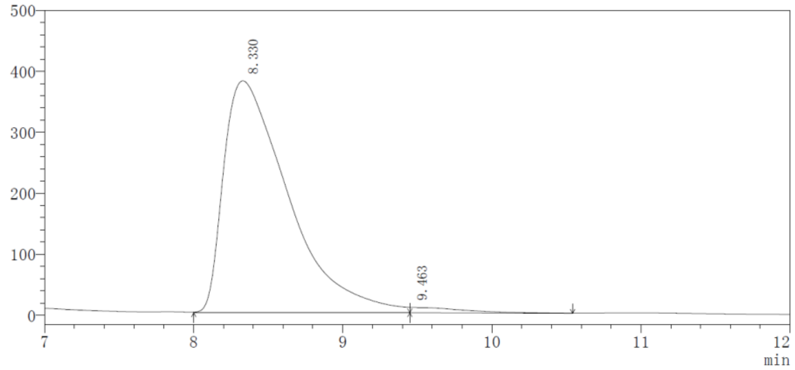

Detector: 220nm

ID#	Start	End	Ret. Time	Height	Area	Area%
1	8.000	9.450	8.330	380359	11527404	98.101
2	9.450	10.542	9.463	8997	223186	1.899
Total				389357	11750590	100.000

Run 3

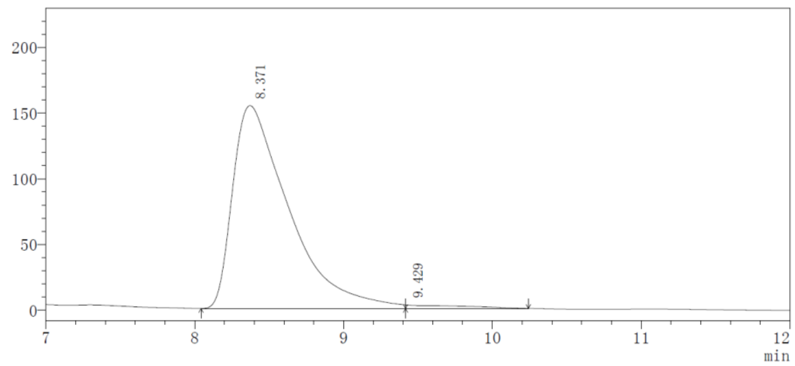

Detector: 220nm

ID#	Start	End	Ret. Time	Height	Area	Area%
1	8.042	9.417	8.371	154487	4062940	98.266
2	9.417	10.242	9.429	2652	71696	1.734
Total				157138	4134635	100.000

Run 4

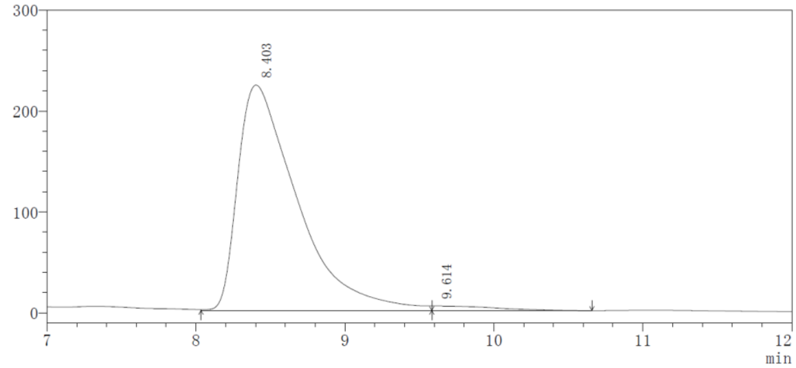

Detector: 220nm

ID#	Start	End	Ret. Time	Height	Area	Area%
1	8.033	9.583	8.403	223310	6210321	98.011
2	9.583	10.658	9.614	4463	126028	1.989
Total				227773	6336348	100.000

Run 5

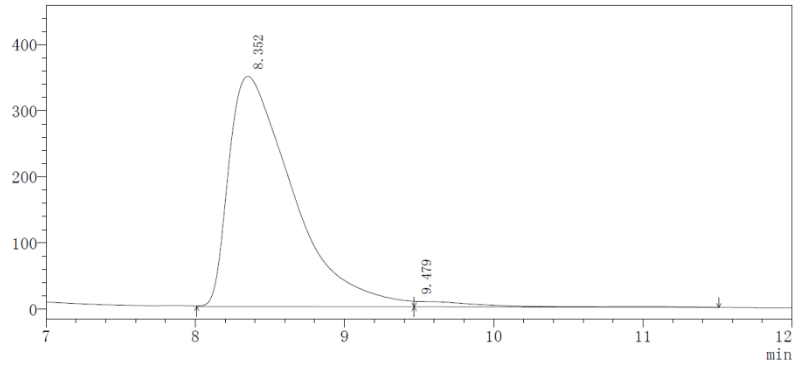

Detector: 220nm

ID#	Start	End	Ret. Time	Height	Area	Area%
1	8.008	9.467	8.352	348745	10394531	97.512
2	9.467	11.508	9.479	8393	265203	2.488
Total				357138	10659734	100.000

Run 6

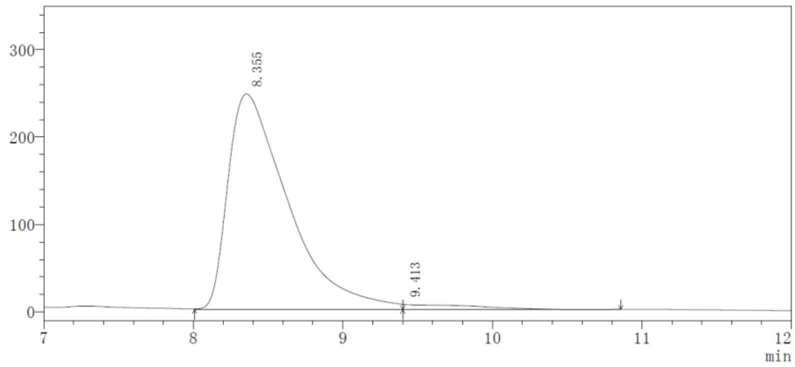

Detector: 220nm

ID#	Start	End	Ret. Time	Height	Area	Area%
1	8.008	9.400	8.355	246724	6908627	97.290
2	9.400	10.858	9.413	5855	192445	2.710
Total				252579	7101072	100.000

Run 7

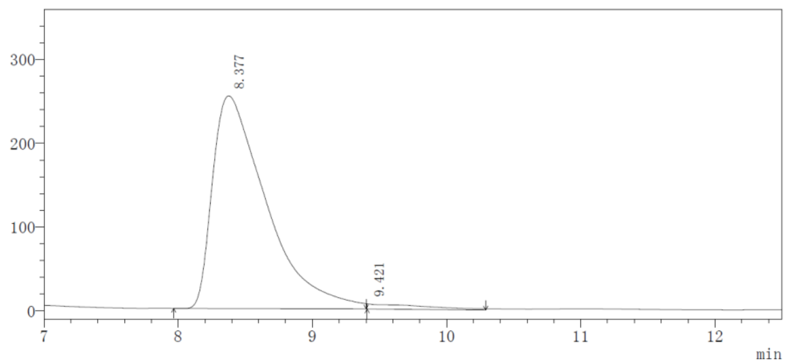

Detector: 220nm

ID#	Start	End	Ret. Time	Height	Area	Area%
1	7.967	9.400	8.377	253888	7077056	97.409
2	9.408	10.292	9.421	6034	188217	2.591
Total				259922	7265273	100.000

Run 8

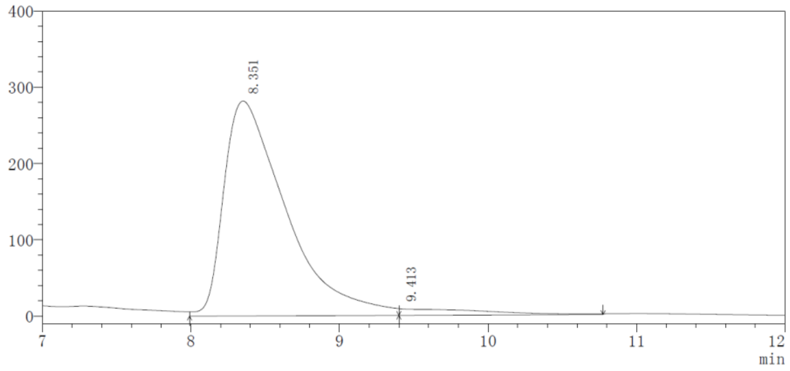

Detector: 220nm

ID#	Start	End	Ret. Time	Height	Area	Area%
1	7.992	9.400	8.351	281869	8211241	96.103
2	9.400	10.775	9.413	8634	332993	3.897
Total				290503	8544234	100.000

Run 9

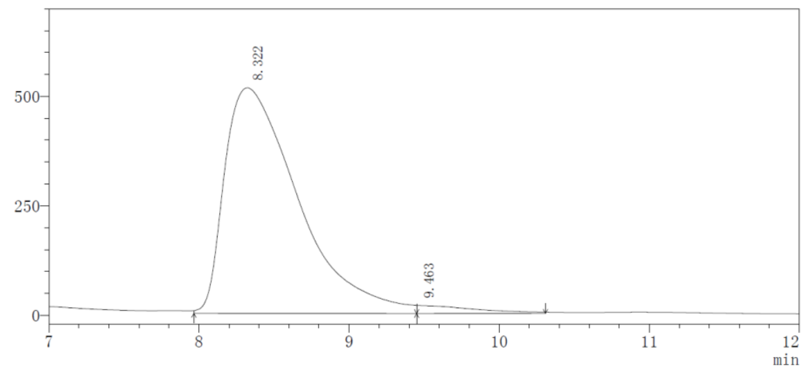

Detector: 220nm

ID#	Start	End	Ret. Time	Height	Area	Area%
1	7.967	9.450	8.322	515310	17653289	97.298
2	9.450	10.308	9.463	18401	490218	2.702
Total				533711	18143506	100.000

Run 10

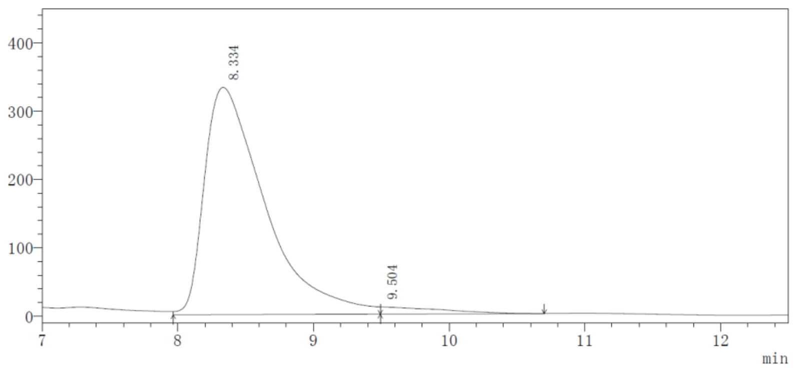

Detector: 220nm

ID#	Start	End	Ret. Time	Height	Area	Area%
1	7.967	9.492	8.334	332811	10330840	96.883
2	9.492	10.700	9.504	10594	332352	3.117
Total				343405	10663191	100.000

17.8 Recycled experiments of Aminolysis of trans-Stilbene Oxide by UiO-68-Cr

Run 1

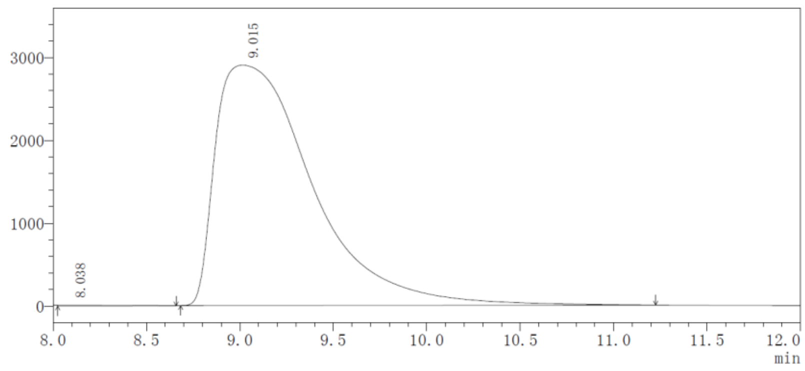

Detector:230nm

ID#	Start	End	Ret. Time	Height	Area	Area%
1	8.025	8.658	8.038	10687	247757	0.235
2	8.683	11.225	9.015	2904446	105097360	99.765
Total				2915134	105345117	100.000

Run 2

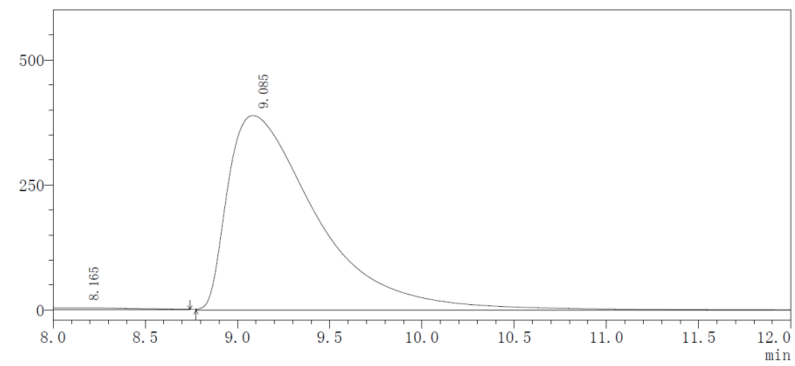

Detector:250nm

ID#	Start	End	Ret. Time	Height	Area	Area%
1	7.983	8.742	8.165	3794	123949	0.932
2	8.775	12.617	9.085	388750	13178708	99.068
Total				392545	13302657	100.000

Run 3

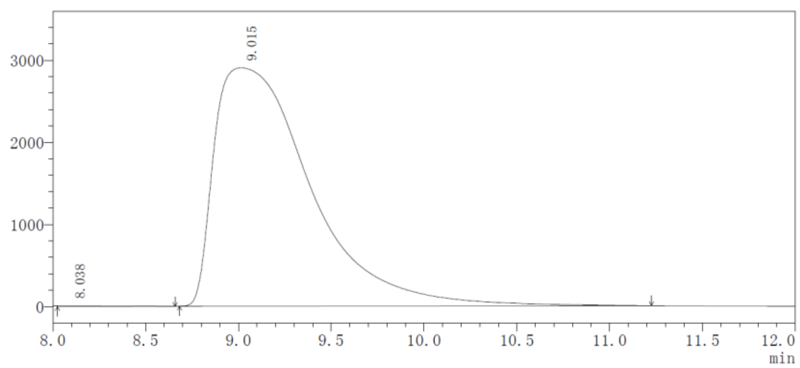

Detector:230nm

ID#	Start	End	Ret. Time	Height	Area	Area%
1	8.025	8.658	8.038	10687	247757	0.235
2	8.683	11.225	9.015	2904446	105097360	99.765
Total				2915134	105345117	100.000

Run 4

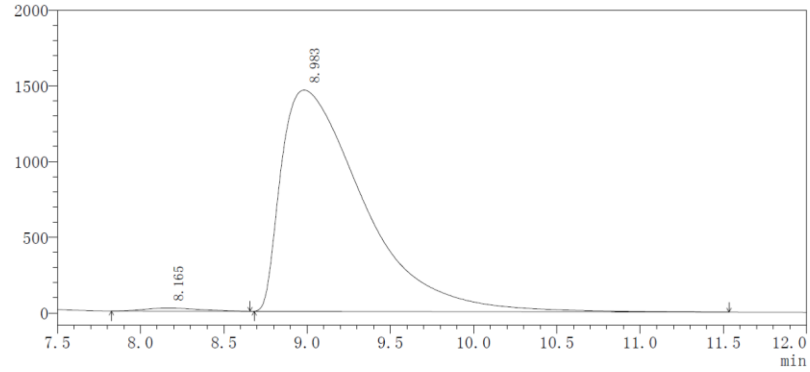

Detector: 240nm

ID#	Start	End	Ret. Time	Height	Area	Area%
1	7.825	8.658	8.165	20268	472139	0.928
2	8.683	11.533	8.983	1461261	50396719	99.072
Total				1481528	50868858	100.000

Run 5

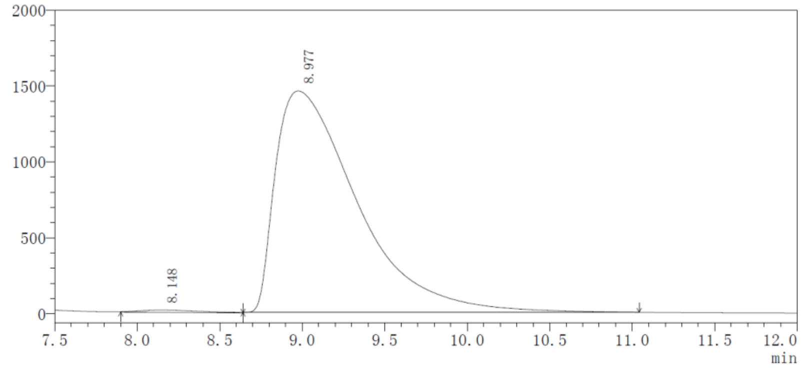

Detector: 240nm

ID#	Start	End	Ret. Time	Height	Area	Area%
1	7.900	8.642	8.148	15418	424234	0.836
2	8.642	11.042	8.977	1459229	50322138	99.164
Total				1474647	50746372	100.000

Run 6

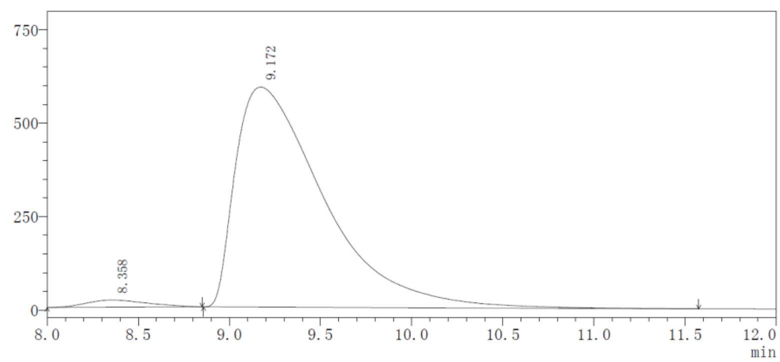

ID#	Start	End	Ret. Time	Height	Area	Area%
1	8.000	8.850	8.358	19181	451033	2.216
2	8.858	11.575	9.172	588984	19902316	97.784
Total				608165	20353349	100.000

Run 7

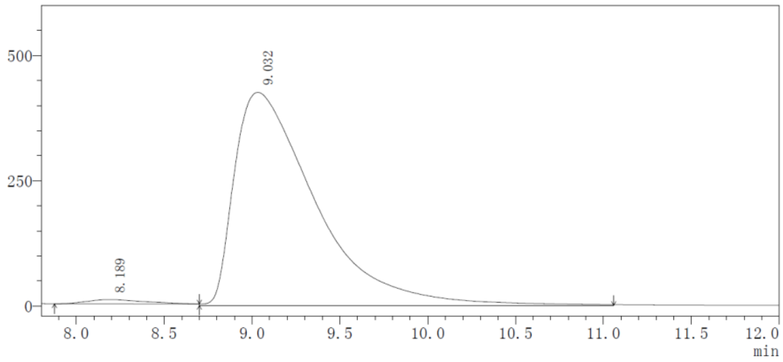

ID#	Start	End	Ret. Time	Height	Area	Area%
1	7.875	8.700	8.189	8509	192117	1.384
2	8.700	11.058	9.032	425345	13688636	98.616
Total				433854	13880753	100.000

Run 8

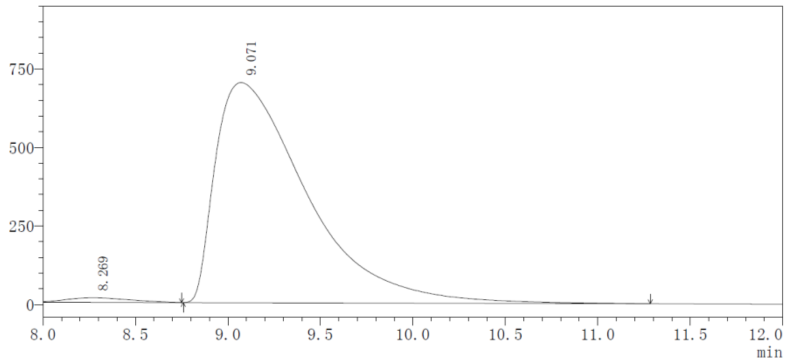

ID#	Start	End	Ret. Time	Height	Area	Area%
1	7.917	8.750	8.269	14523	344411	1.406
2	8.758	11.283	9.071	700591	24147442	98.594
Total				715114	24491853	100.000

Run 9

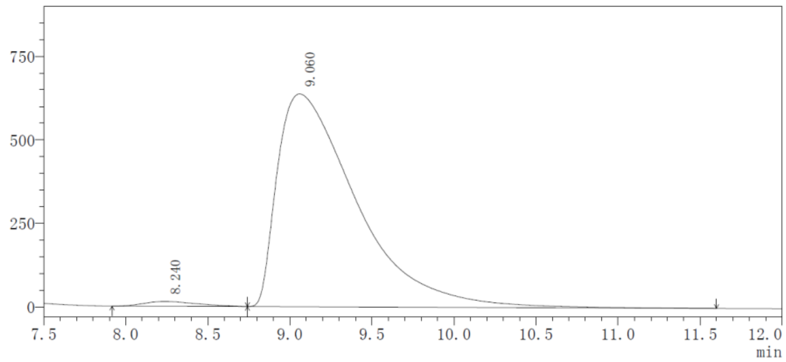

ID#	Start	End	Ret. Time	Height	Area	Area%
1	7.917	8.742	8.240	14629	330870	1.518
2	8.742	11.600	9.060	637396	21465372	98.482
Total				652025	21796242	100.000

Run 10

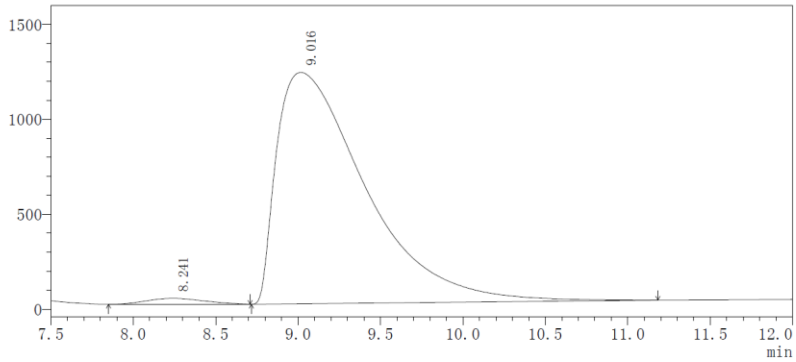

ID#	Start	End	Ret. Time	Height	Area	Area%
1	7.850	8.708	8.241	31780	772223	1.657
2	8.717	11.183	9.016	1218892	45829837	98.343
Total				1250672	46602060	100.000

18. References

[1] (a) Yuan, G.; Zhu, C.; Liu, Y.; Cui, Y. *Chem. Commun.* **2011**, *47*, 3180-3182. (b) Xi, W.; Liu, Y.; Xia, Q.; Li, Z.; Cui, Y. *Chem. Eur. J.*, **2015**, *21*, 12581-12585. (c) Song, F.; Wang, C.; Falkowski, J.; Ma, L.; Lin, W. *J. Am. Chem. Soc.*, **2010**, *132*, 15390-15398. (d)Liu, Y.; Li, Z.; Yuan, G.; Xia, Q.; Yuan, C.; Cui, Y.; *Inorg. Chem.*, **2016**, 55, 12500-12503. (e) Zhu, C.; Yuan, G.; Chen, X.; Yang, Z.; Cui, Y. *J. Am. Chem. Soc.*, **2012**, *134*, 8058-8061.

[2] (a) Yuan, S.; Chen, Y. P.; Qi n, J. S.; Lu, W.; Zou, L.; Zhang, Q.; Wang, X.; Sun, X. and Zhou, H. C. *J. Am. Chem. Soc.* **2016**, *138*, 8912-8919. (b) Jiang, H. L.; Feng, D.; Liu, T. F.; Li, J. R. and Zhou, H. C. *J. Am. Chem. Soc.*, **2012**, *134*, 14690-14693. (c) Manna, K.; Zhang, T.; Carboni, M.; Abney, C. W. and W. Lin. *J. Am. Chem. Soc.* **2014**, *136*, 13182-13185 (d) Li, B.; Gui, B.; Hu, G.; Yuan, D and Wang, C. *Inorg. Chem.*, **2015**, *54* 5139-5141.